Hydrodynamic Analysis of Wave Slamming on a Horizontal Circular Cylinder

By

Shamima Akter

A Thesis submitted to the

Department of Naval Architecture and Marine Engineering

in partial fulfilment of the requirements for the degree of

MASTER OF SCIENCE

in

NAVAL ARCHITECTURE AND MARINE ENGINEERING

BANGLADESH UNIVERSITY OF ENGINEERING AND TECHNOLOGY

Dhaka-1000

January 2011

CERTIFICATE OF APPROVAL

A Thesis titled ***"Hydrodynamic Analysis of Wave Slamming on a Horizontal Circular Cylinder"*** submitted by **Shamima Akter**, Roll No. 0409122011F, Session: April, 2009 has been accepted as satisfactory in partial fulfilment of the requirements for the degree of Master of Science in Naval Architecture and Marine Engineering on January 11, 2011.

Board of Examiners

1.	Dr. Gazi Md. Khalil Professor Department of Naval Architecture & Marine Engineering Bangladesh University of Engineering & Technology Dhaka 1000, Bangladesh.	Chairman (Supervisor)
2.	Dr. Md. Mashud Karim Professor and Head Department of Naval Architecture & Marine Engineering Bangladesh University of Engineering & Technology Dhaka 1000, Bangladesh.	Member (Ex-Officio)
3.	Dr. Md. Refayet Ullah Professor Department of Naval Architecture & Marine Engineering Bangladesh University of Engineering & Technology Dhaka 1000, Bangladesh.	Member
4.	Dr. Md. Shahjada Tarafder Professor Department of Naval Architecture & Marine Engineering Bangladesh University of Engineering & Technology Dhaka 1000, Bangladesh.	Member
5.	Dr. A. K. M. Sadrul Islam Professor Department of Mechanical & Chemical Engineering Islamic University of Technology, Board Bazar, Gazipur.	Member (External)

DECLARATION

This is to certify that this research work has been done by me and has not been submitted elsewhere for the award of any Degree or Diploma.

Shamima Akter

CERTIFICATE OF RESEARCH

This is to certify that this work has been done by the candidate and it was not submitted elsewhere for the award of any degree or diploma.

____________________ Supervisor

____________________ Candidate

Dedicated to my

BELOVED PARENTS

AND

RESPECTED TEACHERS

ACKNOWLEDGEMENT

First of all I am grateful to Almighty Allah for the successful completion of this work. All praises are for Him. Then I would like to express my sincere gratitude to my supervisor, Dr. Gazi Md. Khalil, Professor, Department of Naval Architecture and Marine Engineering, BUET, who provided me with constant encouragement, guidance, valuable suggestions, sincere efforts, direction and careful supervision throughout this research in the department. He has continually given me valuable and helpful advices regarding my thesis work and always kindly helped me to overcome difficulties. I take with me a small part of his knowledge as well as his philosophy in studying and dealing with problems. I would also like to address a special word of thank to Dr. Md. Shahjada Tarafder, Professor, Department of Naval Architecture & Marine Engineering, BUET for his academic advices and nice cooperation during the research. He helped me a lot to enrich the quality of this work.

I would like to pay my special thanks to Prof. Dr. A. K. M. Sadrul Islam, Prof. Dr. Md. Mashud Karim and Prof. Dr. Md. Refayet Ullah for their valuable suggestions which have improved the quality of the thesis. Special thanks to the office staffs of the department of Naval Architecture and Marine Engineering for their cooperation during my research work in the department.

I also wish to thank Mrs. Suraiya Begum, Librarian, Central Library, BUET for allowing me to use the Journal Library and supplying me with some useful papers.

I would also appreciate the efforts of those who have helped me directly or indirectly during the different stages of this work.

Among my personal friends I would like to thank all those who took interest in my work, especially my parents for their encouragement and kind help during this work.

ABSTRACT

Information about the forces acting on cylindrical structures subjected to wave impact is of significant importance in ocean engineering and naval architecture. The design of structures that must survive in a wave environment depends on knowledge of the forces that occur at impact. Impact loads due to wave slamming on horizontal members of an offshore structure are of considerable interest in the context of offshore design, particularly because such loads can give rise to structural failure. Predictions of the wave slamming force generally involve the use of a slamming coefficient. The purpose of this thesis is to analyse the wave impact forces acting on a fixed, slender, horizontal circular cylinder in the vicinity of the free surface, taking account of the intermittent submergence and wave slamming. It presents a new mathematical model for the impact forces acting on a horizontal circular cylinder from the instant of impact to full immersion. Two new expressions are derived for the slamming coefficient, the first expression as a function of the Froude number and the second expression as a function of the Keulegan-Carpenter number. A computer program is developed on the basis of the aforesaid theoretical analysis. The program is written in Fortran 90/95 and executed on the personal computer. The computational results are plotted to show the variation of the slamming coefficient with the Froude number, Keulegan-Carpenter number, wave amplitude, cylinder diameter, depth of cylinder immersion, instantaneous height of the wave surface above the mean water level and the added mass per unit length of the cylinder. In order to check the validity of the mathematical model developed, the present results are compared with the theoretical and experimental results of other investigators.

TABLE OF CONTENTS

LISTS OF SYMBOLS

A	Amplitude of the free surface oscillations
A_i	Immersed sectional area of the circular cylinder
C_S	Slamming coefficient
C_S^0	Slamming coefficient at the instant of impact
D	Diameter of the circular cylinder
F	Total vertical force acting on the cylinder section due to wave slamming
F_b	Buoyant force acting on the cylinder
F_i	Inertial hydrodynamic force acting on the cylinder
Fr	Froude number
g	Acceleration due to gravity
h	Height of the bottom of the horizontal circular cylinder above the mean water level
h'	Height of the centre of the horizontal circular cylinder above the mean water level
KC	Keulegan-Carpenter number
L	Wave length
m	Added mass per unit length of the cylinder
m'	Non-dimensional added mass per unit length of the circular cylinder $\left(= m / \rho D^2\right)$
R	Radius of the circular cylinder
S	Instantaneous depth of cylinder immersion
T	Period of the free surface oscillations
t	Time
U_m	Maximum velocity of the free surface oscillations
α	Half the angle subtended at the centre of the circular cylinder by the water level
η	Instantaneous height of the wave surface above the mean water level
θ	Angle subtended at the centre of the circular cylinder by the water level
ρ	Density of water

LISTS OF FIGURES

CHAPTER 1

INTRODUCTION

1.1 Introduction

Hydrodynamic impact may be defined in general fashion as the forcible, sudden contact of a body, or any part thereof, with the surface of water. A fast planing craft, running through and into waves, suffers impact loading when a portion of the moving bottom surface meets the advancing side of a wave, practically parallel to it. The vertical forces and changes in acceleration on a small, fast, planing boat are frequently so large as to cause it to jump violently up and down. Impact also occurs when there is sudden contact of a liquid surface with a body or a ship; in other words, when the liquid is moving rather than the ship. Large waves often strike sea walls with impact, and breaking wave's impact upon ships which are not in motion.

Interest in this field of hydrodynamics arose more than a half century ago in connection with the problem of the landing of flying boats and seaplanes. Increases in the takeoff and landing speeds of flying boats and seaplanes, and in the running speeds of racing motorboats, coupled with the use of these crafts in rougher water, brought with them the need to estimate or to predict the water-impact forces and pressures on their bottoms. The latter were almost always wedge-shaped in section. Instrumentation was not then available to record these rapidly applied loads and strains, so the problem was attacked analytically (Szebehely, 1959).

The wave impact is generally defined as the early stages of the penetration of a solid body into a wave surface. At the instant of contact the fluid in the vicinity of the body undergoes large accelerations which give rise to large forces. As the body becomes more fully immersed, forces due to viscous drag and separation effects become predominant. Thus the inertia and drag coefficients used in the classical Morison equation (Morison et al., 1950) are not constant, and the problem becomes very difficult, even for simple geometries.

When a body enters a free water surface at speed it experiences large transient forces due to the acceleration field it sets up within the water. The forces are generally termed impact or slamming loads and are often of considerable practical importance. Offshore structures often have appreciable number of main structural and bracing members near the still water level. As waves pass the structure some of these members are alternately exposed to the air and then submerged in the water. Each time they enter the water there are slamming forces. Failures of some members have been partially attributed to slamming.

1.2 Literature Review

The history of research into slamming and impact loads is relatively recent mainly because it is, as far as naval architecture is concerned, predominantly a high speed phenomenon. The general problem of hydrodynamic impact has also been studied extensively motivated in part by its importance in ordnance and missile technology. A large number of mathematical models have been developed for cases of simple geometry such as spheres and wedges. These models have been well supported by experiment. Unfortunately, the special case of wave impact has not been studied extensively.

The early impact theory of von Karman (1929) was based on the principle of conservation of momentum throughout the impact. Prior to impact all momentum is associated with the body, but as the wedge becomes immersed part of the momentum is imparted to a mass of water which is in contact of the bottom and which has the same velocity as the bottom. With a constant momentum, increased mass required a decreased velocity for the system and the change of momentum of the body alone defined the force on the body. von Karman proposed an attached or virtual mass equal to the mass of a half-cylinder of water having a diameter equal to the instantaneous width of the wedge in the plane of the undisturbed water surface. While von Karman's paper was the first, mathematical details came with Wagner's (1931) work published three years later. The basic idea of the mathematical treatment proposed by Wagner can still be recognized in recent papers. In his somewhat difficult-to-read publication he solved the impact problem of the two-dimensional symmetric wedge of small deadrise angle, discussed the concept of similarity solution, computed the piled up water surface, the pressure distribution, spray thickness, gave the equation of a constant force bottom and introduced a deadrise angle correction factor. It can be stated without exaggeration that von Karman's physical picture and Wagner's mathematical treatment are still valid and useful, and form the basis of most later papers.

When considering the various forces acting on offshore drilling platforms at sea, an important class of forces for which there is no extensive history of study are the impact forces that act on horizontal structural members in the so called *splash zone*. The splash zone is a region wherein the particular horizontal members of the platform are not usually considered to have continuous contact with the waves, but which are located at a height relative to the mean water surface so that only occasional contact with the water will occur (see *Figure 1*). The nature of the forces that occur during such contacts is essentially impulsive, and thus somewhat similar to the forces associated with the often-encountered *slamming* of ships, where the relative emersion and immersion of a portion of the ship bow region with respect to the sea surface produces impacts on the ship.

Wave forces on structures composed of slender members are traditionally calculated on the basis of the classical Morison equation, in which the force at any section of a member is expressed directly in terms of the fluids kinematics that would occur at that section's location (Morison et al., 1950). However, the Morison equation is generally applicable only to portions of an immersed body that are in full contact with the water continually, and as such there is a question as to whether that particular approach can be considered applicable to the present impact force problem for horizontal members.

Kaplan and Silbert (1976) developed a mathematical model for determining time histories of vertical impact forces on platform horizontal structural members in the splash zone.

Dalton and Nash (1976) conducted slamming experiments with a 1.27 cm diameter cylinder with small amplitude waves generated in a laboratory tank. But their data exhibited large scatter and showed no particular correlation with either the predictions of hydrodynamic theory or identifiable wave parameters.

Miller (1977) developed a computer model for the vertical wave force on an instrumented cylinder which behaves as a two degree-of-freedom dynamic system. The slamming force was assumed to increase linearly to a peak value over a specific rise time, and to decrease linearly to zero over a specific decay-time. The drag and inertia components were assumed to act only when the cylinder was fully immersed and were computed from constant drag and inertia coefficients. The resulting combined force exhibits discontinuities in magnitude and the buoyancy component had to be reduced when the water surface was reducing in order to avoid an unrealistic dynamic response during that stage. Miller also identified loading regimes associated with wave slamming and described slamming tests on a cylinder in waves. Tests conducted for 3 cylinder elevations indicated an average value of C_S^0 of 3.6, although there was appreciable scatter in the results. He concluded that this was consistent with the theoretical value of π and attributed the observed higher value to dynamic amplification effects. The effects of the slamming force rise time on the dynamic response were illustrated by simulating numerically the vertical wave force using a dynamic analogue and comparing the computed force traces with the experimental records.

Faltinsen et al. (1977) investigated the load acting on horizontal circular cylinders (with end plates and length-to-diameter ratios of about 1) which were forced with constant velocity through an initially calm free surface. They found that the slamming coefficient ranged from 4.1 to 6.4. They also conducted experiments with flexible horizontal cylinders and found that the analytically predicted values were always lower (50 to 90 per cent) than those found experimentally.

Sarpkaya (1978) conducted slamming experiments with harmonically oscillating flow impacting a horizontal cylinder and found that: (a) the dynamic response of the system is as important as the impact force (that is, one cannot be determined without accounting for the other); (b) the initial value of the slamming coefficient is essentially equal to its theoretical value of π; (c) the system response may be amplified or attenuated, depending on its dynamic characteristics; (d) the buoyancy-corrected normalized force in the drag-dominated region reaches a maximum at a relative fluid displacement of about 1.75; and (e) roughness increases the rise time of the force and tends to decrease the amplification factor.

Kaplan (1979) described some of the problems associated with the measurement of high frequency impact forces on offshore structures. The effects of various elements of the measuring and data processing systems on the data, as well as the correlation with theory, were presented in detail. Theoretical representations of the various physical mechanisms contributing to the total forces, both vertical and horizontal, were described and exhibited in the results. Comparisons between theory and experiment were presented in the form of time history characteristics as well as analysis of peak values for use in design estimation. He found that the slamming coefficient ranged from 1.88 to 5.11, with just as many values above the theoretical value of π as below, and a mean value of $C_S = 2.98$.

Miller (1980) has shown that for most structures the current practice of applying a constant slamming coefficient of 3.5 is conservative when estimating extreme stresses. For fatigue estimation this appears to be the case irrespective of the member geometry.

Campbell and Weynberg (1980) measured spanwise and circumferential pressures in addition to the vertical force on horizontal and inclined cylinder driven through a still water surface. They observed that the slamming force was predominant for tests involving a Froude number ($Fr = U/\sqrt{gD}$, where U is the fluid velocity, g is the gravitational acceleration and D is the cylinder diameter) higher than 0.6. They also indicate that the slamming force was masked by the dynamic response of the force transducer and the scatter in the observed data was the result of variable rise-times which were sensitive to small variation in the slope of the cylinder. It was also noted that drips from the cylinder had a significant effect on the response. They summarized their results by proposing an empirical equation that relates the slamming coefficient and cylinder submergence, and which uses C_{S0} = 5.15. This equation is independent of the Froude number and was not corrected for buoyancy effects.

Cointe and Armand (1987) used the method of matched asymptotic expansions to solve the boundary value problem for water-cylinder impact. They too conclude that C_S^0 is 2π rather than π as given by some of the earlier theories.

Greenhow and Li (1987) reviewed a number of different formulations for evaluating the added mass of a horizontal circular cylinder moving near the free surface and conclude that the effects of free surface deformation on the slamming coefficient is significant and must be included in any theoretical treatment. They recommend two different methods to calculate the added mass for small and large cylinder submergence respectively which both indicate a C_{S0} value of $4\pi/3$.

Isaacson and Subbiah (1990) described random wave forces acting on a fixed, slender, horizontal circular cylinder in the vicinity of the free surface, taking account of the intermittency of submergence and wave slamming. They derived expressions for the probability density and the mean of the force maxima, and calculated the expected value of the single largest force maximum occurring within a given duration. These predictions were based on the assumptions of linear wave theory and a narrow-band wave spectrum. They presented useful numerical results and discussed the effects of intermittent submergence and wave slamming.

Miao (1990) computed the bending stress on a flexible cylinder subjected to water impact. The hydrodynamic force was computed as the sum of the momentum, drag and buoyancy forces and the equation of motion was solved for various end fixity conditions using the mode superposition approach. Computed bending stresses compared well with his experimental observation of slamming on a cylinder driven into still water. Miao also reported results from experiments on a 1.52 m long flexible horizontal cylinder which was driven at a constant velocity through a stationary water surface. He proposed an expression for the variation of C_S with submergence which indicates a C_{S0} value of 6.1 and also concluded that for typical truss members in heavy seas, thy dynamic application of the response and the induced stresses ranged from 0.3 to 0.6 due to the short impulse times observed in the experiments.

Chan et al. (1991) presented the results of an experimental study of plunging wave action on a large horizontal cylinder in the splash zone. Impact pressures were found to range from localized impulsive pressures with time scales in the range of 0.001T to synchronous low frequency pressure oscillations with oscillation time scale around 0.01T (T being the characteristic wave period). The peak impact force was about $8.6\rho c^2R$ per unit length of the cylinder (where ρ is the water density, C is the characteristic phase speed of the wave and R is the radius of the cylinder. Overall, the incident wave profile trajectory and the entrapped air were found to influence the impact load significantly.

Isaacson and Prasad (1992 and1994) described a numerical and experimental study of the vertical force acting on a section of a fixed, horizontal circular cylinder located near the free surface. The two-dimensional case of unidirectional waves propagating in a direction orthogonal to the cylinder axis has been considered. Numerical models are developed for the time-varying vertical force on fixed and dynamically responding cylinders on the basis of specified empirical force coefficients. As an alternative to the conventional approach involving the slamming coefficient, the suitability of an impulse coefficient which combines the impact force and rise time into a single dimensionless quantity has also been examined.

Khalil and Ali (1994) conducted an investigation into wave slamming loads on horizontal circular cylinders. They provided an analytical approach for deriving an expression for the slamming coefficient. Subsequently, they developed a computer code based on the theoretical analysis and generated computational results. The results of computation were plotted graphically with a view to explaining the salient features of wave slamming on cylindrical structures like the braces between legs of an offshore platform.

Cortel and Grilli (2006) studied the impact on cylindrical piles of extreme waves, generated by directional wave focusing. Waves were numerically modeled based on a boundary element discretization of fully non-linear potential flow equations with free surface elevation. Finally, the full loading on a cylindrical tower structure, due to a freak wave, was determined.

Zylinsky (2009) performed finite element analysis of wave slamming on offshore structure. He focuses on the analysis of wave slamming on floating platform column. Dynamic analysis has been performed with non-linear finite element method software package *ABAQUS*.

Khalil, Tarafder and Akter (2009) presented a mathematical model for the wave impact forces acting on a horizontal circular cylinder from the instant of impact to full immersion. They derived an expression for the slamming coefficient as a function of the Keulegan-Carpenter number, wave amplitude, diameter of the circular cylinder, instantaneous height of the wave surface above the mean water level, depth of immersion and added mass per unit length of the cylinder. A computer code is developed on the basis of the aforesaid theoretical analysis. The computational results are plotted in order to show the variation of the slamming coefficient with the Keulegan-Carpenter number, non-dimensional immersed area, non-dimensional added mass and relative submergence.

1.3 Present Research

The purpose of the present research is to analyse the wave impact forces acting on a fixed, slender, horizontal circular cylinder located above the still water level. It presents a new mathematical model for the impact forces acting on a horizontal circular cylinder from the instant of impact to full immersion. Two different expressions are developed for the slamming coefficient. The first expression is a function of the Froude number whereas the second expression is a function of the Keulegan-Carpenter number. It may be noted that the Froude number and the Keulegan-Carpenter number are two important dimensionless parameters associated with wave mechanics. These two parameters are used extensively in the design of offshore structures. Thus the expressions of the slamming coefficient which include the aforesaid dimensionless parameters are expected to be very useful in the analysis of wave impact forces on offshore structures.

A computer program is developed on the basis of the aforesaid theoretical analysis. The computational results are plotted in order to show the variation of the slamming coefficient with the Froude number, Keulegan-Carpenter number, cylinder diameter-to-wave amplitude ratio, non-dimensional immersed area, non-dimensional added mass, relative submergence and wave steepness. In order to check the validity of the mathematical model developed, the present computational results are compared with the theoretical and experimental results of other investigators.

CHAPTER 2

THEORETICAL FORMULATION

The general case of hydrodynamic impact is usually described by using incompressible potential flow theory. The compressibility of water and air and the cushioning effect of air (air boundary layer, depression of the water surface just before impact, etc.) are ignored. For a moving body with mass M, and velocity v_0, impacting a quiescent surface, the system momentum is Mv_0. Neglecting non-conservative forces, the momentum of the system is unchanged during penetration. However, the mass of the system increases because of the fluid set in motion near the body. Also known as added mass, m results in reducing the velocity. Thus, the system momentum after penetration is $(M+m)v = Mv_0$. The impact force at any instant is a function of the added mass m and its time derivative $\dot{m}$. Therefore, the solution requires knowledge of the added mass and its time derivative. The determination of the added mass is not a simple matter and the results depend on the assumptions made (Moran, 1965). The following analysis is based on the added mass calculated by Taylor (1930).

This section presents a two-dimensional analysis of the hydrodynamic forces acting on a fixed horizontal circular cylinder in the vicinity of the free surface, taking account of the intermittent submergence and wave slamming. The following assumptions are made in the present theoretical analysis:

(i) The wave system propagates in a direction normal to the axis of the horizontal circular cylinder.

(ii) The motion of the free surface is assumed to be a sinusoidally oscillating one.

(iii) The water is assumed to be inviscid, incompressible and the flow is irrotational.

(iv) The diameter of the cylinder is assumed to be much smaller than the wave length.

(v) The free surface on the small circular cylinder is assumed to be flat.

Let us now analyse the hydrodynamic forces acting on a fixed horizontal circular cylinder located near the free surface, taking account of the intermittent submergence and wave slamming. It is assumed that the wave system propagates in a direction normal to the horizontal cylinder. The particular problem considered here is shown in *Figure 2,* where *h* is the height of the bottom of the cylinder above the mean water level, η is the instantaneous height of the wave surface above the mean water level, and *S* is the instantaneous depth of cylinder immersion and A_i is the immersed area.

The total vertical force acting on the immersed cylinder section is made up of a buoyant force and a hydrodynamic force of inertial nature due to the body-wave interaction. The force on the circular cylinder can be expressed as

$$F = F_b + F_i \tag{1}$$

where F_b is the force of buoyancy and F_i is the inertial hydrodynamic force.

The tendency of a fluid to uplift a submerged body, because of the upward thrust of the fluid, is known as the force of buoyancy or simply buoyancy. It is always equal to the weight of the fluid displaced by the body. Thus the force of buoyancy is given by

$$F_b = \rho g A_i \tag{2}$$

where ρ represents the density of water, *g* is the gravitational acceleration and A_i is the immersed area of the cylinder.

The inertial hydrodynamic force F_i is obtained by generalizing the relations given by Kaplan (1957) and Kaplan and Hu (1959) for body-wave interaction, which leads to the expression

$$F_i = \rho A_i \ddot{\eta} + \frac{\partial}{\partial t}\left(m\dot{\eta}\right) \tag{3}$$

in which m represents the vertical added mass per unit length of the circular cylinder. The first and second derivatives of η with respect to time are denoted by $\dot{\eta}$ and $\ddot{\eta}$ which represent the vertical wave velocity and vertical wave acceleration respectively. The first term in Equation (3) arises due to the spatial variation of the wave characteristics and the second term arises from the time rate of change of fluid momentum associated with the immersed portion of the cylinder section.

The expression for F_i can be simplified as:

$$F_i = \rho A_i \ddot{\eta} + m\ddot{\eta} + \dot{\eta}\frac{\partial m}{\partial t}$$

or,

$$F_i = (m + \rho A_i)\ddot{\eta} + \dot{\eta}\frac{\partial m}{\partial S}\frac{\partial S}{\partial t}$$

or,

$$F_i = (m + \rho A_i)\ddot{\eta} + \frac{\partial m}{\partial S}\dot{\eta}^2 \tag{4}$$

Thus, the total vertical force acting on the immersed cylinder section is given by

$$F = \rho g A_i + (m + \rho A_i)\ddot{\eta} + \frac{\partial m}{\partial S}\dot{\eta}^2 \tag{5}$$

This expression holds good only if there is water contact and resulting immersion of a portion of the circular section. An evaluation of this force expression, which is a two-dimensional force per unit length of the cylinder, requires determination of the immersed area A_i and the vertical added mass m, as well as its rate of change with immersion $\partial m / \partial S$.

Referring to *Figure 2*, we can perform a simple geometrical analysis to obtain an expression for the immersed area of the horizontal circular cylinder. Let *O* be the centre and *D* be the diameter of the circular cylinder. *AB* is the water level and *OC* is drawn vertically downwards from the centre. *ACB* is the immersed area of the circular cylinder and α is half of the angle subtended at the centre by the water level.

From the geometry of the figure, we find that

OA = *OB* =*R*

where *R* is the radius of the circular cylinder.

$\angle AOE = \angle BOE = \alpha$

$OE = R\cos\alpha$

$EB = R\sin\alpha$

Area of $\Delta OEB = \frac{1}{2}R^2 \sin\alpha\cos\alpha$

Area of $\Delta OAE = \frac{1}{2}R^2 \sin\alpha\cos\alpha$

Area of $\Delta OAB = R^2 \sin\alpha \cos\alpha$ (6)

The wetted perimeter = $P = 2R\alpha$ (7)

$\therefore$ Area of $OACB = R^2\alpha$ (8)

From Equations (6) and (8), we get the immersed area

$$A_i = R^2\alpha - R^2 \sin\alpha \cos\alpha$$

or,

$$A_i = R^2\alpha - R^2 \frac{\sin 2\alpha}{2}$$

or,

$$A_i = R^2\left(\alpha - \frac{\sin 2\alpha}{2}\right) \tag{9}$$

But we know that

$$\theta = 2\alpha$$

where θ is the total angle subtended at the centre by the water level. Thus, we can write

$$A_i = R^2\left(\frac{\theta}{2} - \frac{\sin\theta}{2}\right)$$

or,

$$A_i = \frac{R^2}{2}(\theta - \sin\theta) \tag{10}$$

or,

$$A_i = \frac{D^2}{8}(\theta - \sin\theta) \tag{11}$$

where $D = 2R$.

Equation (11) can be rewritten as

$$A_i = \frac{D^2}{8} f_1(\theta) \tag{12}$$

where

$$f_1(\theta) = \theta - \sin\theta \tag{13}$$

The instantaneous depth of cylinder immersion S can be related to the variables D and θ by

$$S = \frac{D}{2}\left(1 - \cos\frac{\theta}{2}\right)$$

or,

$$\frac{S}{D}=\frac{1}{2}\left(1-\cos\frac{\theta}{2}\right) \tag{14}$$

The problem of the vertical added mass of segments of a circle has been solved by Lockwood Taylor (1930). He has shown that the added mass is given by

$$m=\frac{\rho D^2}{8}\left[\frac{2\pi^3}{3}\frac{(1-\cos\theta)}{(2\pi-\theta)^2}+\frac{\pi}{3}(1-\cos\theta)+(\sin\theta-\theta)\right] \tag{15}$$

Thus, we can write

$$m=\frac{\rho D^2}{8}f_2(\theta) \tag{16}$$

where

$$f_2(\theta)=\frac{2\pi^3}{3}\frac{(1-cos\,\theta)}{(2\pi-\theta)^2}+\frac{\pi}{3}(1-cos\,\theta)+(sin\,\theta-\theta) \tag{17}$$

Equation (17) clearly shows that at $\theta=2\pi$, $f_2(\theta)$ takes the indeterminate form $0/0$. In such a case, applying L' Hospital's rule (Smirnov, 1964), we get

$$\underset{\theta\to 2\pi}{Lt}\, f_2(\theta)=\frac{\pi^3}{3}-2\pi \tag{18}$$

(The detailed evaluation of the above function is presented in Appendix I).

Differentiating both sides of Equation (15) with respect to θ, we have

$$\frac{\partial m}{\partial\theta}=\frac{\rho D^2}{8}\left[\frac{2\pi^3}{3}\left\{\frac{\sin\theta}{(2\pi-\theta)^2}+\frac{2(1-\cos\theta)}{(2\pi-\theta)^3}\right\}+\frac{\pi}{3}\sin\theta+(\cos\theta-1)\right] \tag{19}$$

From Equation (14), we obtain

$$\frac{\partial S}{\partial\theta}=\frac{D}{4}\sin\frac{\theta}{2} \tag{20}$$

Now

$$\frac{\partial m}{\partial S}=\frac{\partial m}{\partial\theta}\frac{\partial\theta}{\partial S}$$

or,

$$\frac{\partial m}{\partial S}=\frac{\partial m}{\partial\theta}\Big/\frac{\partial S}{\partial\theta} \tag{21}$$

Combining Equations (19), (20) and (21), we get

$$\frac{\partial m}{\partial S}=\frac{\rho D}{2\sin\frac{\theta}{2}}\left[\frac{2\pi^{3}}{3}\left\{\frac{\sin\theta}{(2\pi-\theta)^{2}}+\frac{2(1-\cos\theta)}{(2\pi-\theta)^{3}}\right\}+\frac{\pi}{3}\sin\theta+(\cos\theta-1)\right] \tag{22}$$

Equation (22) can be presented in the following form:

$$\frac{\partial m}{\partial S}=\frac{\rho D}{2}f_{3}(\theta) \tag{23}$$

where

$$f_{3}(\theta)=\frac{1}{sin\frac{\theta}{2}}\left[\frac{2\pi^{3}}{3}\left\{\frac{sin\theta}{(2\pi-\theta)^{2}}+\frac{2(1-cos\theta)}{(2\pi-\theta)^{3}}\right\}+\frac{\pi}{3}sin\theta+(cos\theta-1)\right] \tag{24}$$

Differentiating both sides of Equation (17) with respect to θ, we have

$$\frac{df_{2}}{d\theta}=\frac{2\pi^{3}}{3}\left[\frac{sin\theta}{(2\pi-\theta)^{2}}+\frac{2(1-cos\theta)}{(2\pi-\theta)^{3}}\right]+\frac{\pi}{3}sin\theta+(cos\theta-1) \tag{25}$$

Combining Equations (24) and (25), we obtain

$$f_{3}(\theta)=\frac{df_{2}}{d\theta}/\,sin\frac{\theta}{2} \tag{26}$$

Equation (24) clearly shows that at $\theta=0$ and 2π, $f_{3}(\theta)$ takes the indeterminate form $0/0$. Then, according to L' Hospital's rule, we get

$$\underset{\theta\to 0}{Lt}\,f_{3}(\theta)=\pi \tag{27}$$

and

$$\underset{\theta\to 2\pi}{Lt}\,f_{3}(\theta)=\frac{\pi^{3}}{9}-\frac{2\pi}{3} \tag{28}$$

(The detailed evaluation of the above functions is presented in Appendix I).

The motion of the free surface is related to its maximum amplitude by

$$\eta = A\,sin\left(\frac{2\pi t}{T}\right) \tag{29}$$

where A and T represent the amplitude and period of the free surface oscillations respectively.

Differentiating both sides of Equation (29) with respect to time t, we have

$$\frac{d\eta}{dt}=\dot{\eta}=\frac{2\pi A}{T}cos\left(\frac{2\pi t}{T}\right) \tag{30}$$

Therefore, the maximum velocity U_{m} of the free surface oscillations is given by

$$U_{m}=\frac{2\pi A}{T} \tag{31}$$

From Equations (30) and (31), we obtain

$$\dot{\eta} = U_m \cos\left(\frac{2\pi t}{T}\right)$$

or,

$$\dot{\eta}^2 = U_m{}^2\left[1 - \sin^2\left(\frac{2\pi t}{T}\right)\right] \tag{32}$$

From Equations (29) and (32), we can write

$$\dot{\eta}^2 = U_m{}^2\left[1 - \left(\frac{\eta}{A}\right)^2\right] \tag{33}$$

Differentiating both sides of Equation (29) twice with respect to t, we have

$$\ddot{\eta} = -\frac{4\pi^2}{T^2} A \sin\left(\frac{2\pi t}{T}\right) \tag{34}$$

Combining Equations (29), (31) and (34), we get

$$\ddot{\eta} = -\frac{U_m{}^2}{A^2}\eta \tag{35}$$

The expression for the slamming coefficient C_S can be written as

$$C_S = \frac{F}{\frac{1}{2}\rho U_m{}^2 D}$$

or,

$$C_S = \frac{2F}{\rho U_m{}^2 D} \tag{36}$$

Combining Equations (5) and (36), we have

$$C_S = \frac{2\rho g A_i + 2(m + \rho A_i)\ddot{\eta} + 2\frac{\partial m}{\partial S}\dot{\eta}^2}{\rho U_m{}^2 D} \tag{37}$$

If a dimensionless relationship is set up between the inertia forces and the gravity forces, there evolves the well-known Froude number. Normally, the Froude number is considered as an indicator of geometrically similar flow, with respect to both velocity and pressure phenomena, when gravity effects such as surface waves are involved. For the present case, it can be represented by

$$Fr = \frac{U_m}{\sqrt{gD}} \tag{38}$$

We can write Equation (37) as

$$C_S = a + b + c \tag{39}$$

where

$$a = \frac{2\rho g A_i}{\rho U_m^{\ 2} D} \tag{40}$$

$$b = \frac{2(m + \rho A_i)\ddot{\eta}}{\rho U_m^{\ 2} D} \tag{41}$$

and

$$c = \frac{2\dfrac{\partial m}{\partial S}\dot{\eta}^2}{\rho U_m^{\ 2} D} \tag{42}$$

Equation (40) can be simplified as:

$$a = \frac{2gA_i}{U_m^{\ 2} D} = 2\left(\frac{gD}{U_m^{\ 2}}\right)\frac{A_i}{D^2} \tag{43}$$

Combining Equations (12), (38) and (43), we have

$$a = \frac{1}{4Fr^2} f_1(\theta) \tag{44}$$

Combining Equations (35) and (41), we get

$$b = -\frac{2(m + \rho A_i)\eta}{\rho A^2 D} \tag{45}$$

From Equations (12), (16) and (45), we may get

$$b = -\frac{1}{4}\frac{\rho D^2 f_2(\theta)\eta}{\rho A^2 D} - \frac{1}{4}\frac{\rho D^2 f_1(\theta)\eta}{\rho A^2 D}$$

or

$$b = -\frac{1}{4}\left[f_1(\theta) + f_2(\theta)\right]\left(\frac{D}{A}\right)\left(\frac{\eta}{A}\right) \tag{46}$$

Combining Equations (23), (33) and (42), we obtain

$$c = \frac{\rho D f_3(\theta) U_m^{\ 2}\left[1 - \left(\dfrac{\eta}{A}\right)^2\right]}{\rho U_m^{\ 2} D}$$

or

$$c = f_3(\theta)\left[1 - \left(\frac{\eta}{A}\right)^2\right] \tag{47}$$

Equations (39), (44), (46) and (47) finally lead to the following expression for the coefficient of slamming:

$$C_S = \frac{1}{4Fr^2} f_1(\theta) - \frac{1}{4}\left[f_1(\theta) + f_2(\theta)\right]\left(\frac{D}{A}\right)\left(\frac{\eta}{A}\right) + f_3(\theta)\left[1 - \left(\frac{\eta}{A}\right)^2\right] \tag{48}$$

The wave elevation may be expressed as:

$$\eta = h + S \tag{49}$$

where h is the height of the bottom of the circular cylinder above the mean water level and S is the depth of immersion of the cylinder .

Dividing both sides of the above expression by A, we get

$$\frac{\eta}{A} = \frac{h}{A} + \left(\frac{S}{D}\right)\left(\frac{D}{A}\right) \tag{50}$$

The hydrodynamic quantities describing the flow around a smooth, circular cylinder in steady currents depend on the Reynolds number. In the case where the cylinder is exposed to an oscillatory flow an additional parameter, the so-called Keulegan-Carpenter number, appears. The Keulegan-Carpenter number is defined by

$$KC = \frac{U_m T}{D} \tag{51}$$

in which U_m is the maximum velocity and T is the period of the oscillatory flow. This parameter expresses the amplitude of fluid motion relative to cylinder size. The magnitude of KC indicates the relative importance of drag and inertia forces (Keulegan & Carpenter, 1958).

Equation (40) can be simplified as:

$$a = \frac{2gA_i}{{U_m}^2 D} = \frac{2gTA_i}{U_m^2 DT} = \frac{2gTA_i}{\left(\frac{U_m T}{D}\right) D^2 U_m} \tag{52}$$

Combining Equations (51) and (52), we get

$$a = \frac{2gTA_i}{KCD^2 U_m} \tag{53}$$

From Equations (31) and (53), we get

$$a = \frac{2gTA_i}{KCD^2\left(\frac{2\pi A}{T}\right)} = \frac{2gT^2A_i}{2\pi AKCD^2} = \frac{gT^2A_i}{\pi AKCD^2} \tag{54}$$

From Equations (12) and (54), we get

$$a = \frac{gT^2}{8\pi AKC} f_1(\theta) \tag{55}$$

The wave form travels over the water surface, and the time for two consecutive crests to pass a point is the wave period. The speed of the wave form is called the velocity of propagation of wave. The classical theory of water waves shows that there is a relation between the velocity of wave propagation *V*, the wave length *L*, and the water depth *d*. This relation is given by (Muckle and Taylor, 1987):

$$V = \sqrt{\frac{gL}{2\pi}\tanh\frac{2\pi d}{L}} \tag{56}$$

Suppose the depth of water is $d = L/2$, then we get

$$V = \sqrt{\frac{gL}{2\pi}\tanh\pi}$$

It may be noted that $\tanh\pi$ is practically equal to unity. Thus, beyond depths of approximately half a wave length the influence of depth is unimportant. We can, therefore, write

$$V = \sqrt{\frac{gL}{2\pi}} \tag{57}$$

Putting $V = L/T$ in Equation (57), we get

$$\frac{L}{T} = \sqrt{\frac{gL}{2\pi}}$$

Simplifying the above expression, we get

$$L = \frac{gT^2}{2\pi} \tag{58}$$

Combining Equations (55) and (58), we get

$$a = \frac{L}{4AKC} f_1(\theta) \tag{59}$$

Equations (39), (46), (47) and (59) finally lead to the following expression for the coefficient of slamming:

$$C_S = \frac{L}{4AKC} f_1(\theta) - \frac{1}{4}\left[f_1(\theta) + f_2(\theta)\right]\left(\frac{D}{A}\right)\left(\frac{\eta}{A}\right) + f_3(\theta)\left[1 - \left(\frac{\eta}{A}\right)^2\right] \qquad (60)$$

The theoretical analysis presented above leads to two different expressions for the slamming coefficient. Equation (48) presents the first expression as a function of the Froude number whereas Equation (60) gives the second expression as a function of the Keulegan-Carpenter number.

It may be noted that the Froude number and the Keulegan-Carpenter number are two important dimensionless parameters associated with wave mechanics. These two parameters are used extensively in the design of offshore structures. Thus the expressions of the slamming coefficient which include the aforesaid dimensionless parameters are expected to be very useful in the analysis of wave impact forces on offshore structures.

CHAPTER 3

RESULTS AND DISCUSSION

A computer program is developed on the basis of the theoretical analysis presented in the preceding chapter. The program is written in Fortran 90/95 and executed on the personal computer. The computational results are plotted in terms of relevant non-dimensional parameters and interpreted with a view to explaining the salient features of wave impact forces on horizontal circular cylinders.

Figure 3 shows the variation of the non-dimensional immersed sectional area (A_i/D^2) of the horizontal circular cylinder as a function of relative submergence (S/D). The non-dimensional immersed sectional area is found to increase almost linearly with relative submergence, and attains a value of 0.785 when relative submergence is unity, that is, the cylinder is completely immersed.

Figure 4 shows the variation of the non-dimensional added mass [$m' = m/ (\rho D^2)$] of the circular cylinder as a function of relative submergence (S/D). It is observed that the non-dimensional added mass increases steadily with relative submergence and attains a value of 0.507 when relative submergence is unity.

Figure 5 shows the variation of the rate of change of added mass [$f_3(\theta) = 2 \frac{\partial m}{\partial s} / (\rho D)$] with relative submergence (S/D). It is observed that $f_3(\theta)$ attains a value of 3.142 when relative submergence is zero. However, $f_3(\theta)$ decreases rapidly as the relative submergence increases and attains the minimum value when relative submergence is 0.75, but it increases again with any further increase of relative submergence.

Figures 6 to 16 presents the variation of the slamming coefficient (C_S) with relative submergence (*S/D*) of the circular cylinder for nine different Froude numbers ($Fr =$ 0.4, 0.5, 0.6, 0.7, 0.8, 0.9, 1.0, 1.1 and 1.2). These results have been computed for a circular cylinder whose different diameter-to-wave amplitude ratios are (*D/A* = 0.1, 0.2, 0.3, 0.4, and 0.5) and the cylinder is placed at different heights (*h /A* = 0.0, 0.1, 0.2, 0.3, 0.4, and 0.5). It is observed that the value of the slamming coefficient decreases as the Froude number increases for any given value of relative submergence (*S/D*).

Figures 6*, 7, 8, 9* and 10 present the results for a cylinder whose diameter-to-wave amplitude ratio (*D/A*) is 0.1, 0.2, 0.3, 0.4 and 0.5 respectively. In all these cases the cylinder height-to-wave amplitude ratio (*h /A*) is equal to zero, which means that the bottom of the cylinder just touches the mean water level. It is also observed that as the *D/A* ratio increases the value of the slamming coefficient decreases with relative submergence and at the instant of impact, the slamming coefficient is approximately equal to 3.142 for all Froude numbers.

Figures 11, 12, 13, 14, 15 and *16* show the results when the cylinder height-to-wave amplitude ratio (*h/A*) is equal to 0.0, 0.1, 0.2, 0.3, 0.4, and 0.5 respectively. It is observed that the slamming coefficient decreases significantly as the height of the cylinder from the mean water level increases. These results are computed assuming that the diameter of the circular cylinder is 20% of the wave amplitude. Hence it may be treated as a slender structure. One of the important assumptions made in the analysis of the present problem is that the cylinder diameter is much smaller than the wave amplitude. The cylinder is placed horizontally at six different heights. In the highest position (*h/A* = 0.5), the height of the bottom line of the cylinder from the mean water level is 50% of the wave amplitude. It is interesting to note that the slamming coefficient is equal to 3.142 when the cylinder height-to-wave amplitude ratio is minimum (*h/A* = 0.0). This is true for all Froude numbers. On the other hand, the slamming coefficient is equal to 2.356 when the cylinder height-to-wave amplitude ratio (*h/A*) is equal to 0.5. It must be mentioned here that the values of the slamming coefficient mentioned above are attained at the instant of impact. It may be further noted that as the relative submergence of the cylinder increases, the value of the slamming coefficient sharply decreases at the beginning and then again increases. This sharp rate of decline of the slamming coefficient at the beginning indicates the impulsive nature of the slamming force. However, it is interesting to note that, the slamming coefficient curves remarkably diverge from one another as the relative submergence increases.

Figures 17 to 24 show the variation of the slamming coefficient $\left(C_S\right)$ with relative submergence (*S/D*) for six different values of *h/A* (*h/A* = 0.0, 0.1, 0.2, 0.3, 0.4 *and* 0.5), where *h* is the height of the bottom of the horizontal circular cylinder above the mean water level and *A* is the wave amplitude. It is observed that the diameter-to-wave amplitude ratio gradually increases from 0.1 to 0.45 for a fixed Froude number (*Fr* = 0.7). These figures are plotted to show the influence of the height of the horizontal cylinder on the slamming coefficient. It is also observed that, the value of the slamming coefficient decreases as *h/A* increases for any given value of relative submergence *(S/D).* Physically it means that, a horizontal cylinder will experience less wave impact force if it is fixed at a relatively higher location from the mean water level.

Figure 25 to 30 are plotted to show the variation of the slamming coefficient $\left(C_S\right)$ with relative submergence (*S/D*) for eight different diameter-to-wave amplitude ratios (*D/A* = 0.1, 0.15, 0.2, 0.25, 0.3, 0.35, 0.4 and 0.45). It is observed that the value of the slamming coefficient decreases as diameter-to-wave amplitude ratio (*D/A*) increases for any given value of relative submergence (*S/D*). It is also observed that the height-to-amplitude ratio gradually increases from 0.0 to 0.5 for a fixed Froude number (*Fr* = 0.7) and the initial value of slamming coefficient changes with *h/A*. As the height-to-amplitude ratio increases the value of the slamming coefficient decreases.

Figure 31 shows the variation of the slamming coefficient $\left(C_S\right)$ with relative submergence *(S/D).* These results have been computed using Equation (48). A comparison of the experimental results of Sarpkaya (1978) and the present theoretical results is shown in this figure. It is clearly observed from this figure that the slamming coefficient and consequently the impact force, is of an impulsive nature beginning with a high value at the instant of impact. It is interesting to note that the theoretical and experimental curves intersect at three different points (*S/D* = 0.05, 0.55 and 0.85). Since viscous forces are neglected in the present analysis, one would expect the solution to deviate from the actual situation as the cylinder becomes more fully immersed. A good agreement is found between the two results for small values of relative submergence up to 0.06 and again from 0.55 to 0.85, beyond which the two curves diverge from each other.

Figure 32 is plotted to show the variation of the slamming coefficient (C_S) as a function of the Froude number. Sarpkaya (1978) conducted slamming experiments with harmonically oscillating flow impacting a horizontal cylinder and presented the values of the slamming coefficient (C_S) at various Froude numbers. The present theoretical results of wave slamming coefficient are compared with those of Sarpkaya (1978), as shown in *Figure 33*. It is interesting to note that the theoretical and experimental curves show the same trend with regard to the variation of the slamming coefficient as a function of the Froude number.

Figure 33 shows the variation of the slamming coefficient (C_S) with relative submergence *(S/D).*These results have been computed using equation (48). It is interesting to note that the curves of the present theoretical value and Sarpkaya's theoretical value are very close to each other and the two curves are almost the same trend. Since viscous forces are neglected in the present analysis, one would expect the solution to deviate from the actual situation as the cylinder becomes more fully immersed. A comparison of the theoretical results of Sarpkaya (1978) and the present theoretical results is shown in this Figure. This figure shows that the value of the slamming coefficient curve decreases with the increase of relative submergence up to 0.6 and again increases.

Figures 34 to 48 present the variation of the slamming coefficient (C_S) with relative submergence (S/*D*) of the circular cylinder for seven different Keulegan-Carpenter numbers (*KC* = 11.0, 11.5, 12.0, 12.5, 13.0, 13.5, and 14.0). These results have been computed for circular cylinders whose diameter-to-amplitude ratios (*D/A*) are 0.1, 0.2, 0.3, 0.4 and 0.5 and the cylinder is placed at different heights (*h /A* = 0.0, 0.1, 0.2, 0.3, 0.4 and 0.5). The corresponding wave length-to-amplitude ratios (*L/A*) are 80, 90, 100 and

110. It is observed that the value of the slamming coefficient decreases as the Keulegan-Carpenter number increases for any given value of relative submergence (*S/D*). At the instant of impact, the slamming coefficient is equal to 3.142 for all the Keulegan-Carpenter numbers. But as the relative submergence of the cylinder increases, the value of the slamming coefficient sharply decreases. The sharp rate of decline of the slamming coefficient curve with the increase of relative submergence indicates the impulsive nature of the slamming force. However, it is interesting to note that the slamming coefficient curves notably diverge from one another as the relative submergence increases. It is also observed that the slamming coefficient attains a maximum value when the Keulegan-Carpenter number is minimum and then it decreases continuously as the Keulegan-Carpenter number increases.

Figures 34, 35, 36, 37 and *38* present the results for a cylinder whose diameter-to-wave amplitude ratios (*D/A*) are 0.1, 0.2, 0.3, 0.4 and 0.5 respectively. In all these cases the cylinder height-to-wave amplitude ratio (*h /A*) is equal to zero and wave length-to-amplitude ratio is 85. The cylinder height-to-wave amplitude ratio is equal to zero implies that the bottom of the cylinder just touches the mean water level. It is also observed that as the cylinder diameter-to-wave amplitude ratio increases the value of the slamming coefficient decreases with the relative submergence. However, at the instant of impact the slamming coefficient is approximately equal to 3.142 for all Keulegan-Carpenter numbers.

Figures 39, 40, 41 and *42* present the results for a cylinder whose wave length-to-amplitude ratios are 80, 90, 100 and 110 respectively. In all these cases the cylinder height-to-wave amplitude ratio (*h /A*) is equal to zero and diameter-to-wave amplitude ratio (*D/A*) is 0.2. It is also observed that as the wave length-to-amplitude ratio increases the value of the slamming coefficient decreases with relative submergence. It is interesting to note that at the instant of impact, the slamming coefficient is also approximately equal to 3.142 for all wave length-to-amplitude ratios and all Keulegan-Carpenter numbers.

Figures 43, 44, 45, 46, 47 and *48* show the results when the cylinder height-to-wave amplitude ratio (*h/A*) is equal to 0.0, 0.1, 0.2, 0.3, 0.4, and 0.5 respectively. It is observed that the slamming coefficient decreases significantly as the height of the cylinder from the mean water level increases. These results are computed assuming that the wave length-to-amplitude ratio is 85 and the diameter of the circular cylinder is 20% of the wave amplitude. Hence it may be treated as a slender structure. One of the important assumptions made in the analysis of the present problem is that the cylinder diameter is much smaller than the wave amplitude. The cylinder is placed horizontally at six different heights. In the highest position (*h/A* = 0.5), the height of the bottom line of the cylinder from the mean water level is 50% of the wave amplitude. It is interesting to note that the slamming coefficient is equal to 3.142 when the cylinder height-to-wave amplitude ratio is minimum (*h/A* = 0.0). This is true for all Keulegan-Carpenter numbers. On the other hand, the slamming coefficient is equal to 2.356 when the cylinder height-to-wave amplitude ratio (*h/A*) is equal to 0.5. It must be mentioned here that the values of the slamming coefficient mentioned above are attained at the instant of impact. It may be further noted that as the relative submergence of the cylinder increases, the value of the slamming coefficient sharply decreases at the beginning and then increases again. This sharp rate of decline of the slamming coefficient at the beginning indicates the impulsive nature of the slamming force. However, it must be pointed out that the slamming coefficient curves notably diverge from one another as the relative submergence increases.

Figures 49 to 61 are plotted to show the variation of the slamming coefficient $\left(C_S\right)$ with relative submergence (*S/D*) for seven different values of cylinder diameter-to-wave amplitude ratios (*D/A* = 0.1, 0.15, 0.2, 0.25, 0.3, 0.35 and 0.4) when cylinder height-to-wave amplitude ratio (*h/A*) varies from 0.0 to 0.5, wave length-to-amplitude ratio (*L/A*) varies from 80 to 110 and Keulegan-Carpenter number (*KC*) is equal to 11. It is observed that the value of the slamming coefficient decreases as the cylinder diameter-to-wave amplitude ratio increases for any given value of relative submergence. Similarly, the slamming coefficient decreases as the cylinder height-to-wave amplitude ratio (*h/A*) increases. Furthermore, as the wave length-to-amplitude ratio increases the value of the slamming coefficient decreases.

Figures 62 to 75 show the variation of the slamming coefficient $\left(C_S\right)$ with relative submergence (*S/D*) for six different values of cylinder height-to-wave amplitude ratio (*h/A* = 0.0, 0.1, 0.2, 0.3, 0.4 and 0.5). In *Figures 62 to 68* the cylinder diameter-to-wave amplitude ratio varies from 0.1 to 0.4 and in *Figures 69 to 75* wave length-to-amplitude ratio varies from 80 to 110. These figures are plotted to show the influence of the height of the horizontal cylinder on the slamming coefficient. It is observed that the value of the slamming coefficient decreases as *h/A* increases for any given value of relative submergence. Physically, it means that a horizontal cylinder will experience less wave impact force if it is fixed at a relatively higher location from the mean water level. However, it is interesting to note that the slamming coefficient curves converge to one another as the relative submergence *(S/D)* increases.

Figures 76 to 82 are plotted to show the variation of the slamming coefficient $\left(C_S\right)$ with relative submergence (*S/D*) for seven different values of wave length-to-amplitude ratio (*L/A* = 80, 85, 90, 95, 100, 105 and 110) when cylinder diameter-to-wave amplitude ratio varies from 0.1 to 0.4. All the slamming coefficient curves are obtained for Keulegan-Carpenter number, *KC* = 11 and cylinder height-to-wave amplitude ratio, *h/A* = 0.0. These curves are found to converge at one point (C_S = 3.142) at the initial impact, when *S/D* = 0, and then diverge from one another as the relative submergence increases. Furthermore, the slamming coefficient is found to increase continuously as the wave length-to-amplitude ratio (*L/A*) increases.

As it was mentioned in the introduction, various analytical and experimental studies have been carried out in order to establish the appropriate values of the maximum slamming coefficient for the common case of a horizontal circular cylinder. The present authors have gone through all the papers and compiled the values of the slamming coefficient as reported by different researchers. Table 1 shows a comparison of the results obtained from the present theoretical model with those of previous researchers.

Table 1. Values of the slamming coefficient obtained by different researchers

Investigators (year)	Nature of investigation	Value of the slamming coefficient
Fabula (1957)	Theoretical	C_S^0 = 6.28
Dalton and Nash (1976)	Experimental	C_S^0 = 1.0 - 6.4
Kaplan and Silbert (1976)	Theoretical	C_S^0 = 3.14
Holmes et al. (1976)	Experimental	C_S^0 = 0.4 - 2.9

Faltinsen et al. (1977)	Theoretical Experimental	C_S^0 = 3.14 C_S^0 = 4.1 - 6.4
Miller (1977)	Experimental	C_S^0 = 1.0 - 6.4
Srpkaya (1978)	Theoretical Experimental	C_S^0 = 3.14 C_S^0 = 1.57 - 5.34
Arhan et al. (1978)	Experimental	C_S^0 = 2.4 - 6.9
Campbell and Weynberg (1980)	Experimental	C_S^0 = 1.0 – 6.4
Armand and Cointe (1986)	Theoretical	C_S^0 = 6.28
Miao (1988)	Experimental	C_S^0 = 6.1
Isaacson and Prasad (1992)	Experimental	C_S^0 = 1.0 - 6.4
Present study (2011)	Theoretical	C_S^0 = 3.142

It is observed that the value of the slamming coefficient at the instant of impact (C_S^0) obtained from the present theoretical model is equal to 3.142 which is exactly the same as those found by Kaplan and Silbert (1976), Faltinsen et al. (1977) and Sarpkaya (1978). However, experimental studies have yielded values of C_S^0 which exhibits a considerable degree of scatter, ranging from about 1.0 to 6.4 (Dalton and Nash, 1976; Miller, 1977; Sarpkaya, 1978; Campbell and Weynberg, 1980 and Isaacson and Prashad, 1992). Thus the present theoretical model yields a value of the initial slamming coefficient which agrees well with the theoretical and experimental results of previous researchers.

CHAPTER 4

CONCLUSIONS

This thesis presents a two-dimensional analysis of the hydrodynamic forces acting on a fixed, horizontal circular cylinder in the vicinity of the free surface, taking account of the intermittent submergence and wave slamming. The theoretical analysis and computational results lead to several important conclusions which may be summarized as follows:

(a) Two new expressions are derived for the slamming coefficient, the first expression as a function of the Froude number and the second expression as a function of the Keulegan-Carpenter number. The Froude number and the Keulegan-Carpenter number are two important dimensionless parameters associated with wave mechanics. These two parameters are used extensively in the design of offshore structures. Thus the expressions of the slamming coefficient which include the aforesaid dimensionless parameters are expected to be very useful in the analysis of wave impact forces on offshore structures.

(b) The non-dimensional added mass (m') of the circular cylinder is observed to increase steadily with relative submergence (S/D).

(c) The rate of change of added mass $f_3(\theta)$ of the circular cylinder attains a value of 3.142 when relative submergence (S/D) is equal to zero. However, $f_3(\theta)$ decreases rapidly as the relative submergence increases and attains the minimum value when S/D = 0.75, but then it increases again with any further increase of relative submergence.

(d) The slamming coefficient can be expressed through the diameter of the circular cylinder, wave amplitude, depth of immersion of the cylinder, instantaneous height of the surface wave above the mean water level and the added mass per unit length of the cylinder.

(e) At the instant of impact, the slamming coefficient (C_S^0) is equal to 3.142 for all Froude numbers and Keulegan-Carpenter numbers. But as the relative submergence of the cylinder increases, the value of the slamming coefficient sharply decreases at the beginning and then increases again. The sudden decline of the slamming coefficient after the initial impact indicates the impulsive nature of the slamming force. The slamming coefficient attains a maximum value when the Froude number or Keulegan-Carpenter number are minimum and then it decreases continuously as these two numbers increase.

(f) The slamming coefficient decreases as the height of the circular cylinder from the mean water level increases. Physically, it means that a horizontal circular cylinder experiences a greater wave impact force if it is located at a relatively lower position from the mean water level.

(g) It is necessary to mention that the proposed theoretical model has been developed without taking viscosity into account. But water is a viscous fluid. This is why some differences are observed between the present theoretical results and previously published experimental data. Evidently, the predictions of the present theoretical model are not valid beyond very small values of relative submergence.

(h) The slamming coefficient, and consequently the impact force, is of an impulsive nature beginning with a finite value (equal to 3.142) at the instant of impact. Since viscous forces are neglected in the analysis of impact forces, one would expect the solution to deviate from the actual situation as the cylinder becomes more deeply immersed. Where this becomes the case the slamming coefficient can only be determined experimentally.

(i) The present theoretical model predicts the slamming coefficient for a horizontal circular cylinder from the instant of impact to full immersion. In order to check the validity of the present theoretical model, the computational results are compared with the theoretical and experimental results of other investigators and satisfactory agreement is found for small values of relative submergence.

REFERENCES

Arhan, M., Deleuil, g., and Doris, C.G. (1978): Experimental study of the impact of horizontal cylinders on a wave surface, *Proceedings of the 10th Offshore Technology Conference,* Houston, Texas, Paper No. OTC 3107, Vol. 1, pp. 485-492.

Armand, J.L. and Cointe, R. (1986): Hydrodynamic impact analysis of a cylinder, *Proceedings of the 5th International Conference on Offshore Mechanics and Arctic Engineering, Vol. 1*, pp. 250-256.

Campbell, I.M.C. and Weynberg, P.A. (1980): *Measurement of Parameters Affecting Slamming*, Report No. 440, Wolfson Unit for Marine Technology and Industrial Aerodynamics, University of Southampton.

Chan, E.S., Cheong, H.F. and Gin, K.Y.H. (1991): Wave impact loads on horizontal structures in the splash zone, *Proc. ISOPE '91*, Edinburgh, 3, pp. 203-209.

Cointe, R. and Armand, J.L. (1987): Hydrodynamic impact analysis of a cylinder, *J. Offshore Mechanics and Arctic Enginering*, *Vol. 109*, pp. 237-243.

Cortel, C. and Grilli, S.T. (2006): Numerical modeling of extreme wave slamming on cylindrical offshore support structures, *Proceedings of the Sixteenth International Offshore and Polar Engineering Conference*, San Francisco, California, USA, May 28-June 2, 2006.

Dalton, C. and Nash, J.M. (1976): Wave slam on horizontal members of an offshore platform, *Proceedings of Offshore Technology Conference*, Houston, Texas, Paper No. OTC 2500, pp. 769-780.

Fabula, A.G. (1957): Ellipse-fitting approximation of two-dimensional normal symmetric impact of rigid bodies on water, *Proceedings of the 5th Midwestern Conference on Fluid Mechanics*, University of Michigan Press, Ann Arbor, Michigan.

Faltinsen, O., Kjaerland, O., Nottveit, A. and Vinje, T. (1977): Water impact loads and dynamic response of horizontal circular cylinder in offshore structures, *Proceedings of Offshore Technology Conference*, Houston, Texas, Paper No. OTC 2741, pp. 119-126.

Greenhow, M. and Li, Y. (1987): Added masses for circular cylinders near or penetrating fluid boundaries--Review, extension and application to water-entry, exit and slamming, *Ocean Engineering, Vol.14, No. 4*, pp. 325-348.

Holmes, P., Chaplin,J.R. and Filld, C. (1976): Wave Slamming Loads on Horizontal Members. Department of Energy Report OT-R-7706.

Isaacson, M. and Prasad, S. (1992): Wave slamming on a horizontal circular cylinder, *Proceedings of Civil Engineering in Oceans V,* ASCE, College Station, Texas, pp. 652-666.

Isaacson, M, and Prasad S (1994): Wave slamming on a horizontal circular cylinder, *International Journal of Offshore and Polar Engineering, Vol. 4, No. 2*, pp. 81-88.

Isaacson, M. and Subbiah, K. (1990): Random wave slamming on cylinders, *Journal of Waterway, Port, Coastal, and Ocean Engineering, Vol. 116, No. 6,* pp. 742-763.

Kaplan, P. and Silbert, M.N. (1976): Impact forces on platform horizontal members in the splash zone, *Proceedings of Offshore Technology Conference*, Houston, Texas, May 3-6, 1976, Paper No. OTC 2498, pp. 749-758.

Kaplan, P. (1957): Application of slender body theory to forces acting on submerged bodies and surface ships in regular waves, *Journal of Ship Research, Vol. 1, No. 3*.

Kaplan, P. (1979): Impact forces on horizontal members, *Proceedings of Civil Engineering in the Oceans, IV*, ASCE, San Francisco, California, 2, pp. 716-731.

Kaplan, P. and Hu, P.N. (1959): Virtual mass and slender body theory for bodies in waves, *Proceedings of the Sixth Annual Conference on Fluid Mechanics*, University of Texas, September 1959.

Keulegan, G.H. and Carpenter, L.H. (1958): Forces on cylinders and plates in an oscillating fluids, *J. Res. Nat. Bureau of Standards, Vol. 60, No. 5*, pp. 423-440.

Khalil, G.M. and Ali, M.T. (1994): An investigation into wave slamming loads on horizontal circular cylinders, *Journal of the Institution of Engineers Malaysis, Volume 55,* pp. 19-28.

Khalil, G.M., Tarafder, M.S. and Akter, S. (2009): Wave slamming on a horizontal circular cylinder located above still water level, *The Journal of NOAMI*, *Volume 26, Number 2,* pp. 21-38.

Miao, G. (1990): Dynamic response of elastic horizontal circular cylinders by wave slamming, *Proceedings of 9th International Conference on Offshore Mechanics and Arctic Engineering*, *Vol. 1*, pp. 239-245.

Miao, G. (1988): Hydrodynamic Forces and Dynamic Response of Circular Cylinders in Wave Zones. Ph.D thesis, University of Trondheim, Norway.

Miller, B.L. (1977): Wave slamming loads on horizontal circular elements of offshore structures, Paper presented at a meeting of the Royal Institution of Naval Architects, London on April 6, pp. 81-98.

Miller, B.L. (1980): *Wave Slamming on Offshore Structures*, Report No. NMI-R81, National Maritime Institute, Feltham, Middlesex, UK.

Moran, J.P. (1965): *On the Hydrodynamic Theory of Water-Exit and Entry*, Thermodynamic Advanced Research Report, TAR-TR-6501.

Morison, J.R., O'Brien, M.P., Johnson, J.W. and Schaaf, S.A. (1950): The force exerted by surface waves on piles, *Petroleum Transactions*, American Institute of Mining Engineering, *Vol. 189*, pp. 149-154.

Muckle, W. and Taylor, D.A. (1987): *Muckle's Naval Architecture, Second Edition*, Butterworths, London, pp.150-151.

Sarpkaya, T (1978): Wave impact loads on cylinders, *Proceedings of Offshore Technology Conference*, Paper No. OTC 3065, Houston.

Smirnov, V. I. (1964), *A Course of Higher Mathematics, Vol. 1*, Pergamon Press, London, pp. 153-155.

Szebehely, V.G. (1959): Hydrodynamic impact, *Applied Mechanics Reviews, Vol. 12, No. 5*, pp. 297-300.

Taylor, J. L. (1930): Some Hydro-dynamical inertia coefficients, *Philosophical Magazine, Series 7, Vol. 9, No. 55*, pp. 161-183.

von Karman, T. and Wattendorf, P.L. (1929): *The Impact on Seaplane Floats During Landing, TN 321*, U.S. National Advisory Committee for Aeronautics, Washington, October.

Wagner, H. (1931): *Landing of Seaplanes*, *TN 622*, U.S. National Advisory Committee for Aeronautics, Washington, May.

Zylinski, B. (2009): Finite element local analysis of wave slamming on offshore structure, *Polish Maritime Research, Vol. 16*, pp. 8-12.

FIGURES

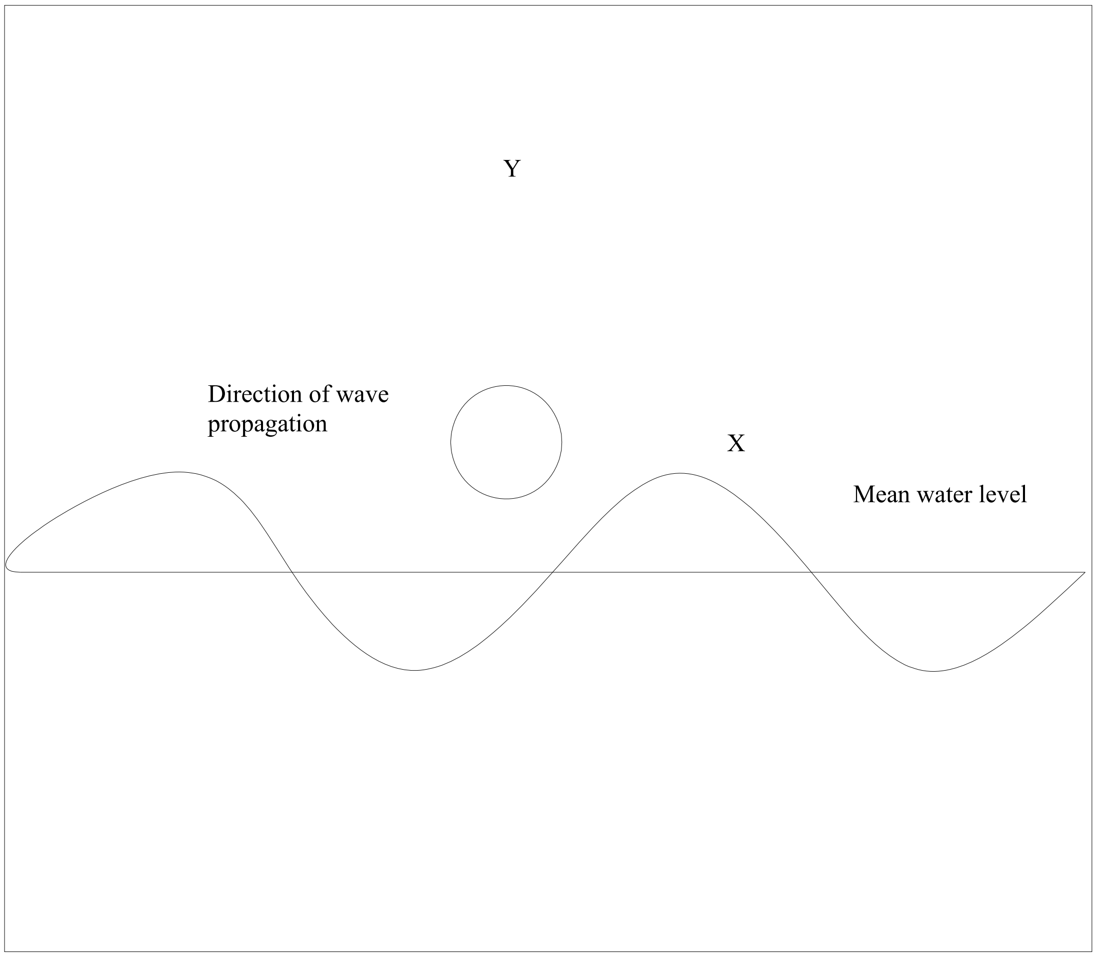

Figure 1. Schematic diagram of a horizontal circular cylinder in the splash zone.

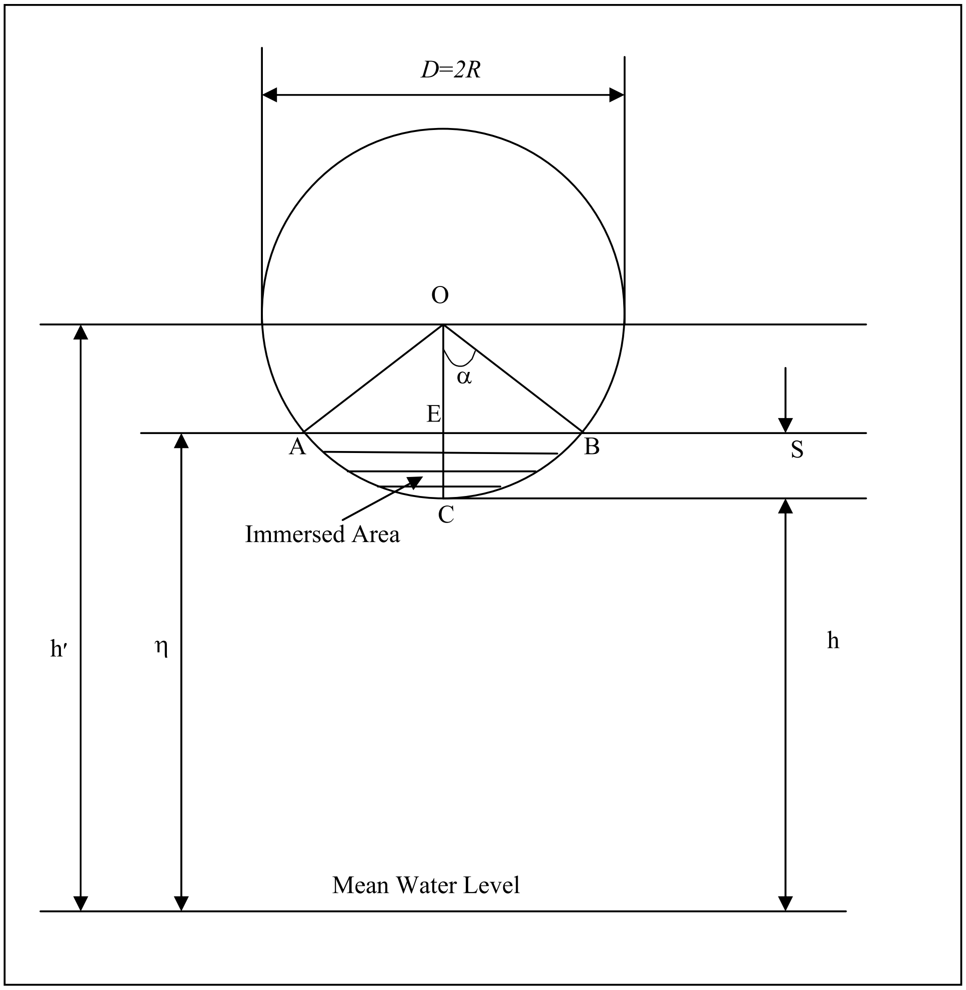

Figure 2. Definition sketch for the analysis of the problem

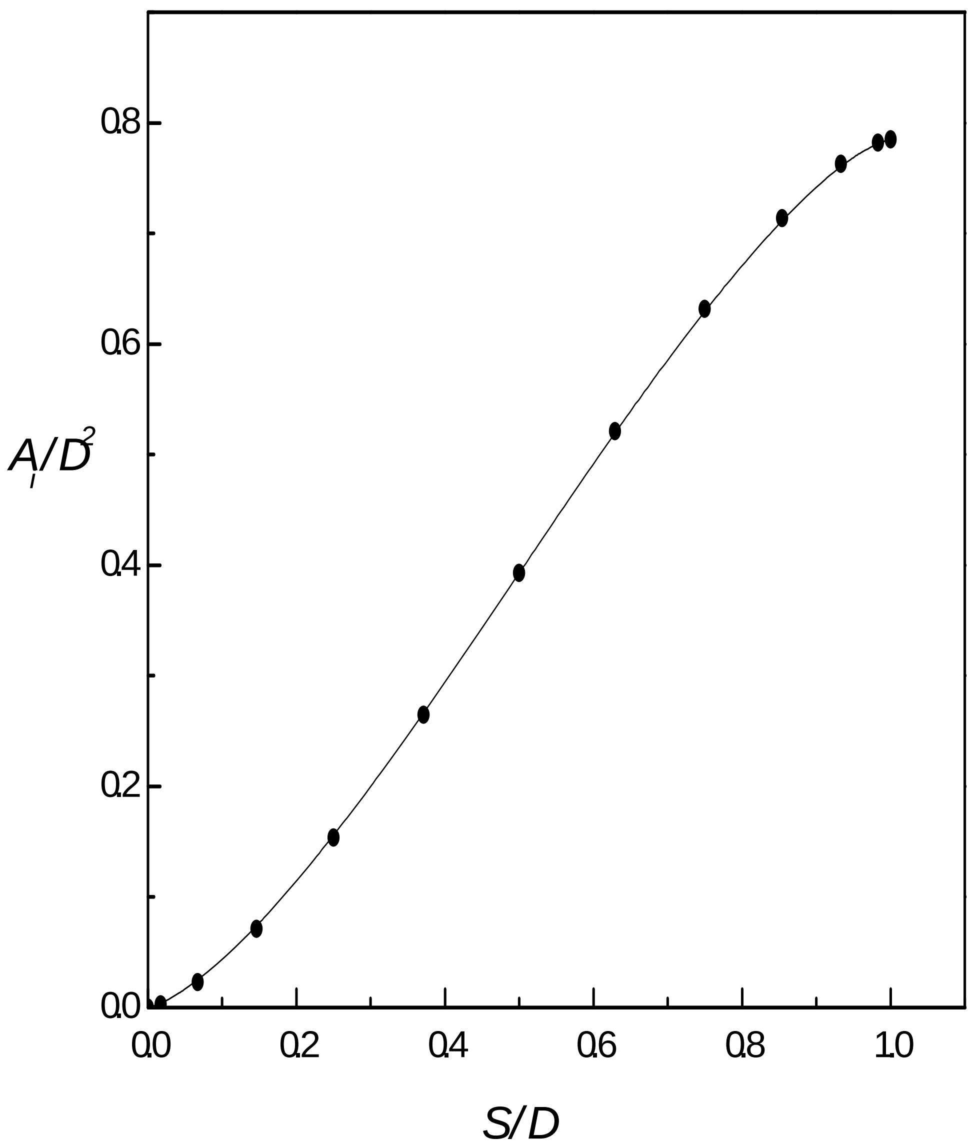

Figure 3. Variation of the non-dimensional immersed area ($A_i\ /D^2$) with relative submergence (*S/D*).

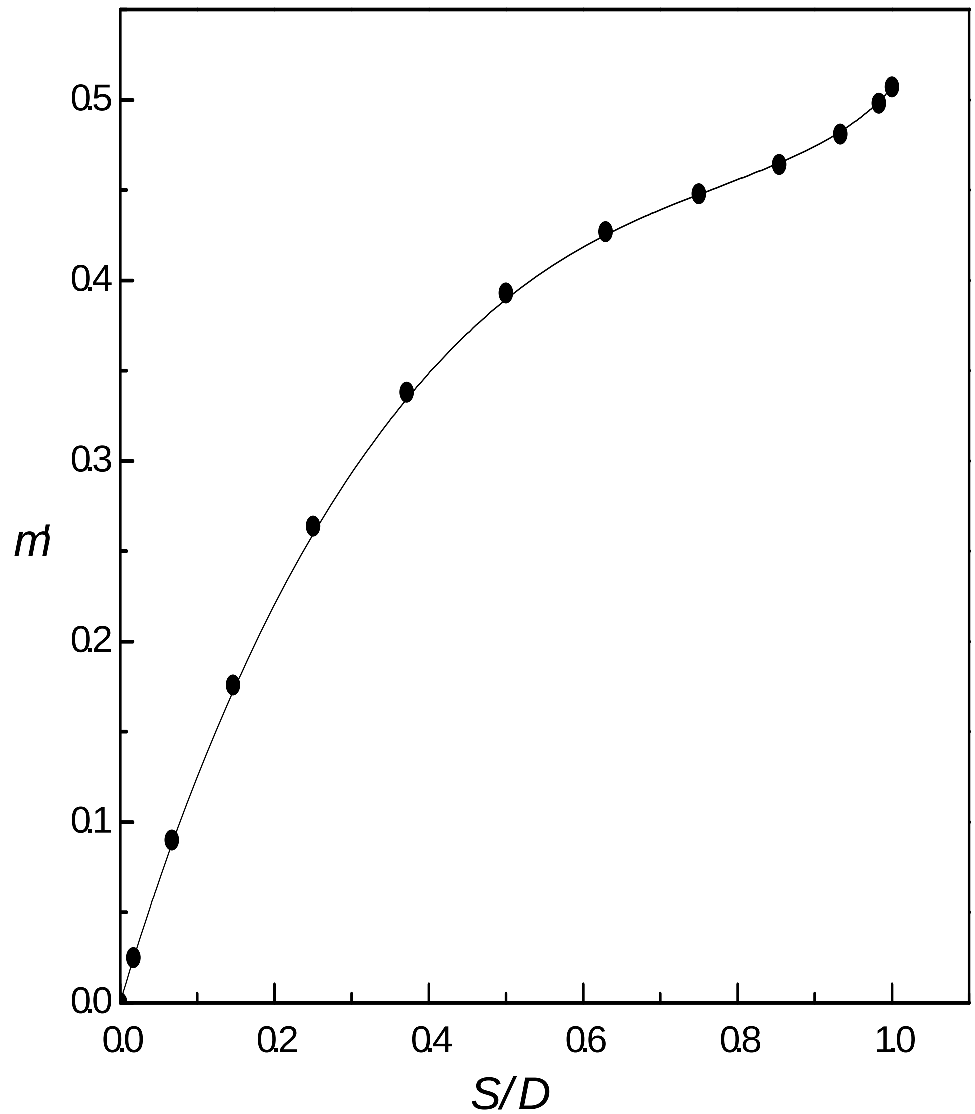

Figure 4. Variation of the non-dimensional added mass [$m' = m/(\rho D^2)$] with relative submergence (*S/D*).

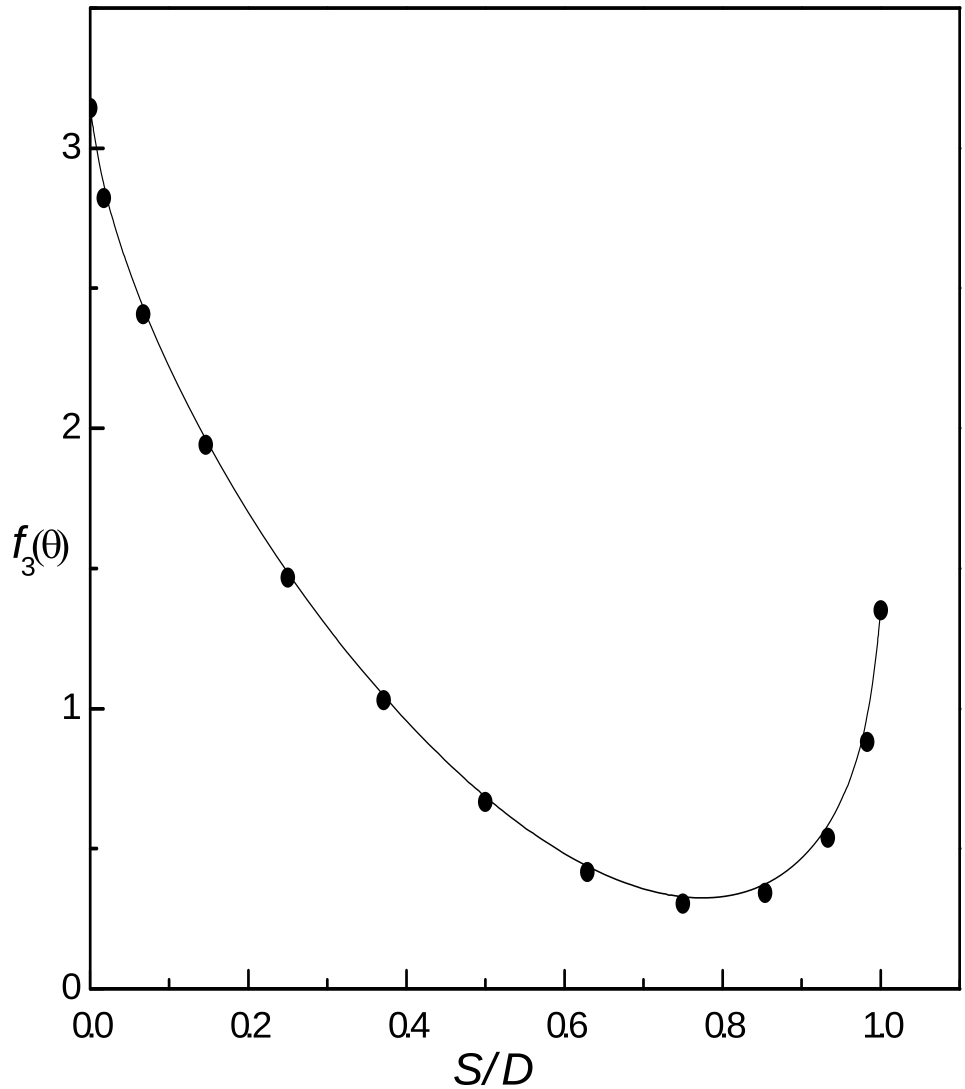

Figure 5. Variation of the rate of change of added mass [$f_3\ (\theta) = 2\frac{\partial m}{\partial s} / (\rho D)$] with relative submergence (S/D).

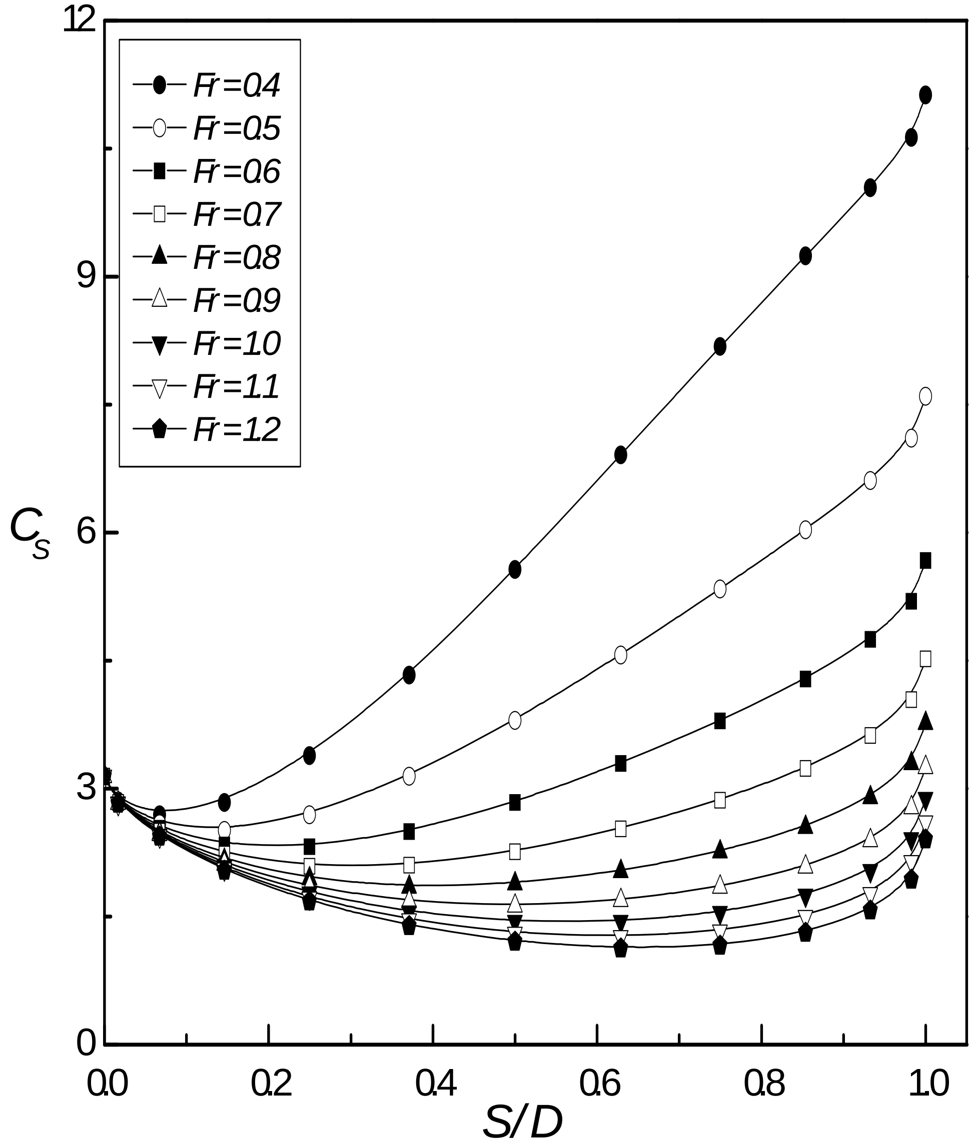

Figure 6. Variation of the slamming coefficient (C_s) with relative submergence (*S/D*) for different Froude numbers (*Fr*) when the cylinder diameter-to-wave amplitude ratio (*D/A*) is 0.1and height-to-wave amplitude ratio (*h/A*) is 0.0.

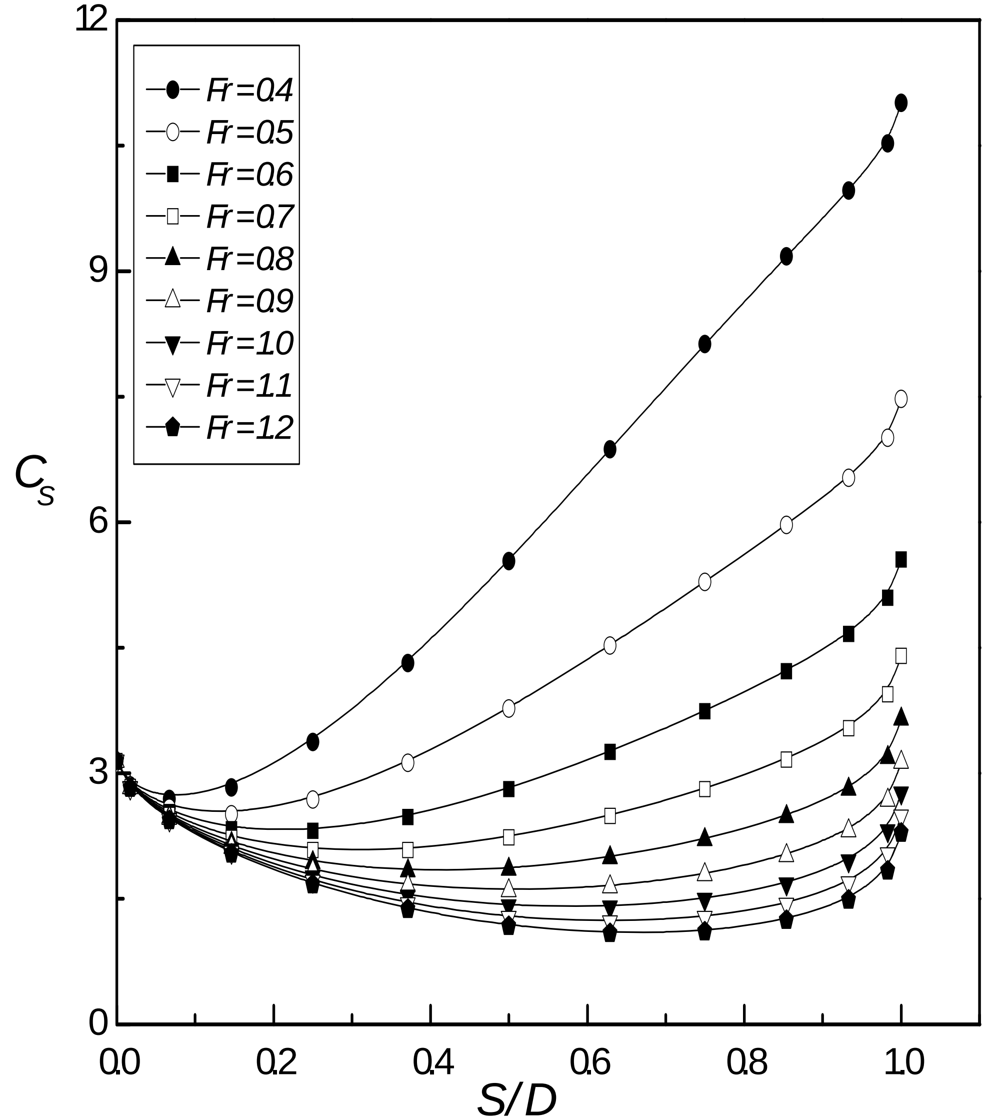

Figure 7. Variation of the slamming coefficient (C_s) with relative submergence (*S/D*) for different Froude numbers (*Fr*) when the cylinder diameter-to-wave amplitude ratio (*D/A*) is 0.2 and height-to-wave amplitude ratio (*h/A*) is 0.0.

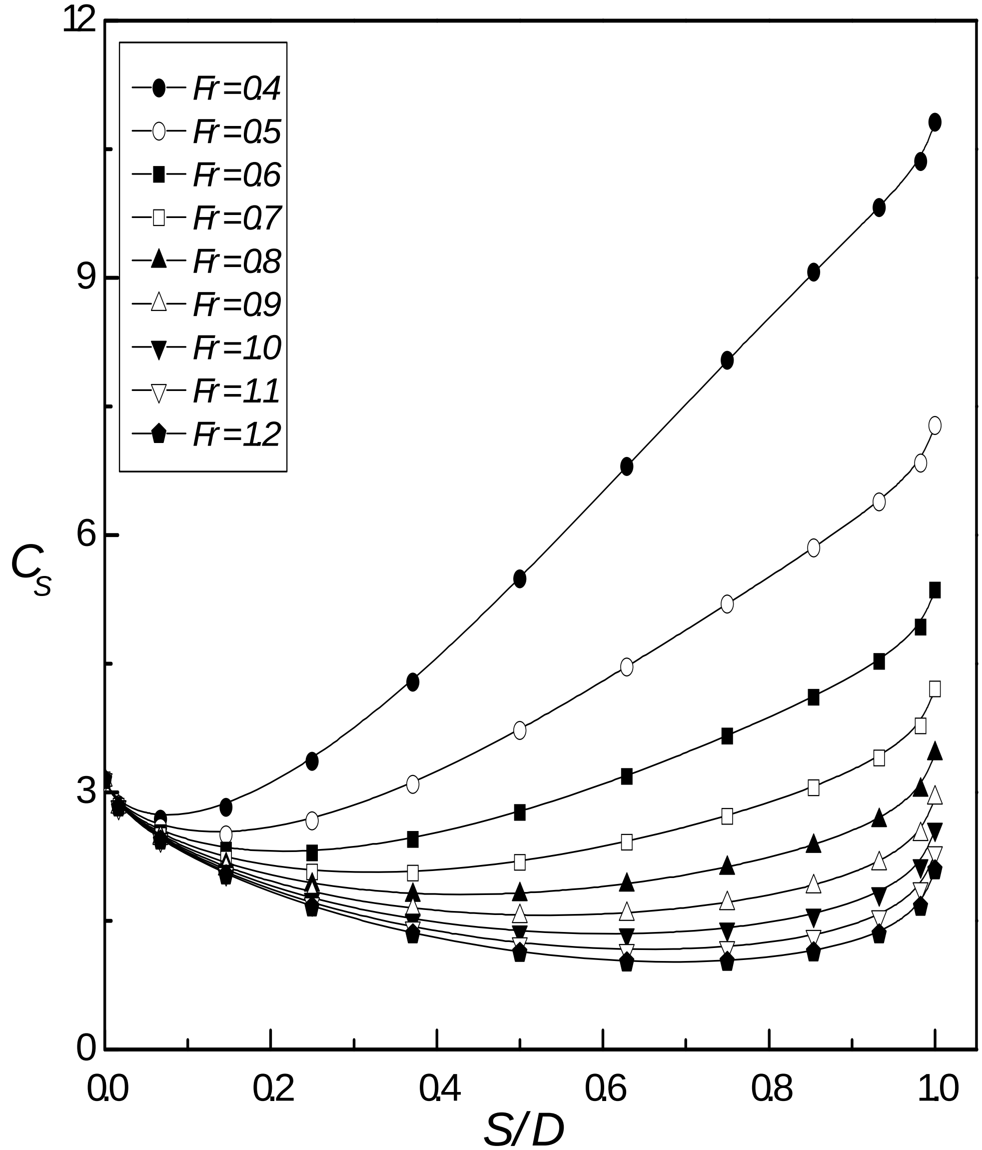

Figure 8. Variation of the slamming coefficient (C_s) with relative submergence (*S/D*) for different Froude numbers (*Fr*) when the cylinder diameter-to-wave amplitude ratio (*D/A*) is 0.3 and height-to-wave amplitude ratio (*h/A*) is 0.0.

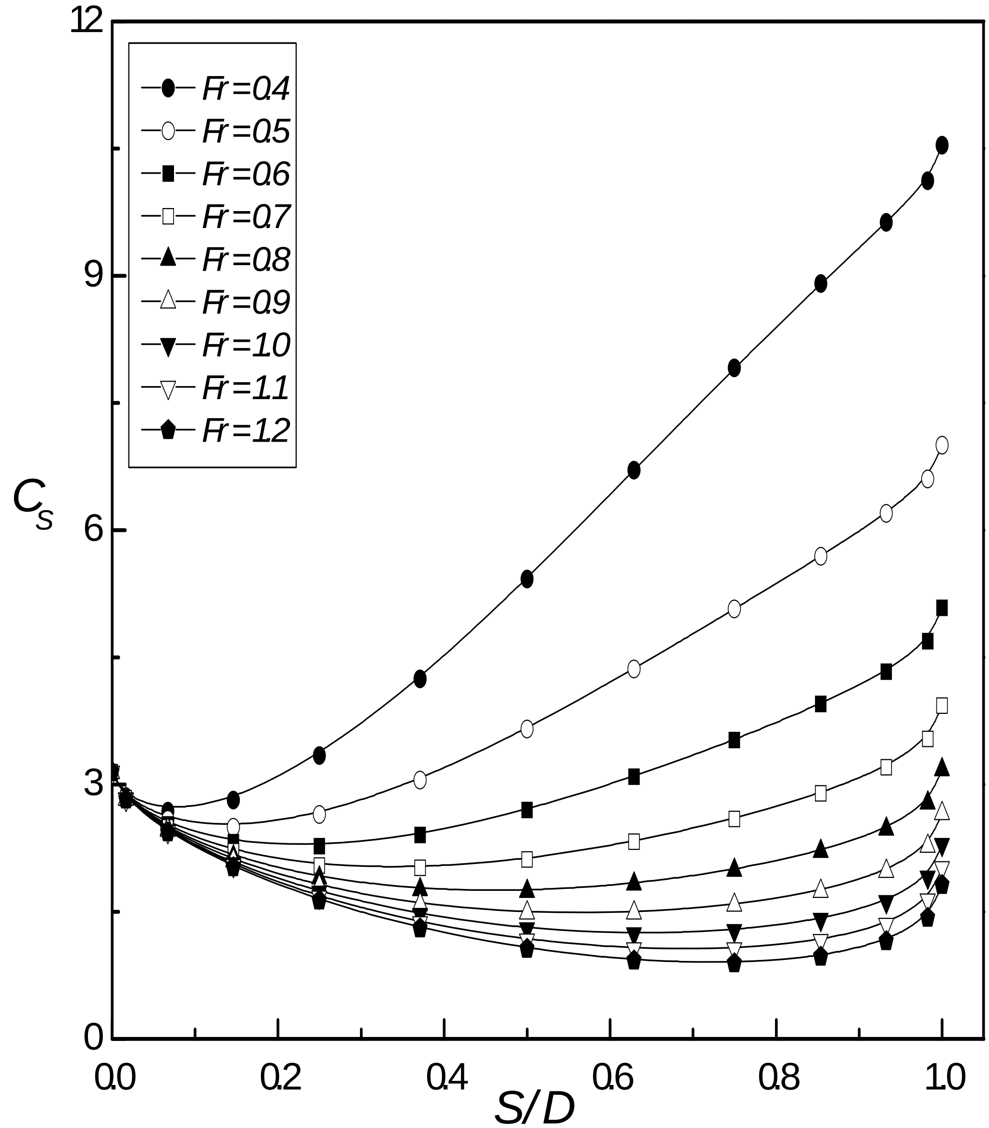

Figure 9. Variation of the slamming coefficient (C_s) with relative submergence (*S/D*) for different Froude numbers (*Fr*) when the cylinder diameter-to-wave amplitude ratio (*D/A*) is 0.4 and height-to-wave amplitude ratio (*h/A*) is 0.0.

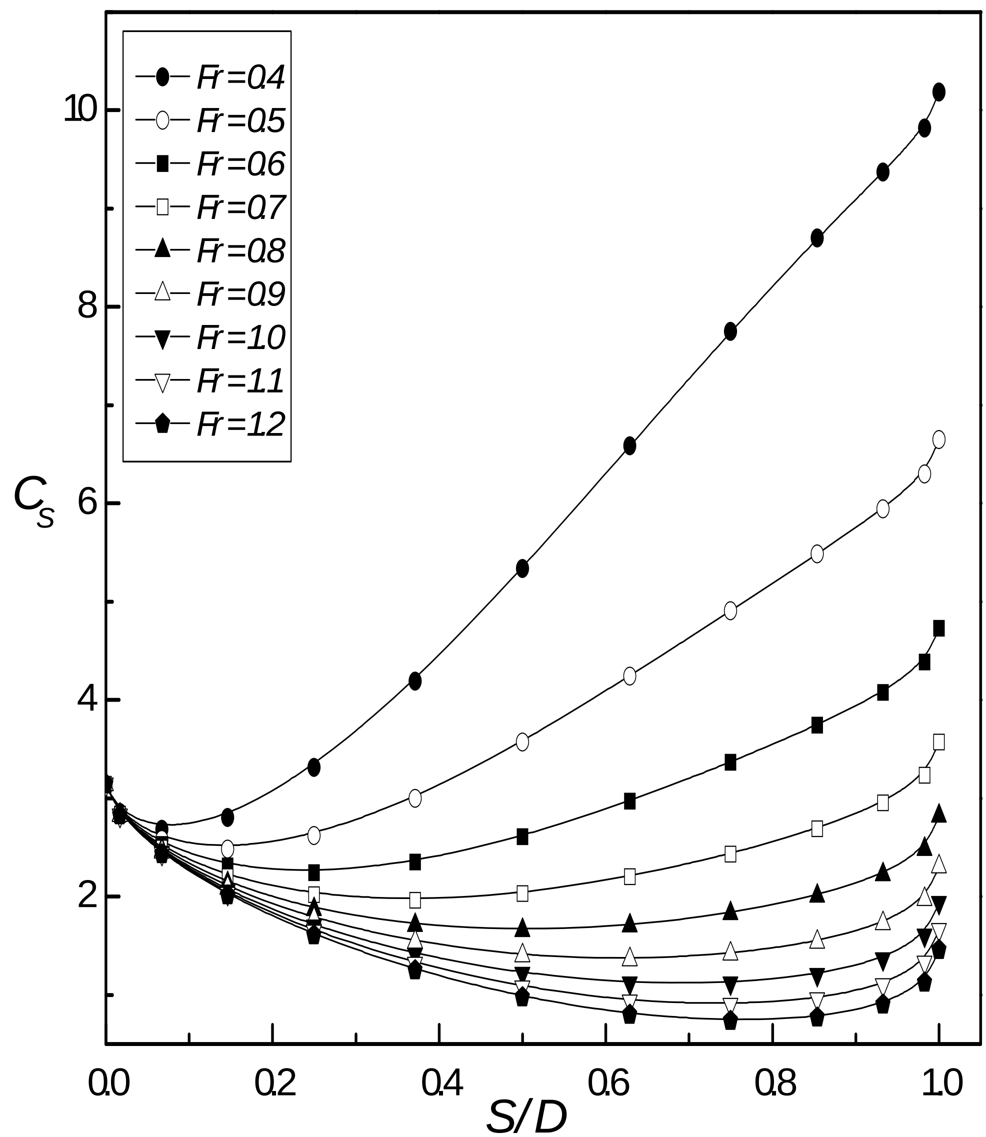

Figure 10. Variation of the slamming coefficient (C_s) with relative submergence (*S/D*) for different Froude numbers (*Fr*) when the cylinder diameter-to-wave amplitude ratio (*D/A*) is 0.5 and height-to-wave amplitude ratio (*h/A*) is 0.0.

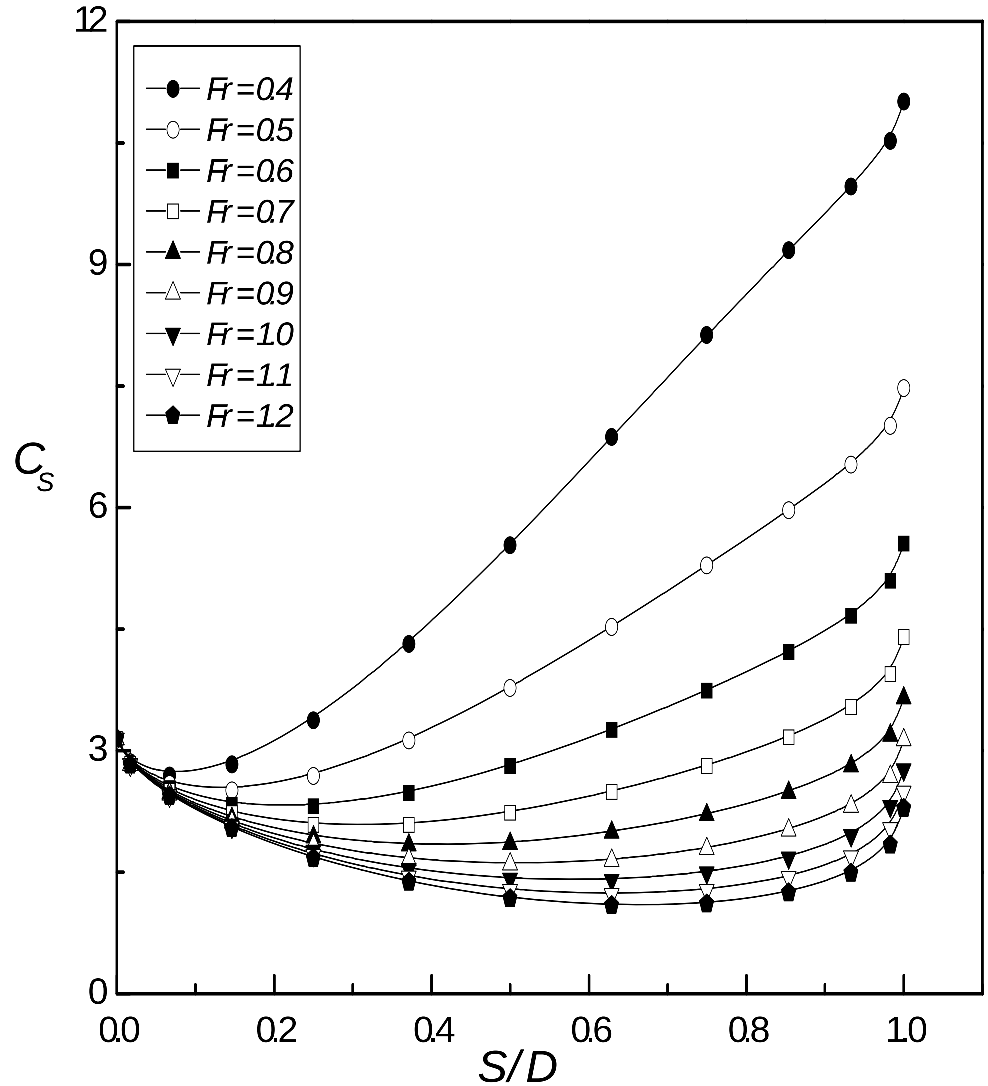

Figure 11. Variation of the slamming coefficient (C_s) with relative submergence (*S/D*) for different Froude numbers (*Fr*) when the cylinder height-to-wave amplitude ratio (*h/A*) is 0.0 and diameter-to-wave amplitude ratio (*D/A*) is 0.2.

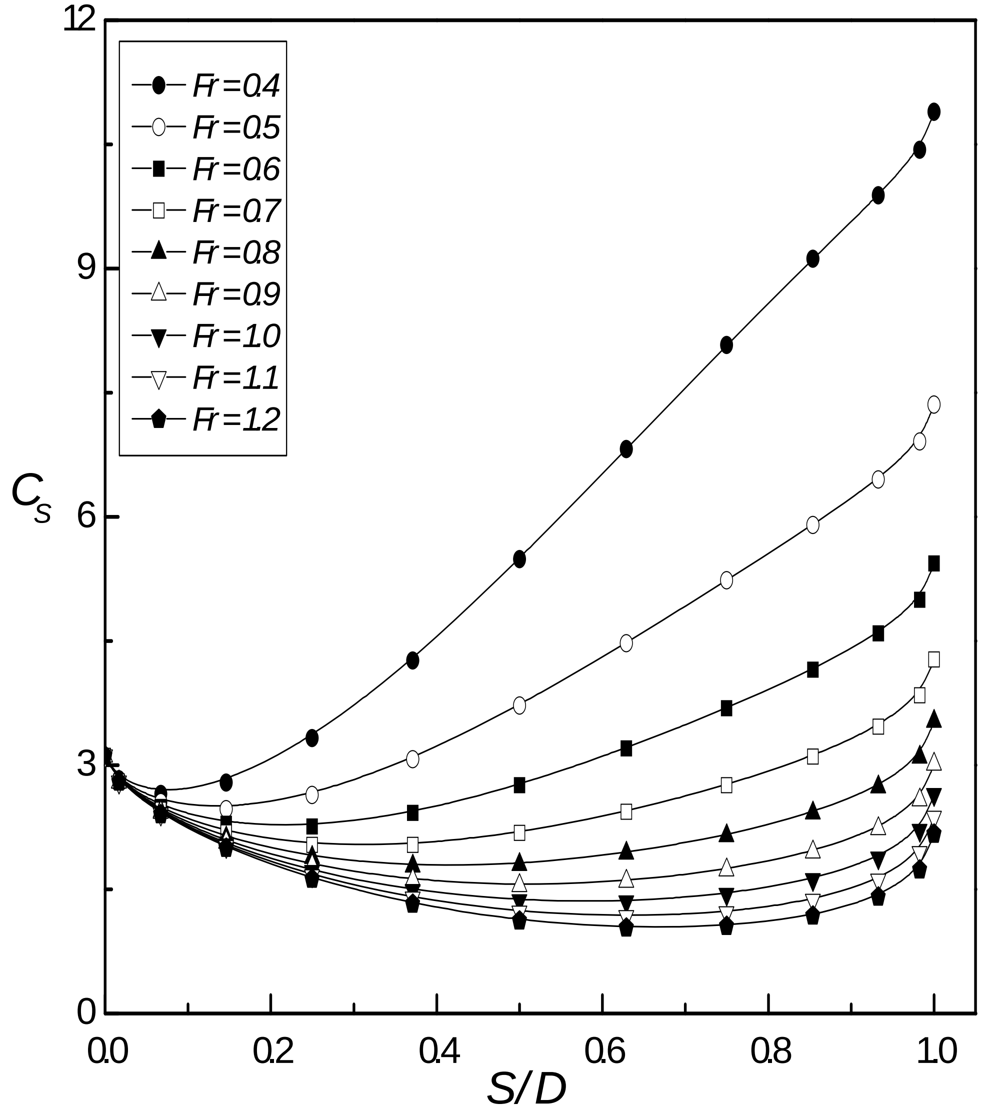

Figure 12. Variation of the slamming coefficient (C_s) with relative submergence (*S/D*) for different Froude numbers (*Fr*) when the cylinder height-to-wave amplitude ratio (*h/A*) is 0.1 and diameter-to-wave amplitude ratio (*D/A*) is 0.2.

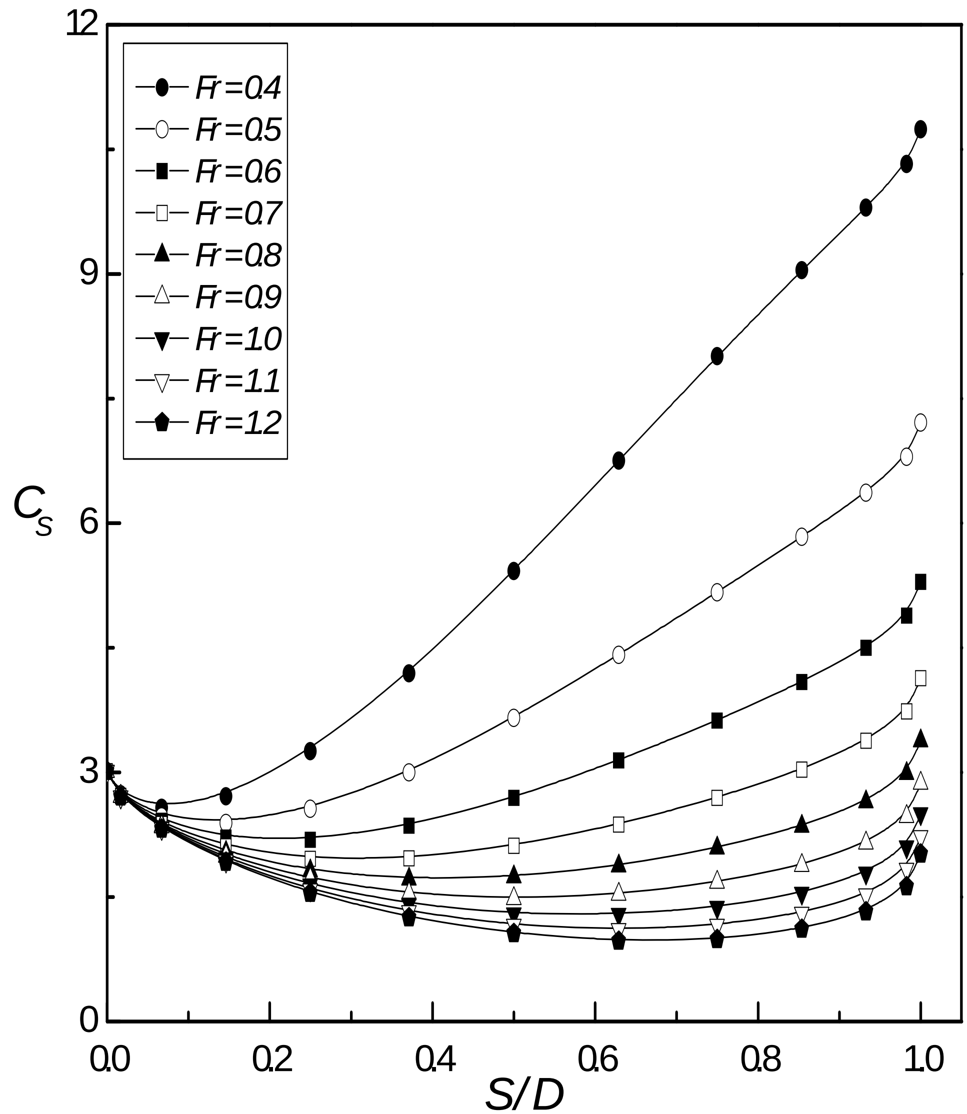

Figure 13. Variation of the slamming coefficient (C_s) with relative submergence (*S/D*) for different Froude numbers (*Fr*) when the cylinder height-to-wave amplitude ratio (*h/A*) is 0.2 and diameter-to-wave amplitude ratio (*D/A*) is 0.2.

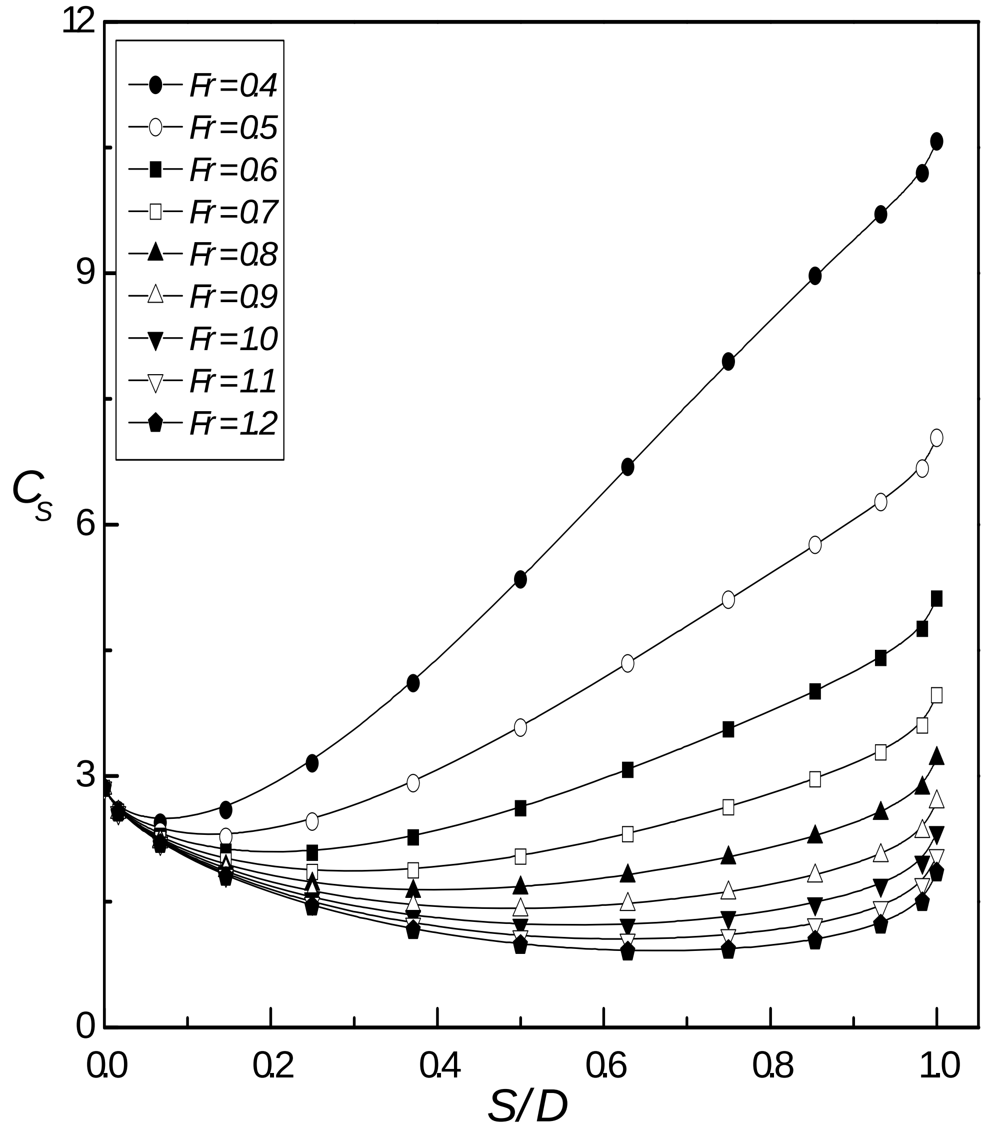

Figure 14. Variation of the slamming coefficient (C_s) with relative submergence (*S/D*) for different Froude numbers (*Fr*) when the cylinder height-to-wave amplitude ratio (*h/A*) is 0.3 and diameter-to-wave amplitude ratio (*D/A*) is 0.2.

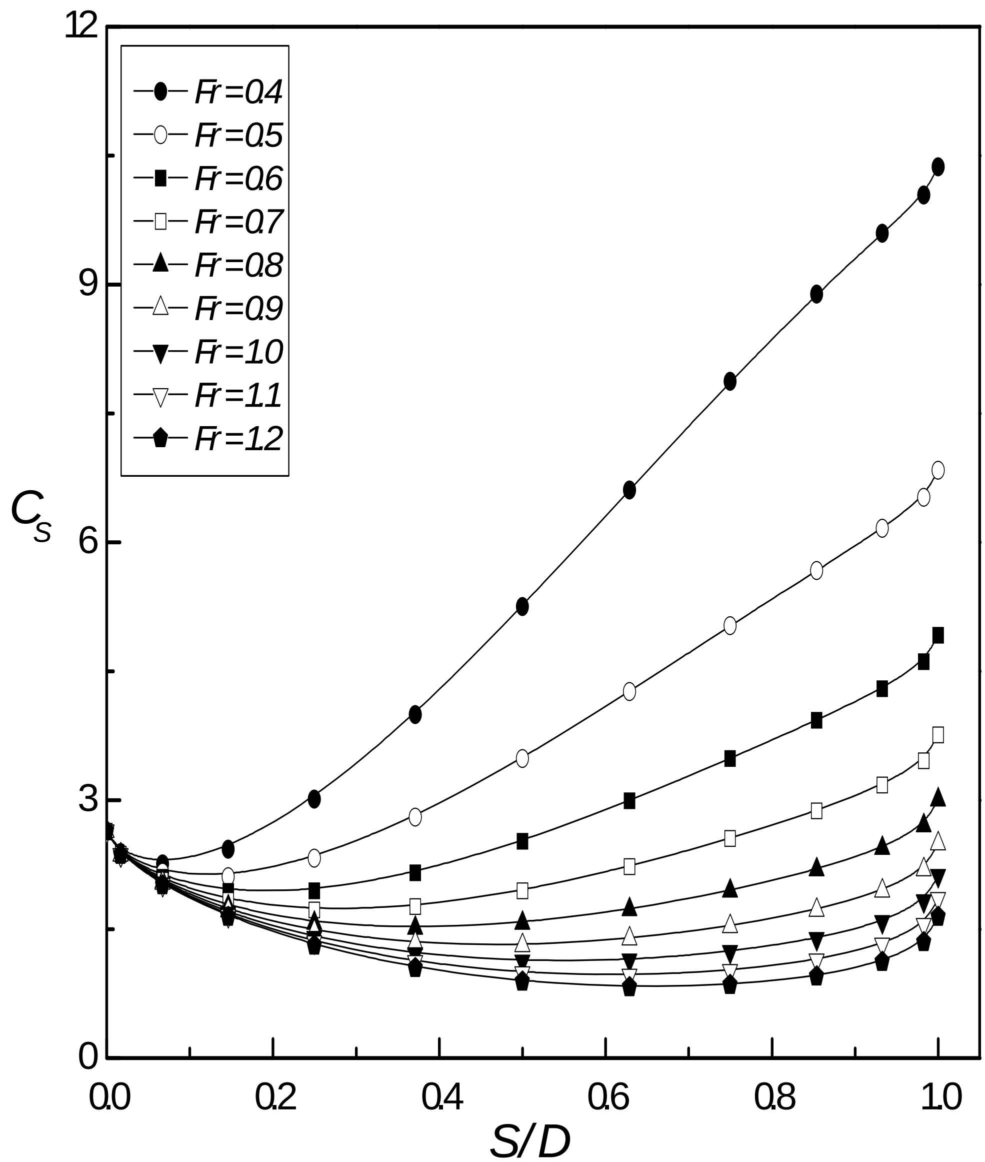

Figure 15. Variation of the slamming coefficient (C_s) with relative submergence (*S/D*) for different Froude numbers (*Fr*) when the cylinder height-to-wave amplitude ratio (*h/A*) is 0.4 and diameter-to-wave amplitude ratio (*D/A*) is 0.2.

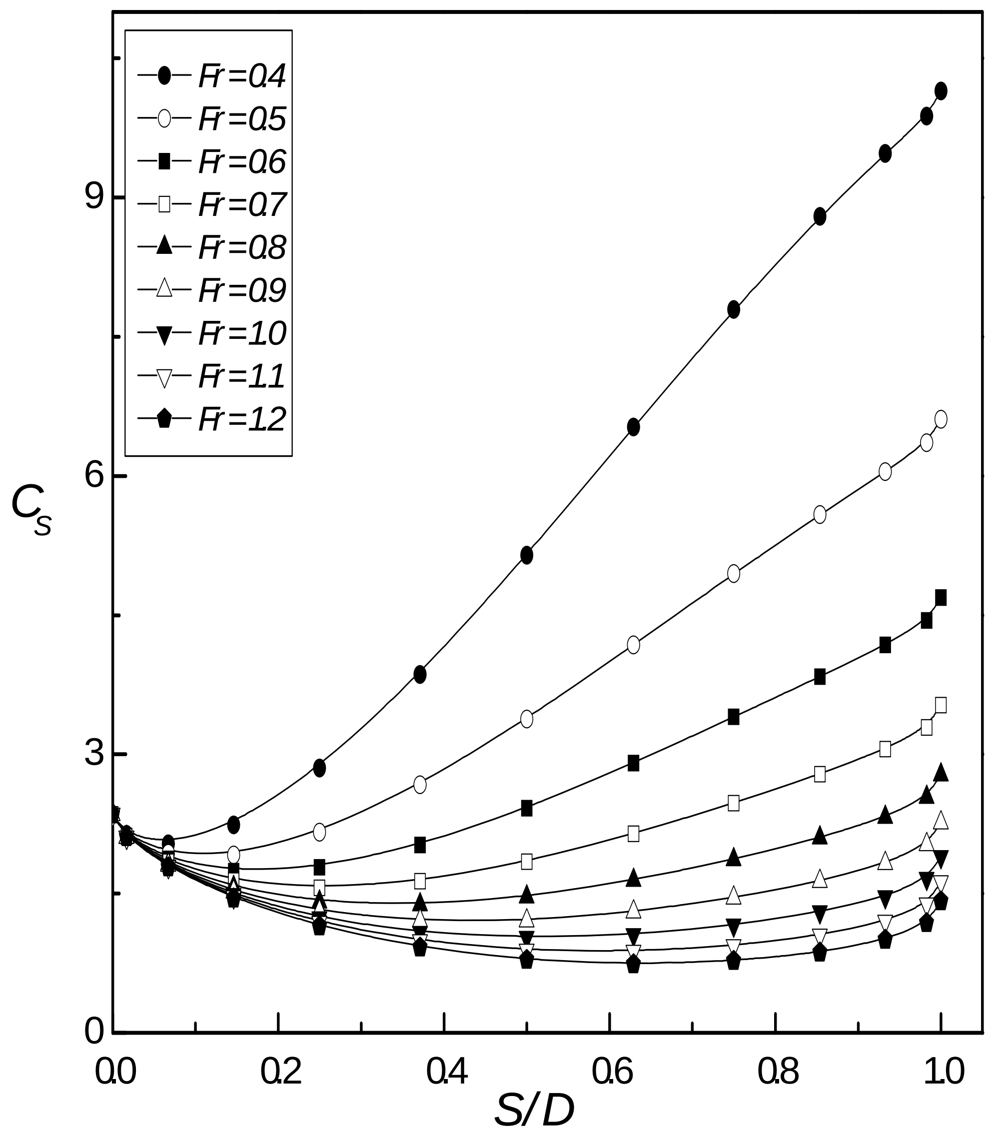

Figure 16. Variation of the slamming coefficient (C_s) with relative submergence (*S/D*) for different Froude numbers (*Fr*) when the cylinder height-to-wave amplitude ratio (*h/A*) is 0.5 and diameter-to-wave amplitude ratio (*D/A*) is 0.2.

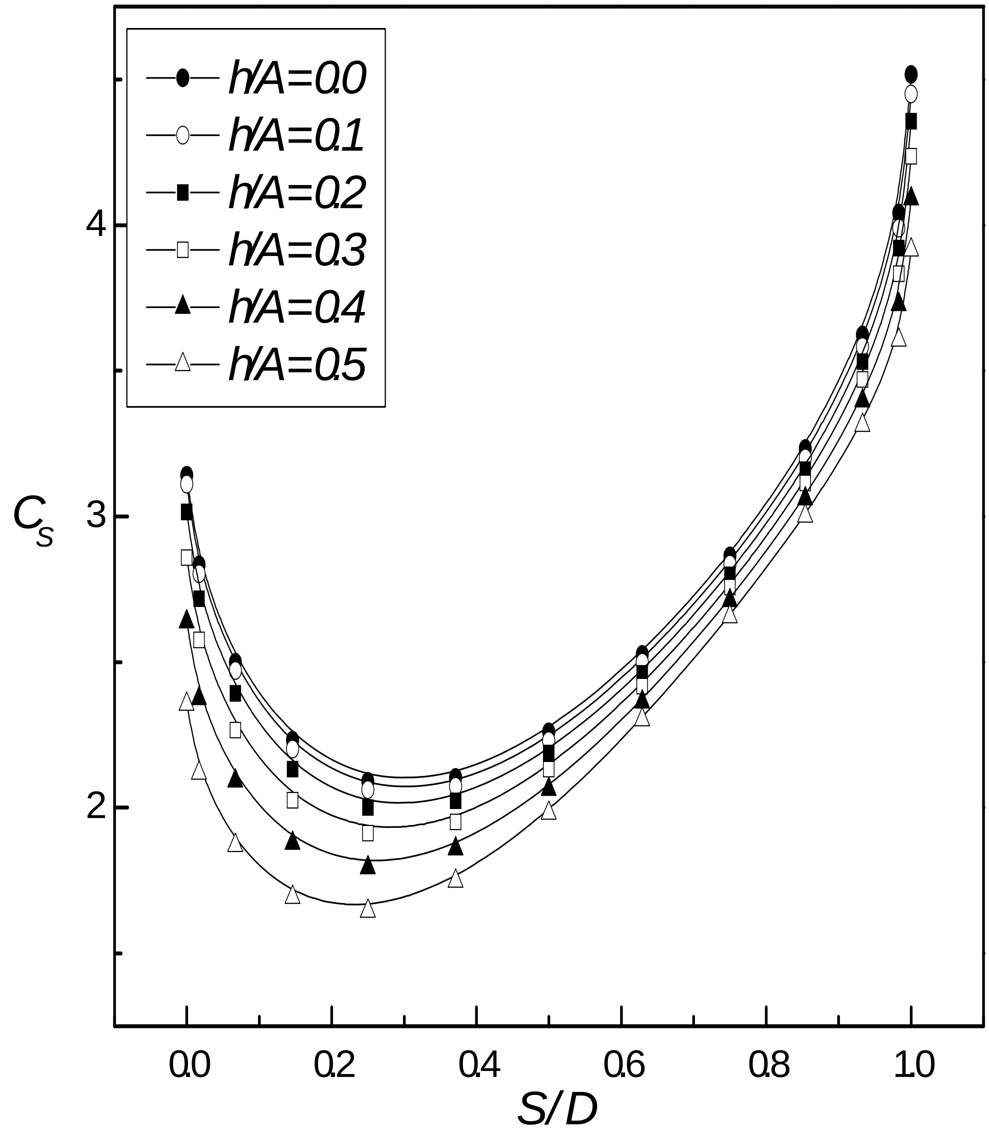

Figure 17. Variation of the slamming coefficient (C_s) with relative submergence (*S/D*) for different values of cylinder height-to-wave amplitude ratio (*h/A*) when the cylinder diameter-to-wave amplitude ratio (*D/A*) is equal to 0.10 and *Fr* = 0.7.

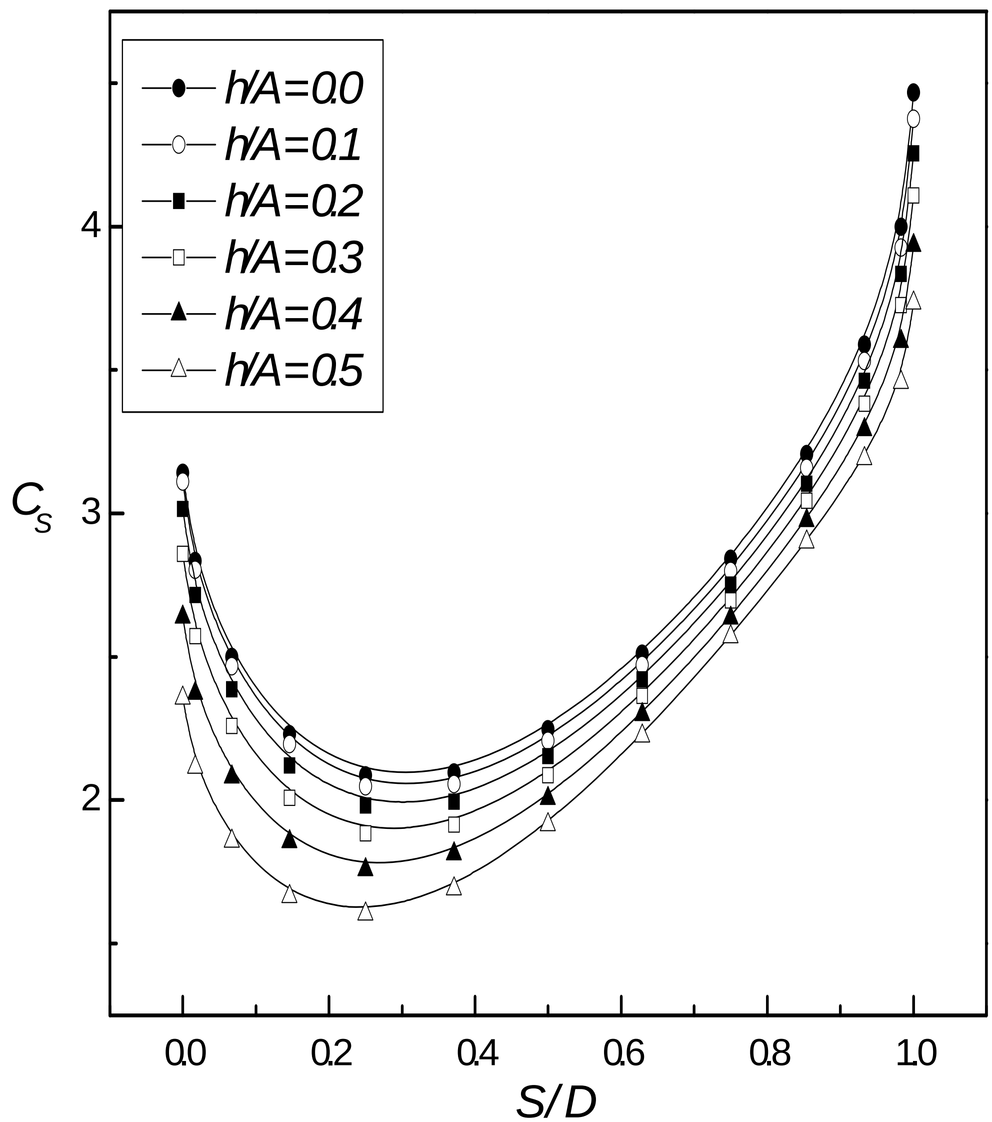

Figure 18. Variation of the slamming coefficient (C_s) with relative submergence (*S/D*) for different values of cylinder height-to-wave amplitude ratio (*h/A*) when the cylinder diameter-to-wave amplitude ratio (*D/A*) is equal to 0.15 and $Fr = 0.7$.

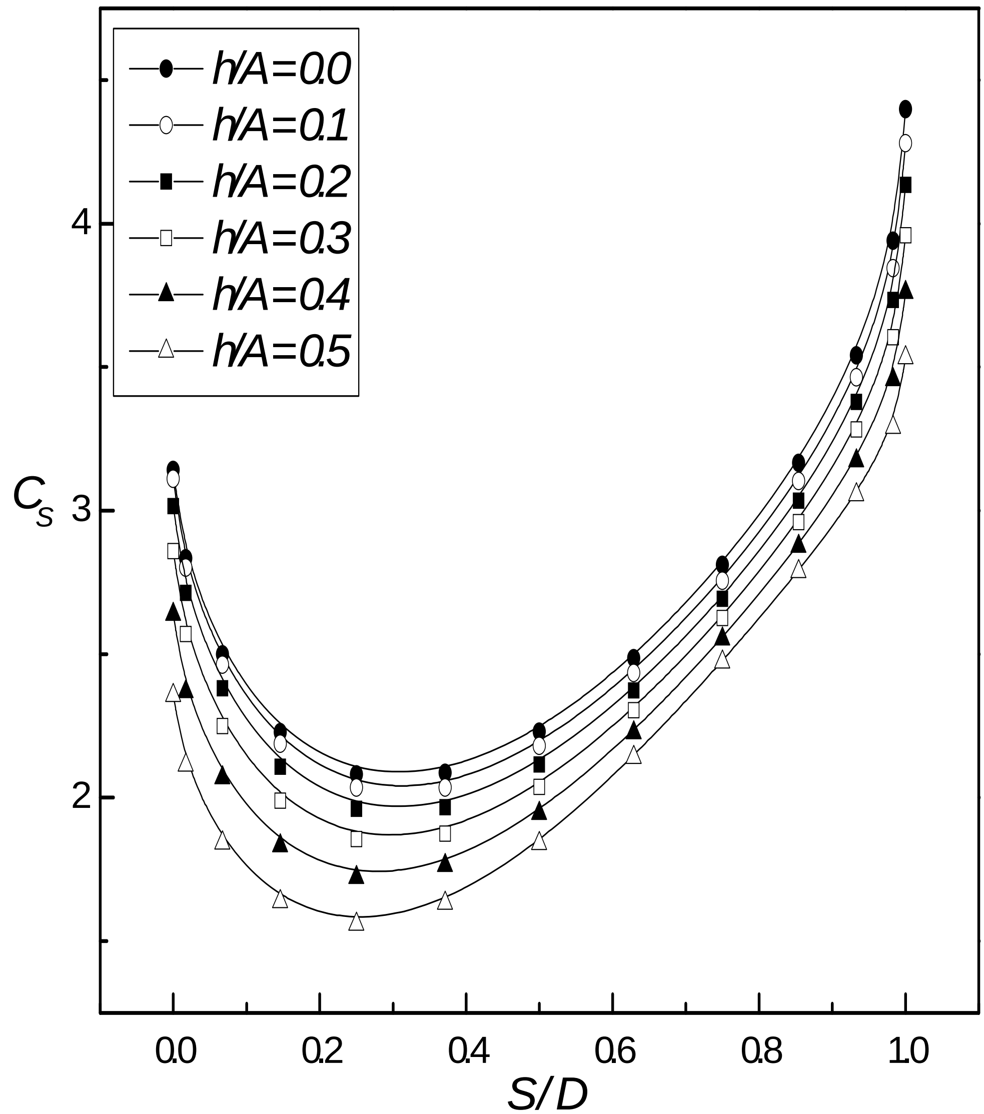

Figure 19. Variation of the slamming coefficient (C_s) with relative submergence (*S/D*) for different values of cylinder height-to-wave amplitude ratio (*h/A*) when the cylinder diameter-to-wave amplitude ratio (*D/A*) is equal to 0.20 and *Fr* = 0.7.

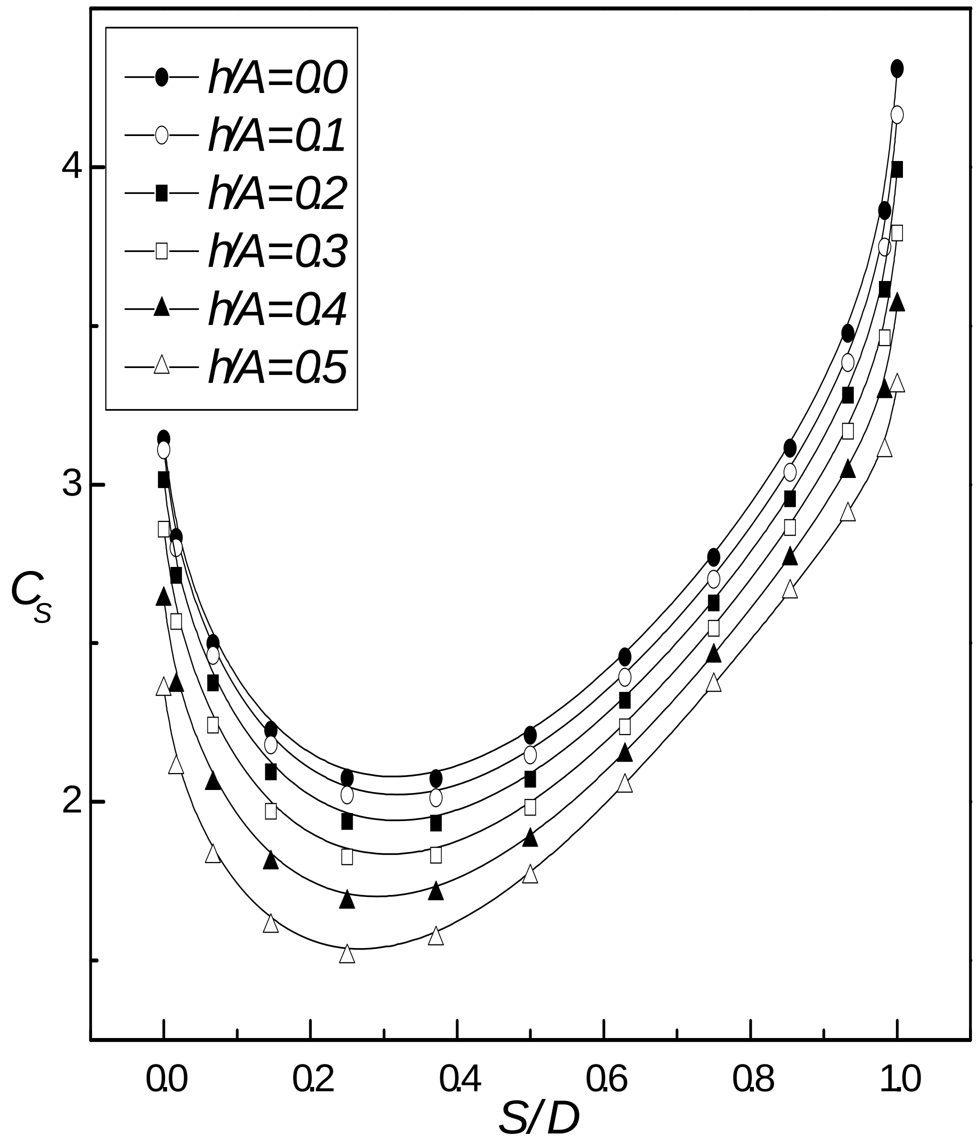

Figure 20. Variation of the slamming coefficient (C_s) with relative submergence (*S/D*) for different values of cylinder height-to-wave amplitude ratio (*h/A*) when the cylinder diameter-to-wave amplitude ratio (*D/A*) is equal to 0.25 and *Fr* = 0.7.

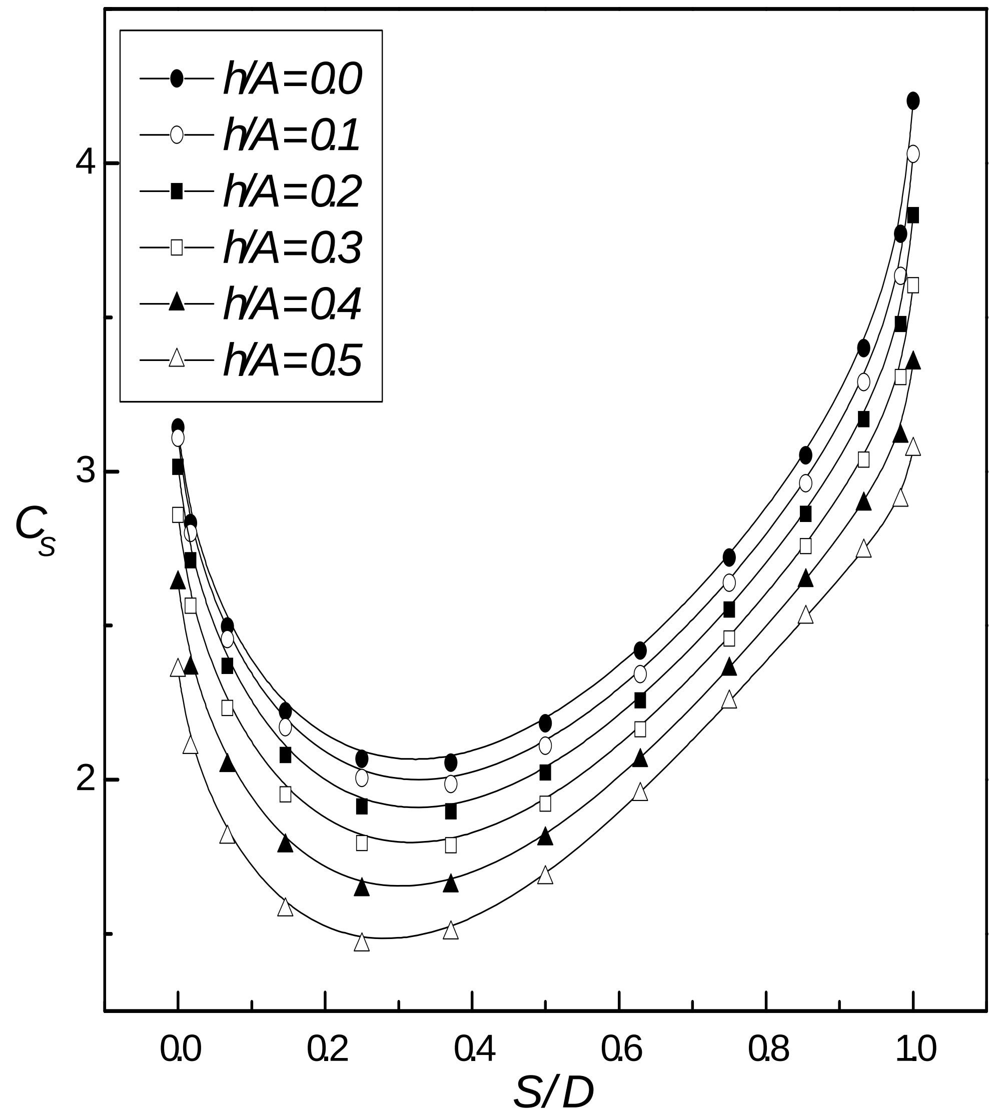

Figure 21. Variation of the slamming coefficient (C_s) with relative submergence (*S/D*) for different values of cylinder height-to-wave amplitude ratio (*h/A*) when the cylinder diameter-to-wave amplitude ratio (*D/A*) is equal to 0.30 and *Fr* = 0.7.

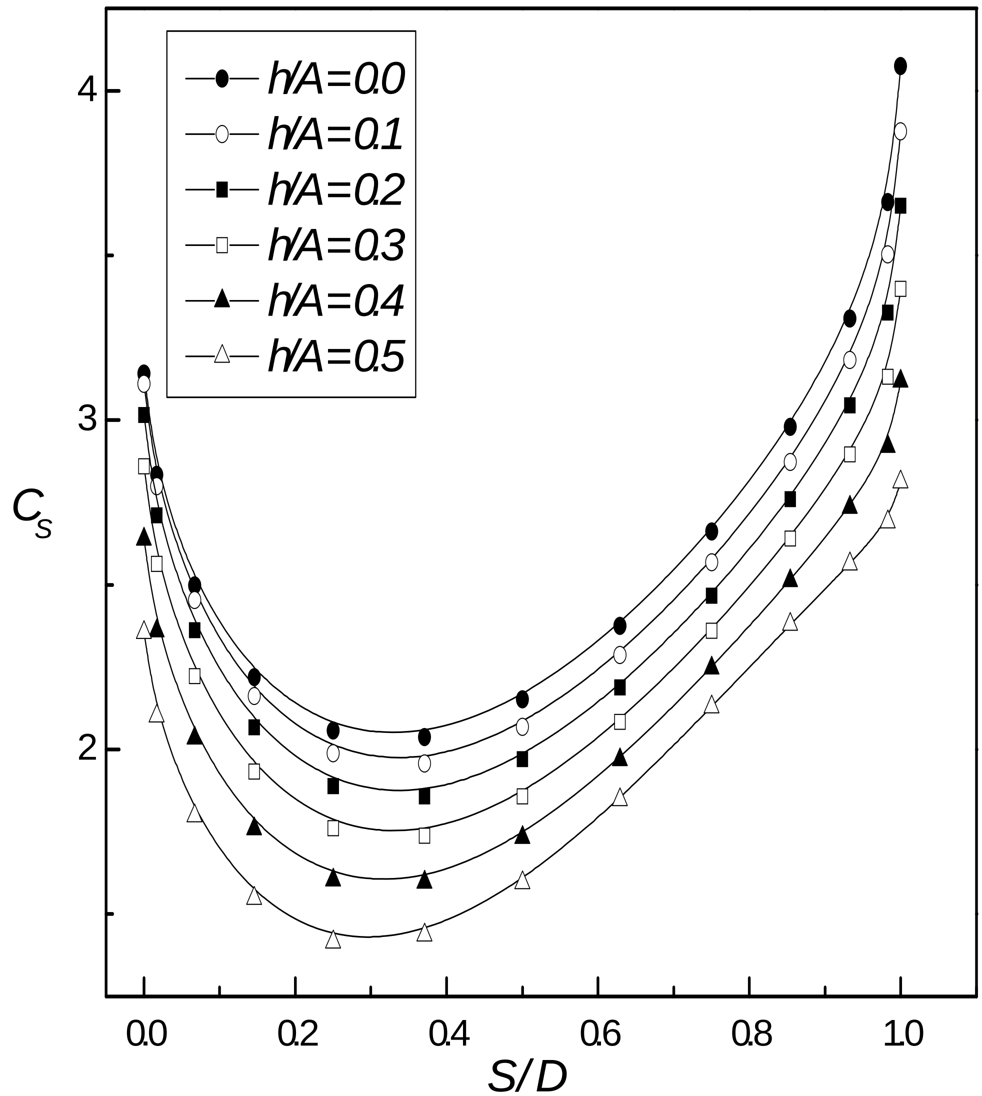

Figure 22. Variation of the slamming coefficient (C_s) with relative submergence (*S/D*) for different values of cylinder height-to-wave amplitude ratio (*h/A*) when the cylinder diameter-to-wave amplitude ratio (*D/A*) is equal to 0.35 and *Fr* = 0.7.

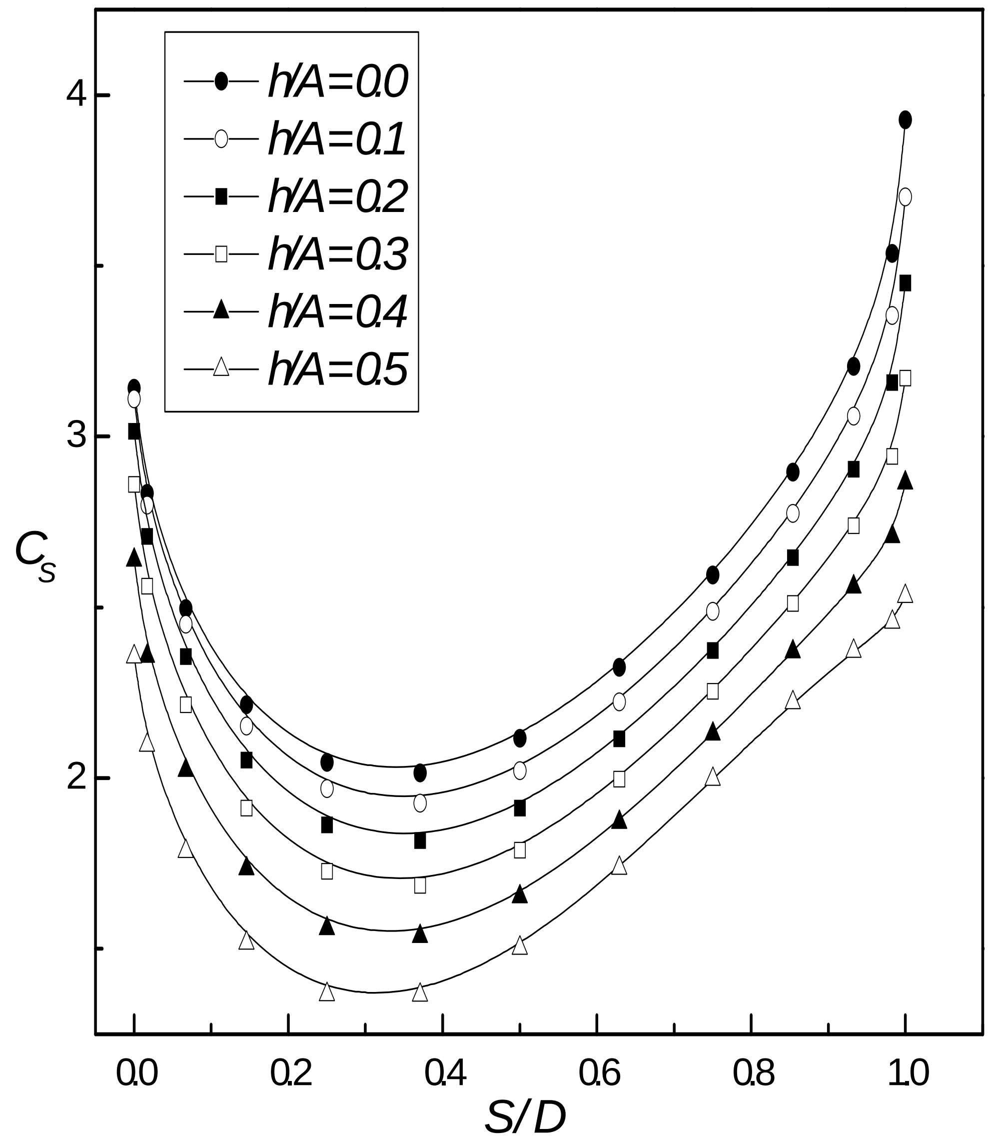

Figure 23. Variation of the slamming coefficient (C_s) with relative submergence (*S/D*) for different values of cylinder height-to-wave amplitude ratio (*h/A*) when the cylinder diameter-to-wave amplitude ratio (*D/A*) is equal to 0.40 and *Fr* = 0.7.

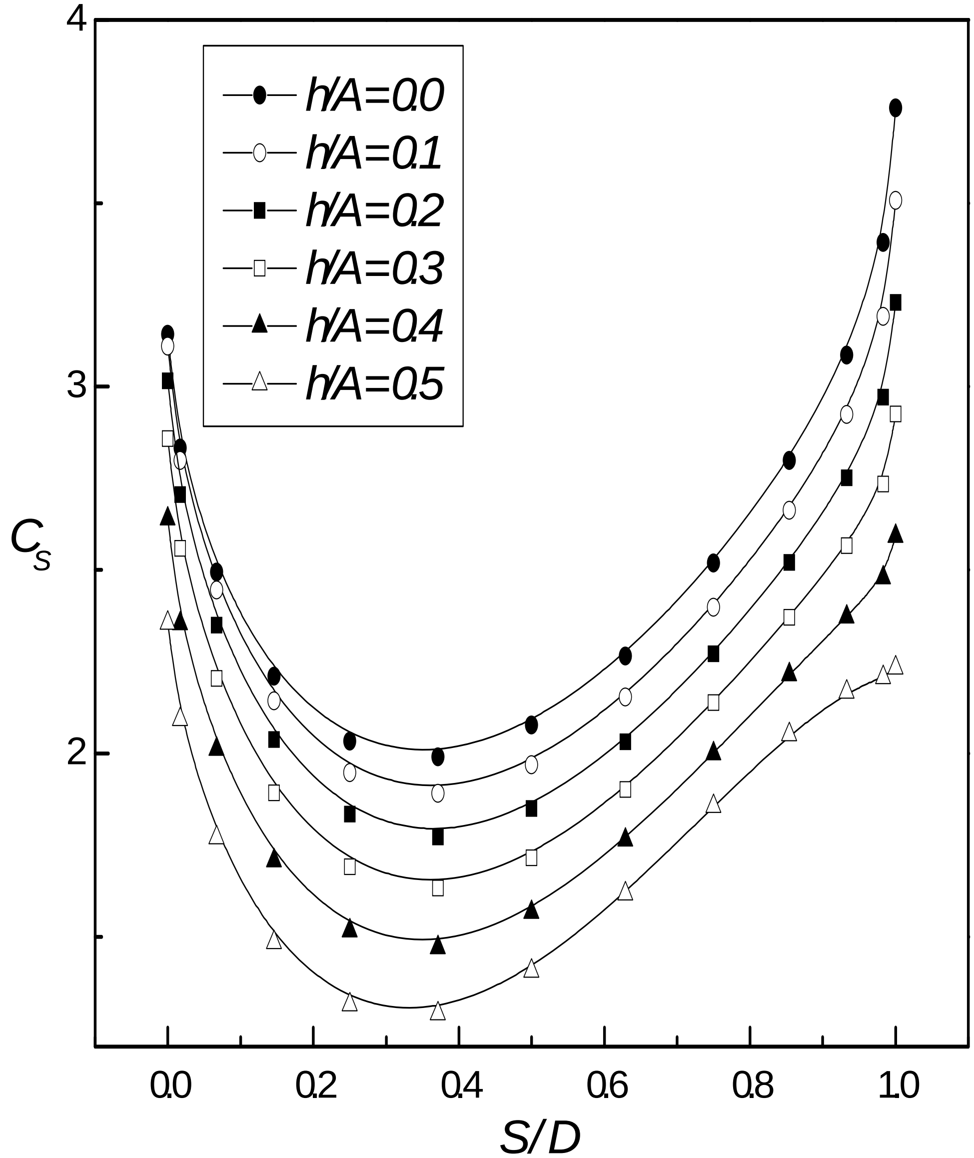

Figure 24. Variation of the slamming coefficient (C_s) with relative submergence (*S/D*) for different values of cylinder height-to-wave amplitude ratio (*h/A*) when the cylinder diameter-to-wave amplitude ratio (*D/A*) is equal to 0.45 and *Fr* = 0.7.

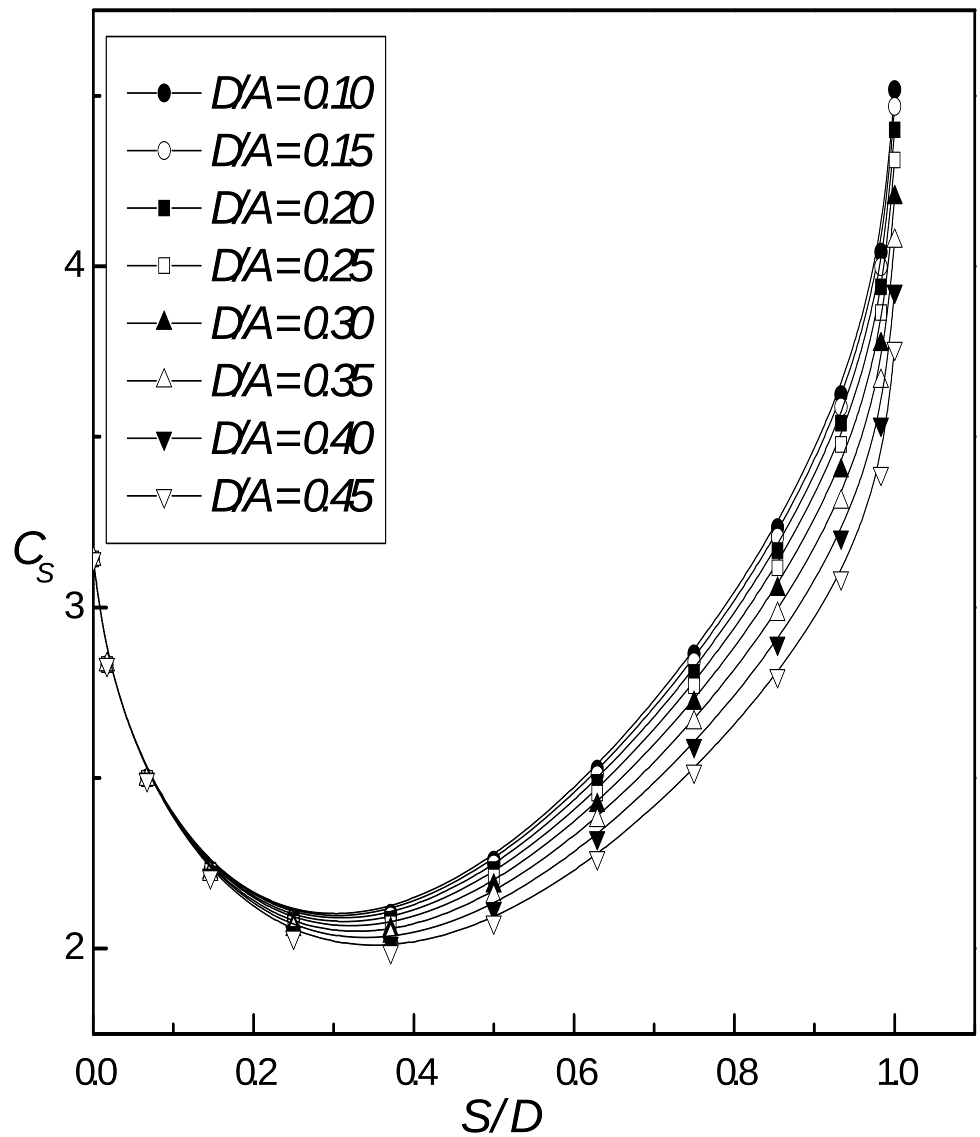

Figure 25. Variation of slamming coefficient (C_S) with relative submergence (S/D) for different diameter-to-wave amplitude ratios (D/A) when h/A = 0.0 and Fr = 0.7.

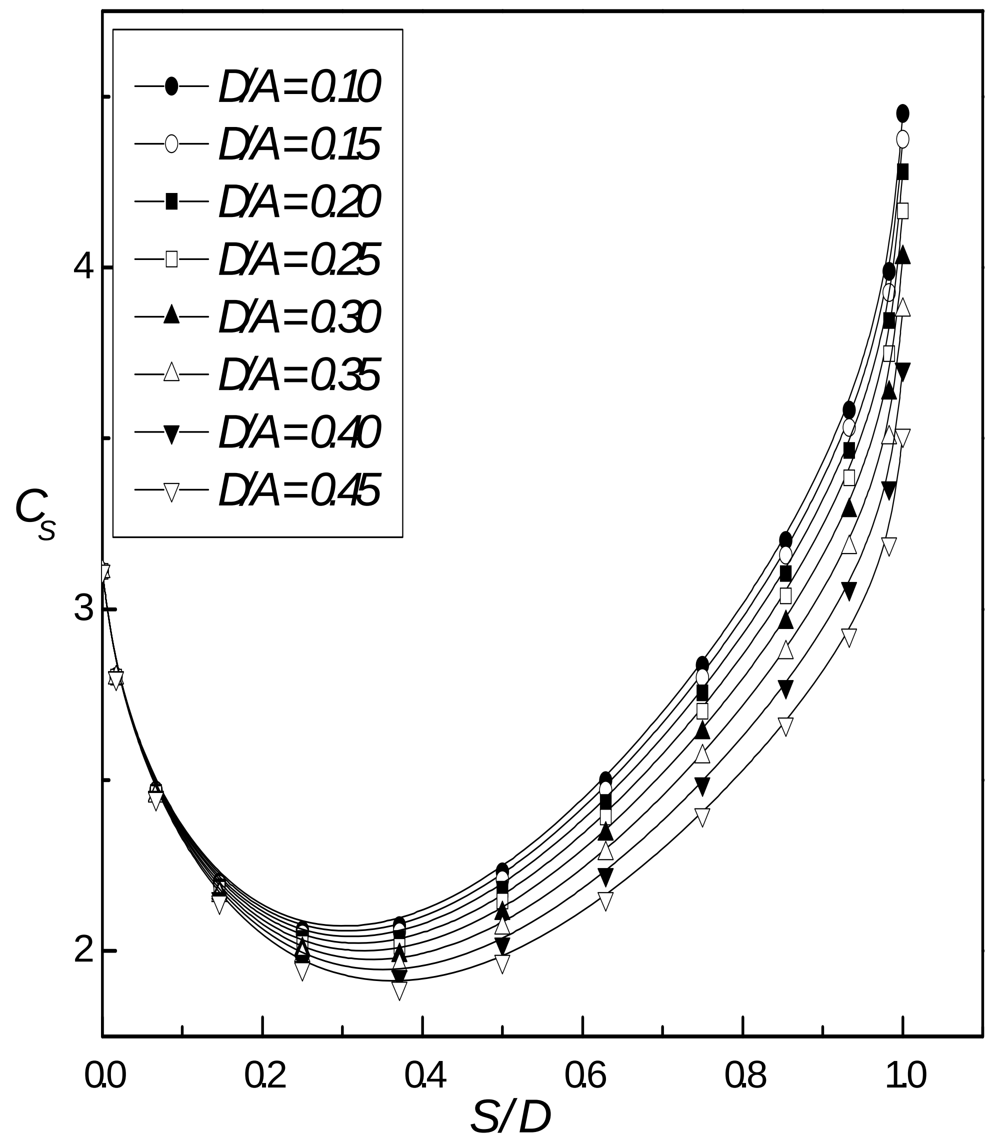

Figure 26. Variation of slamming coefficient (C_S) with relative submergence (S/D) for different diameter-to-wave amplitude ratios (D/A) when h/A = 0.1 and Fr = 0.7.

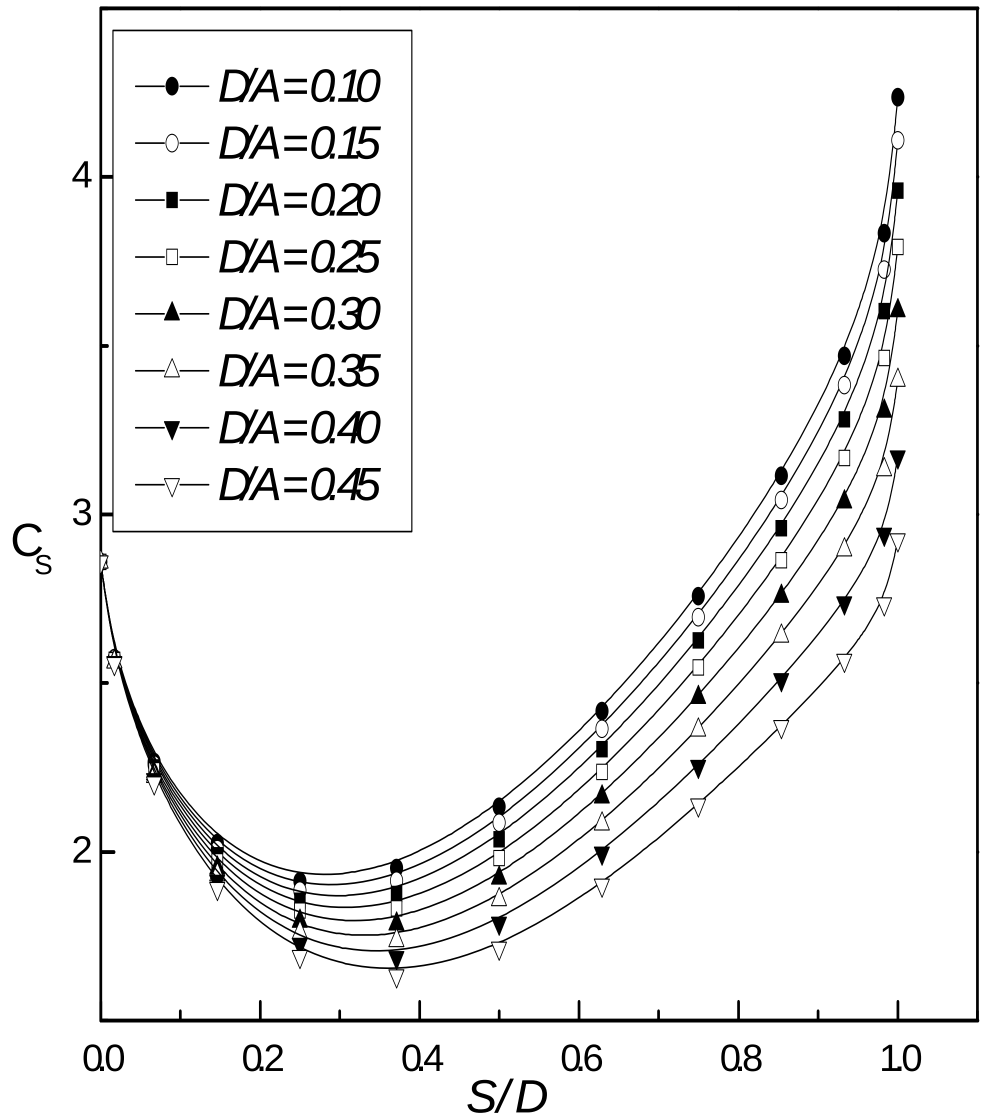

Figure 27. Variation of slamming coefficient (C_S) with relative submergence (*S/D*) for different diameter-to-wave amplitude ratios (*D/A*) when h/A = 0.2 and Fr = 0.7.

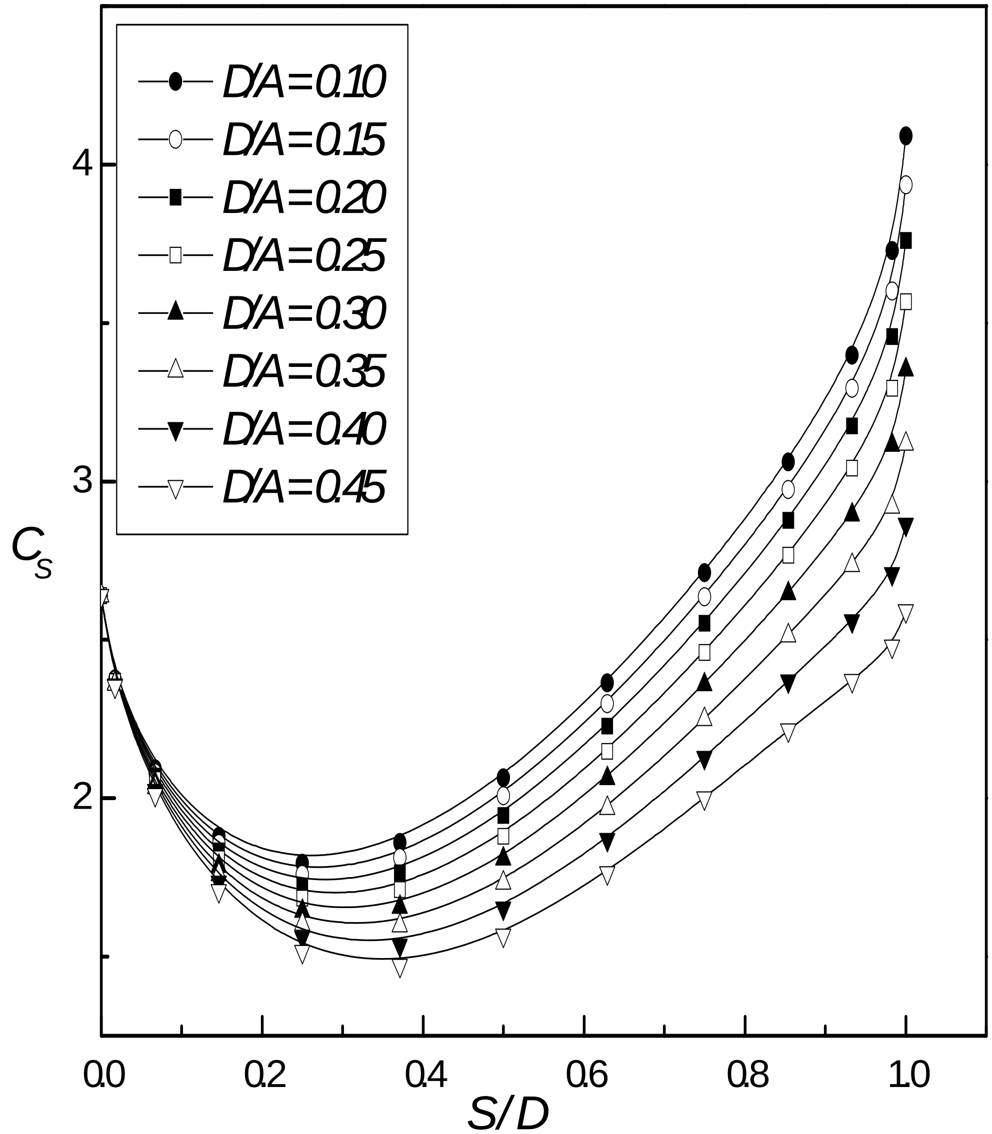

Figure 28. Variation of slamming coefficient (C_S) with relative submergence (*S/D*) for different diameter-to-wave amplitude ratios (*D/A*) when *h/A* = 0.3 and *Fr* = 0.7.

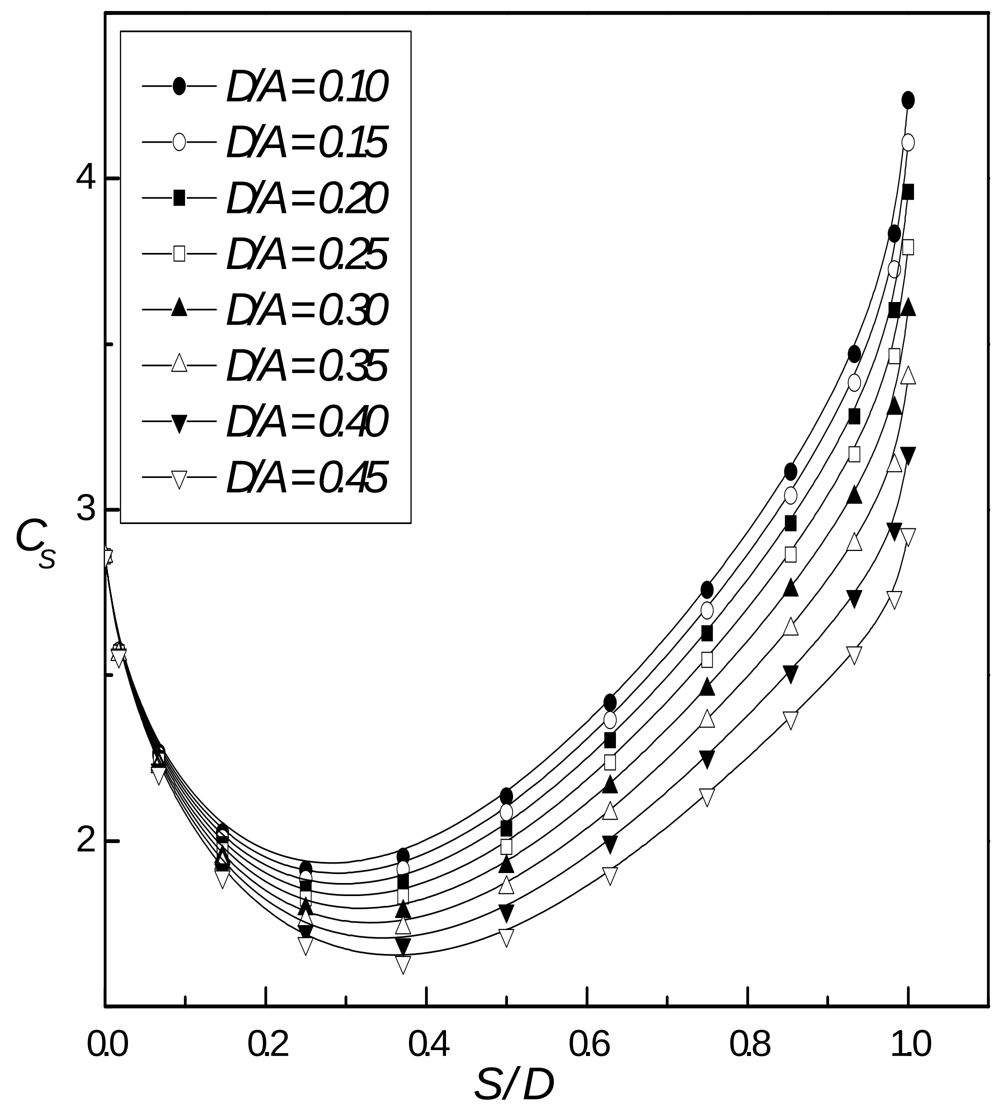

Figure 29. Variation of slamming coefficient (C_S) with relative submergence (S/D) for different diameter-to-wave amplitude ratios (D/A) when h/A = 0.4 and Fr = 0.7.

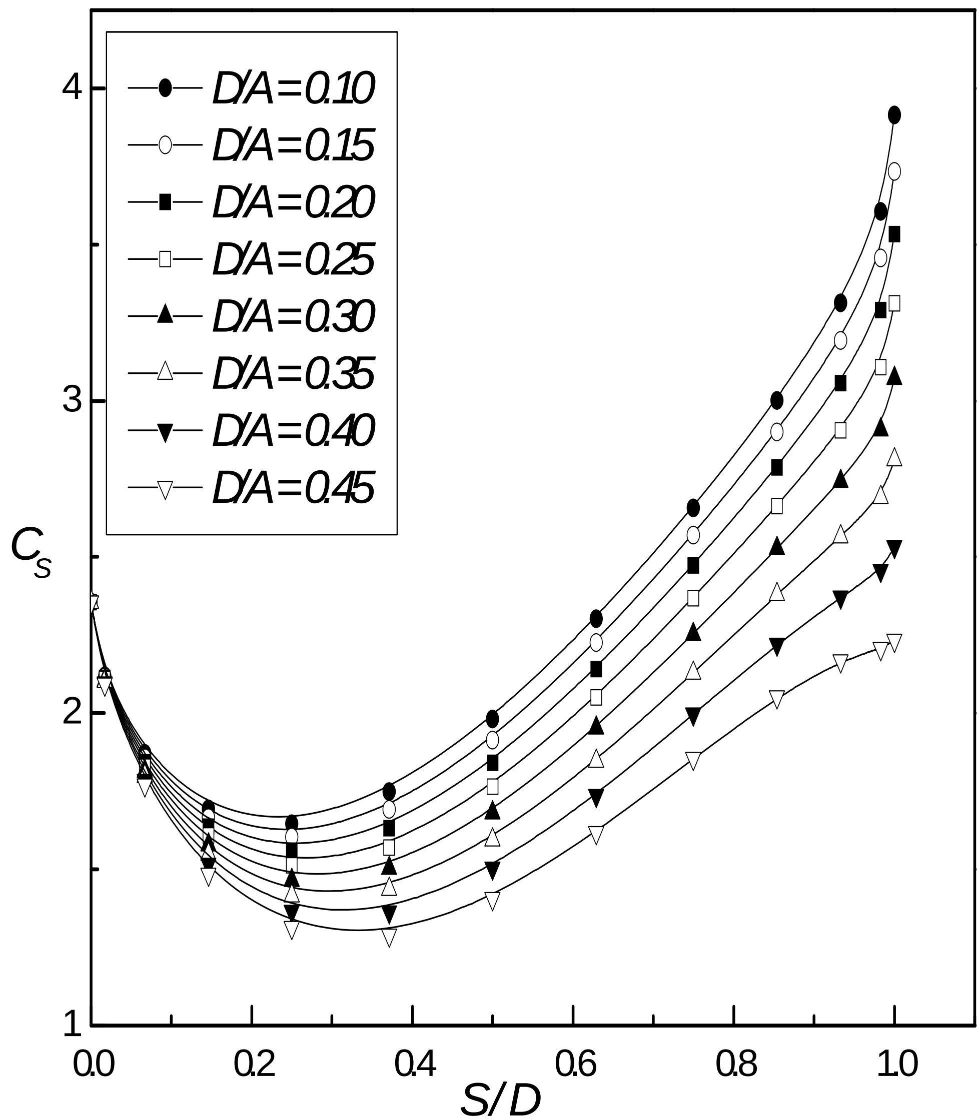

Figure 30. Variation of slamming coefficient (C_S) with relative submergence (*S/D*) for different diameter-to-wave amplitude ratios (*D/A*) when h/A = 0.5 and Fr = 0.7.

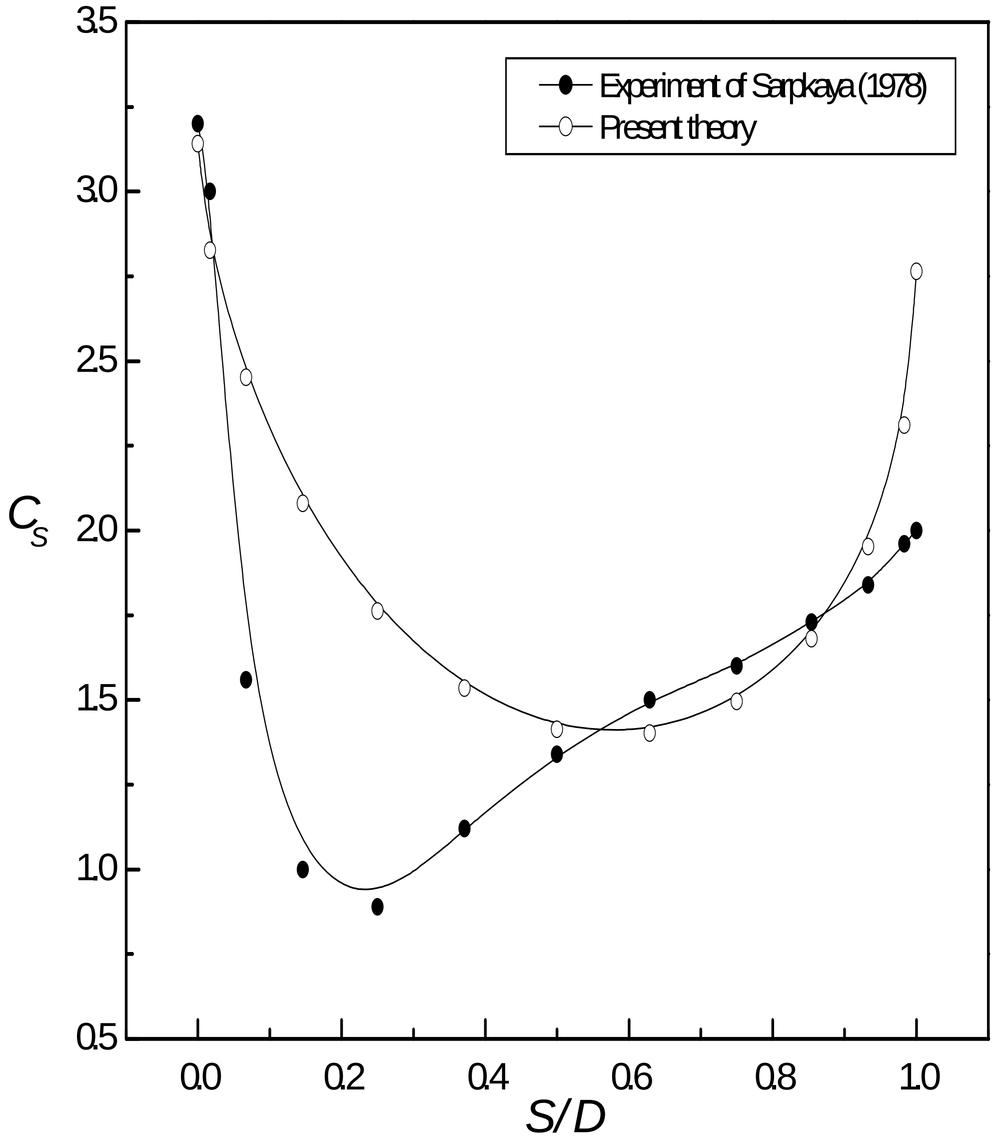

Figure 31. Variation of the coefficient of slamming (C_S) with relative submergence (*S/D*).

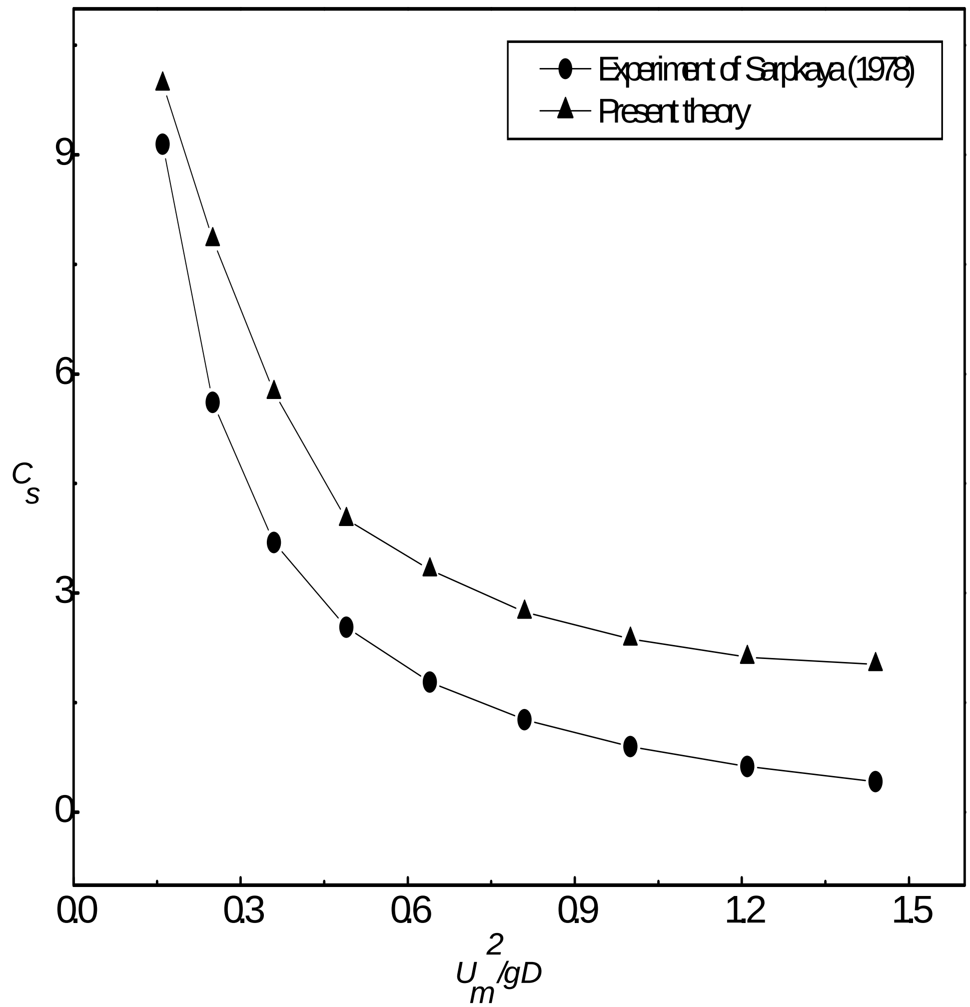

Figure 32.Variation of the slamming coefficient (*Cs*) as a function of the Froude number.

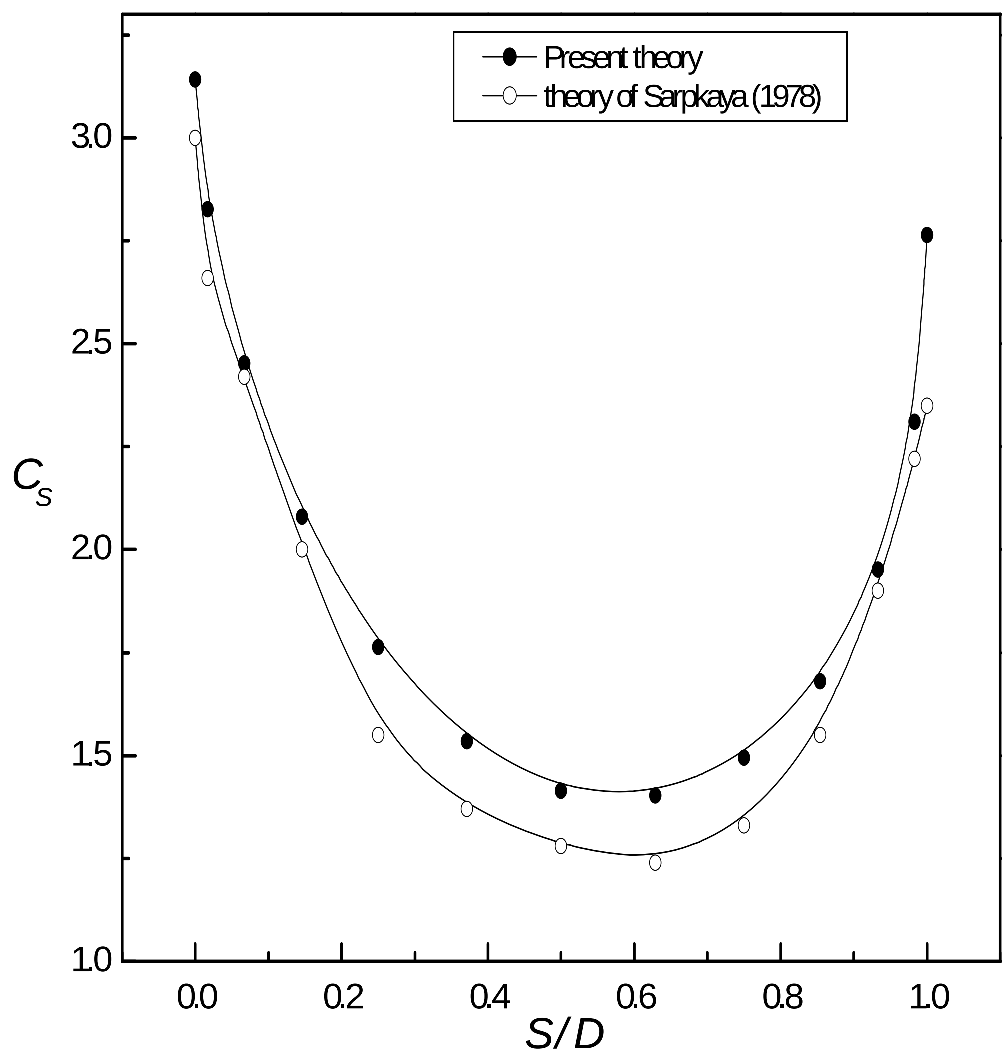

Figure 33. Variation of the coefficient of slamming (C_S) with relative submergence (*S/D*).

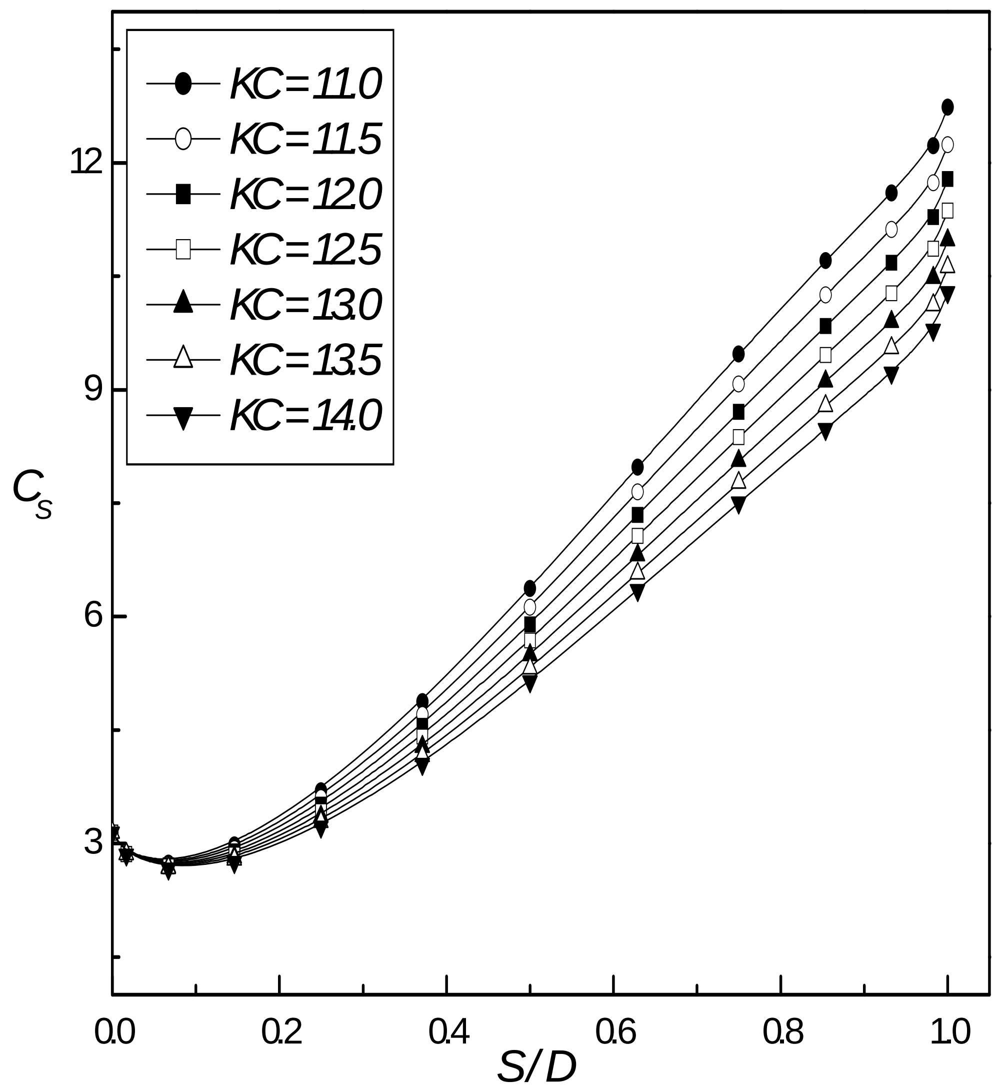

Figure 34. Variation of the slamming coefficient (C_s) with relative submergence (*S/D*) for different Keulegan-Carpenter numbers (*KC*) at diameter-to-wave amplitude ratio (*D/A*) is 0.1 when height-to-wave amplitude ratio (*h/A*) is 0.0 and *L/A* = 85.

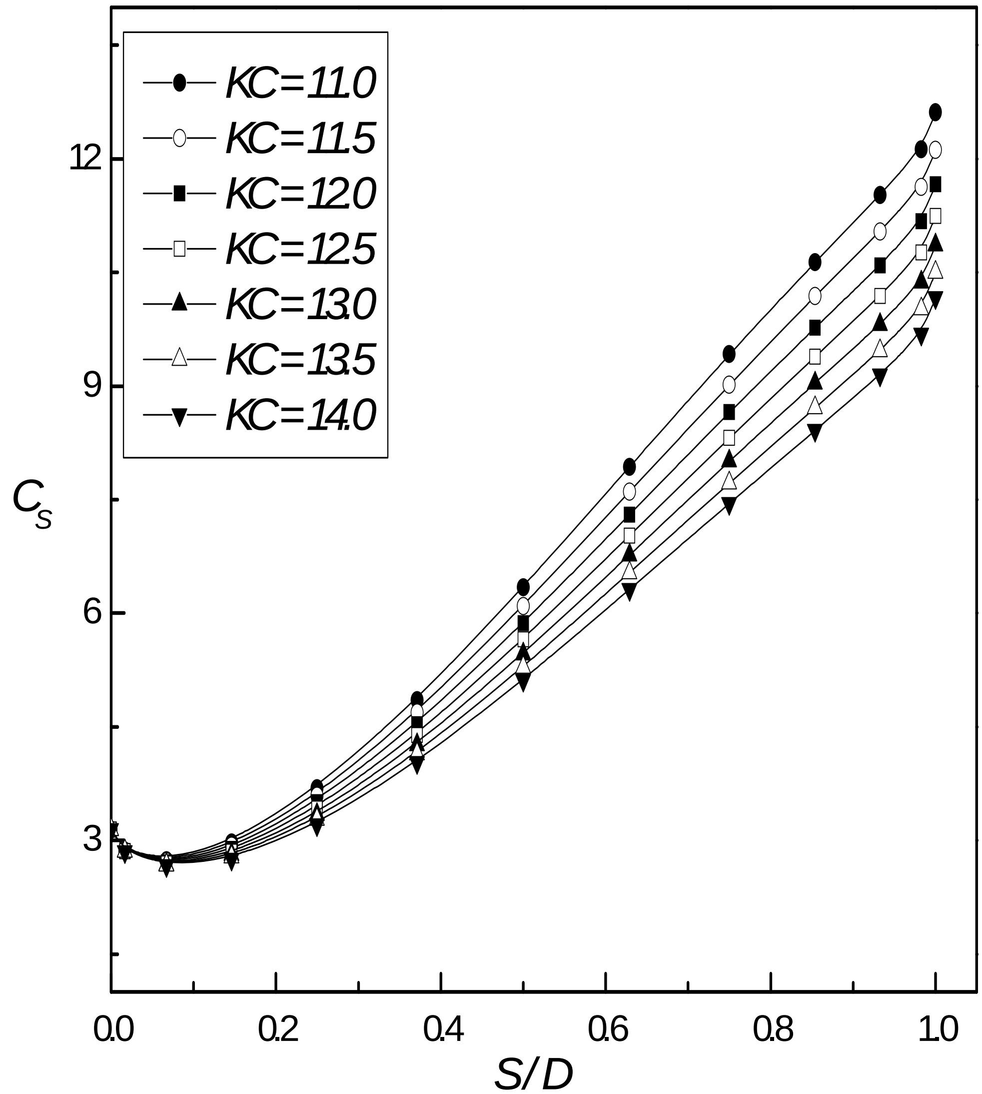

Figure 35. Variation of the slamming coefficient (C_s) with relative submergence (*S/D*) for different Keulegan-Carpenter numbers (*KC*) at diameter-to-wave amplitude ratio (*D/A*) is 0.2 when height-to-wave amplitude ratio (*h/A*) is 0.0 and *L/A* = 85.

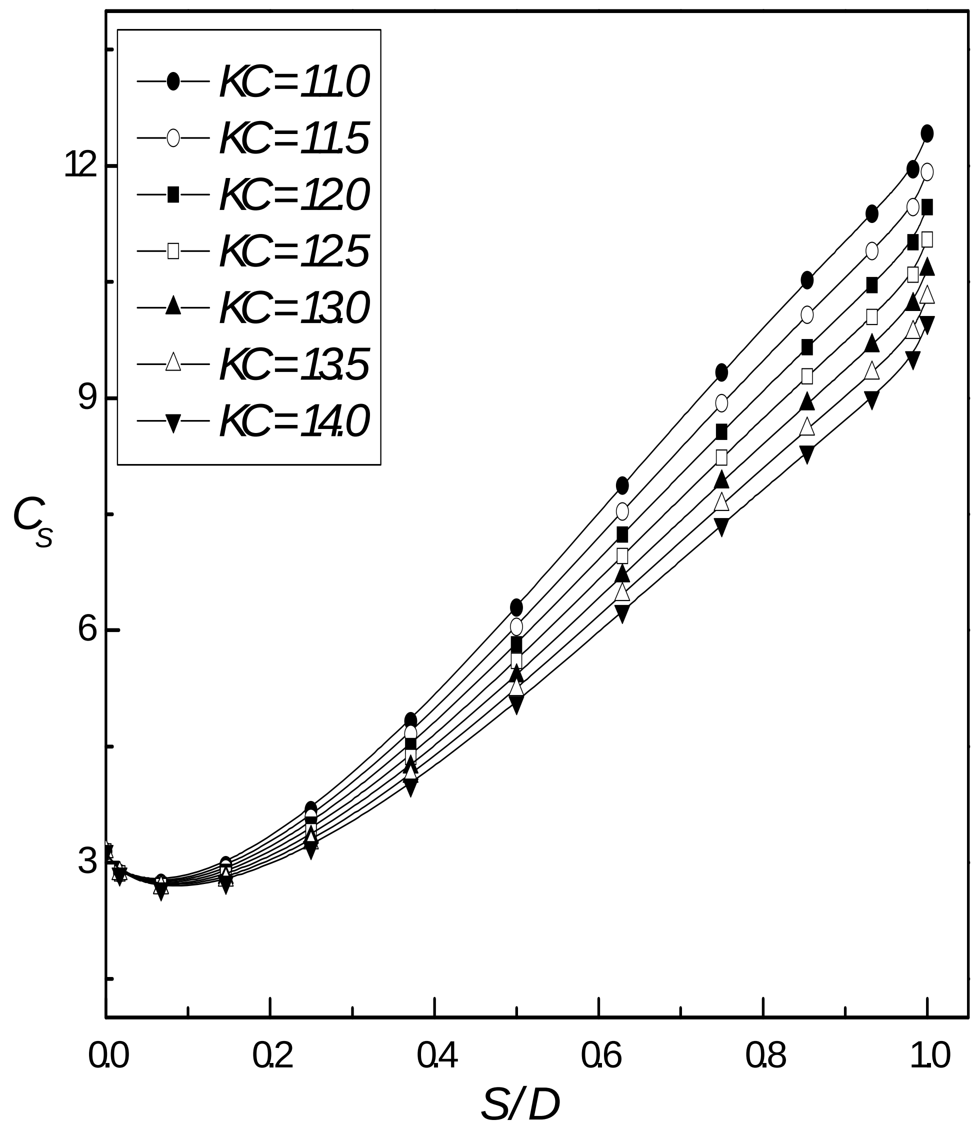

Figure 36. Variation of the slamming coefficient (C_s) with relative submergence (*S/D*) for different Keulegan-Carpenter numbers (*KC*) at diameter-to-wave amplitude ratio (*D/A*) is 0.3 when height-to-wave amplitude ratio (*h/A*) is 0.0 and *L/A* = 85.

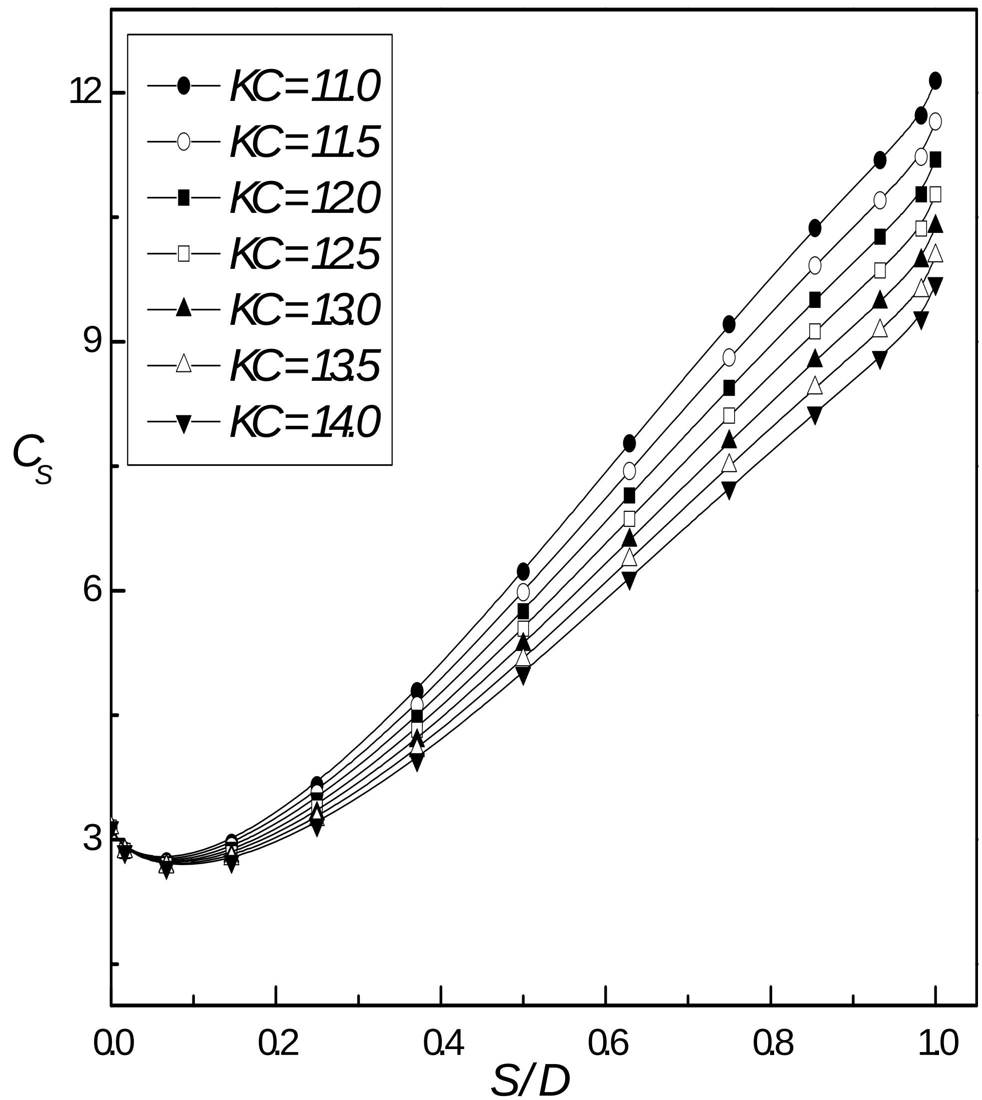

Figure 37. Variation of the slamming coefficient (C_s) with relative submergence (*S/D*) for different Keulegan-Carpenter numbers (*KC*) at diameter-to-wave amplitude ratio (*D/A*) is 0.4 when height-to-wave amplitude ratio (*h/A*) is 0.0 and *L/A* = 85.

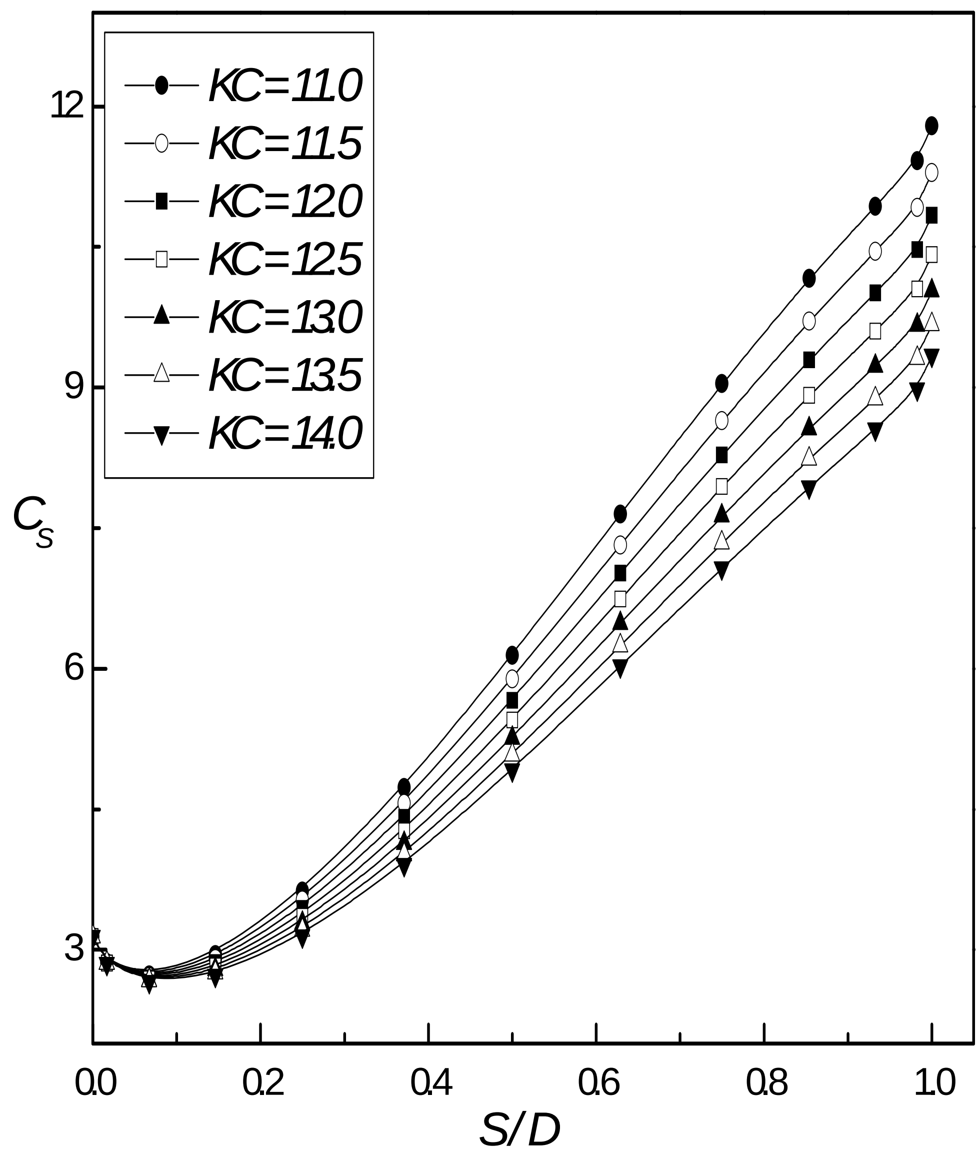

Figure 38. Variation of the slamming coefficient (C_s) with relative submergence (*S/D*) for different Keulegan-Carpenter numbers (*KC*) at diameter-to-wave amplitude ratio (*D/A*) is 0.5 when height-to-wave amplitude ratio (*h/A*) is 0.0 and *L/A* = 85.

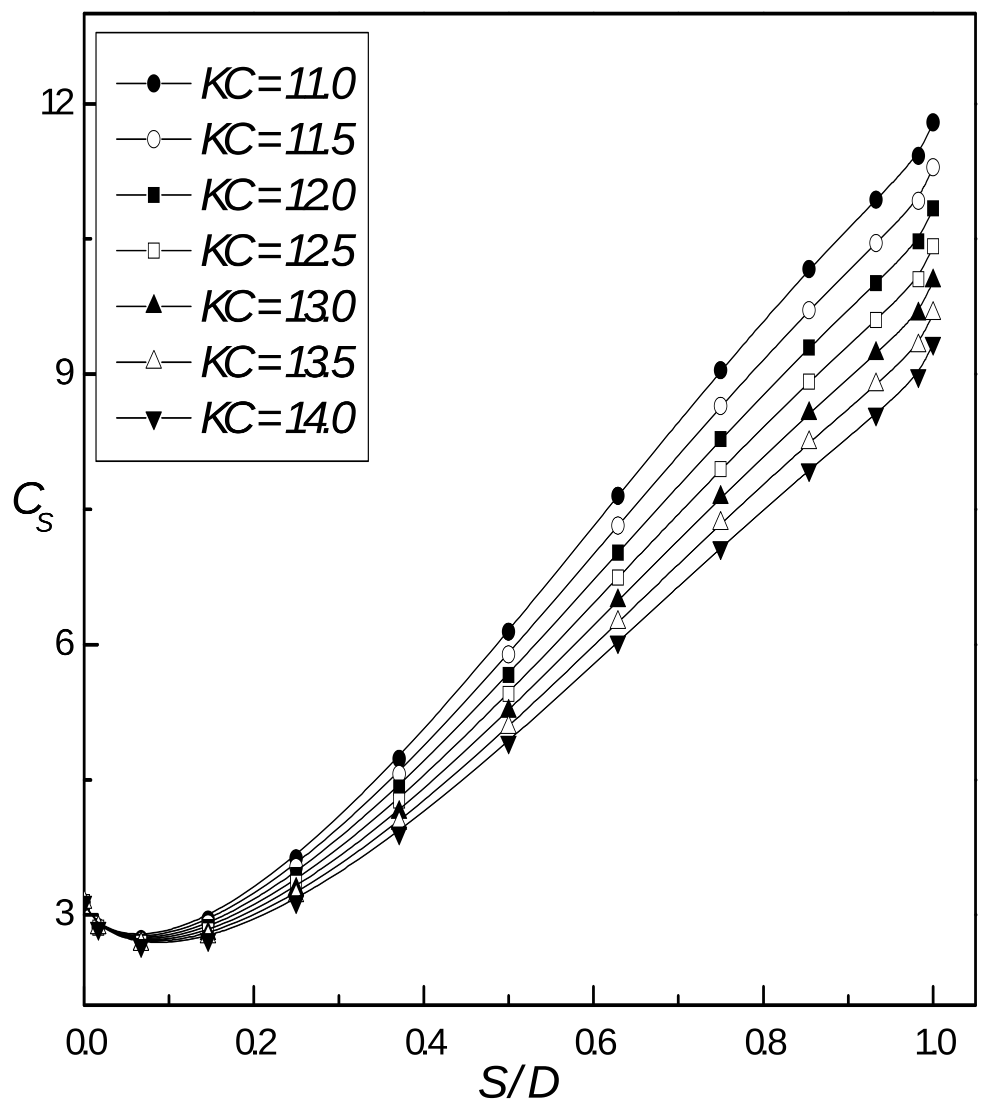

Figure 39. Variation of the slamming coefficient (C_s) with relative submergence (*S/D*) for different Keulegan-Carpenter numbers (*KC*) at wave length-to-amplitude ratio (*L/A*) is 80 when diameter-to-wave amplitude ratio (*D/A*) is 0.2 and height-to-wave amplitude ratio (*h/A*) is 0.0.

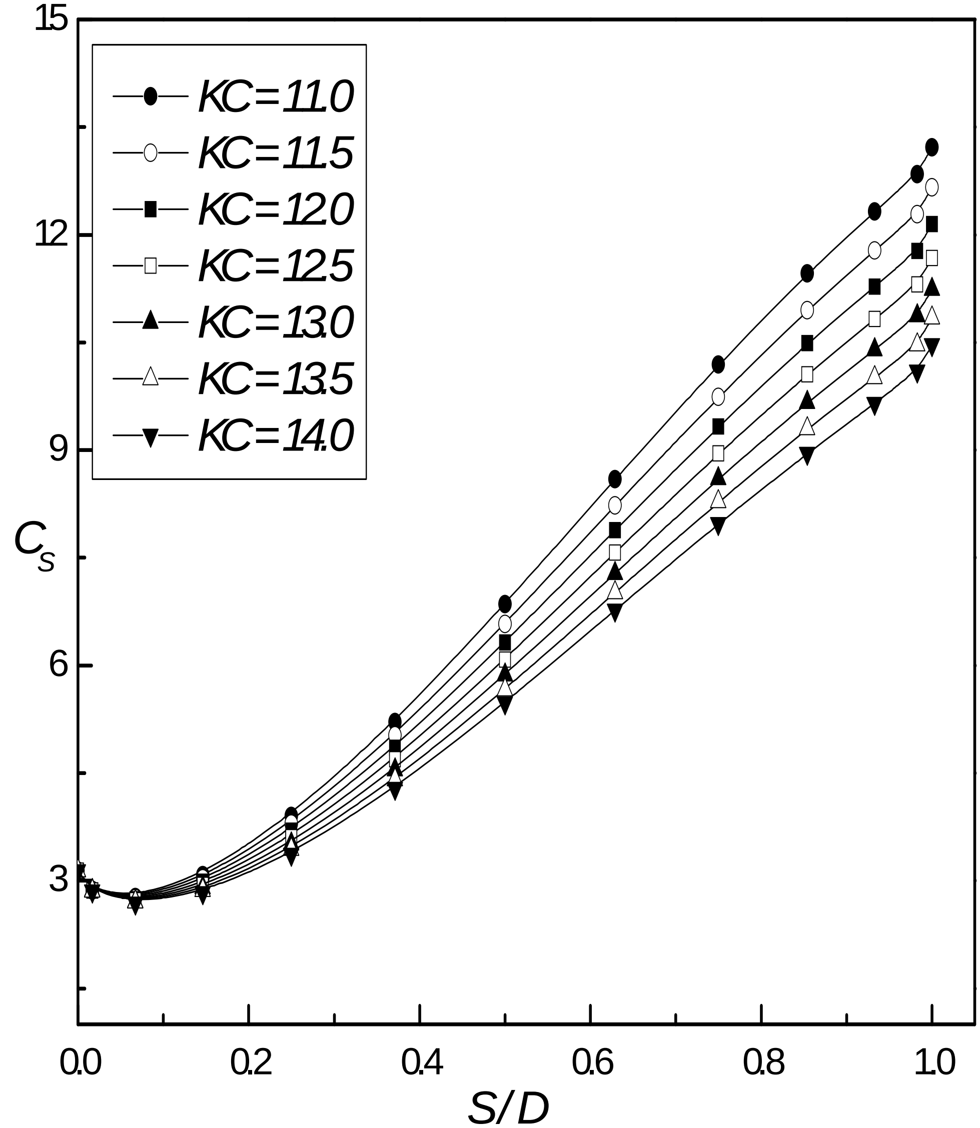

Figure 40. Variation of the slamming coefficient (C_s) with relative submergence (*S/D*) for different Keulegan-Carpenter numbers (*KC*) at wave length-to-amplitude ratio (*L/A*) is 90 when diameter-to-wave amplitude ratio (*D/A*) is 0.2 and height-to-wave amplitude ratio (*h/A*) is 0.0.

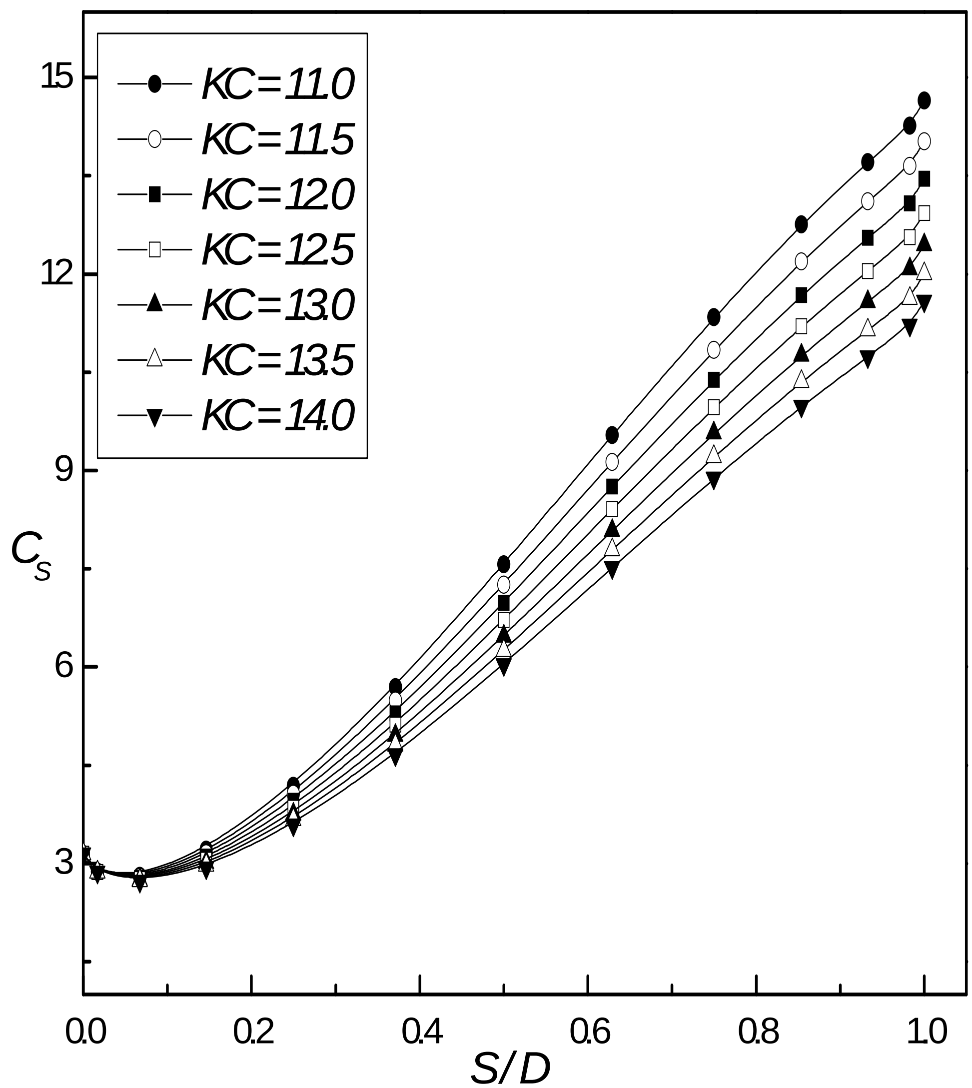

Figure 41. Variation of the slamming coefficient (C_s) with relative submergence (*S/D*) for different Keulegan-Carpenter numbers (*KC*) at wave length-to-amplitude ratio (*L/A*) is 100 when diameter-to-wave amplitude ratio (*D/A*) is 0.2 and height-to-wave amplitude ratio (*h/A*) is 0.0.

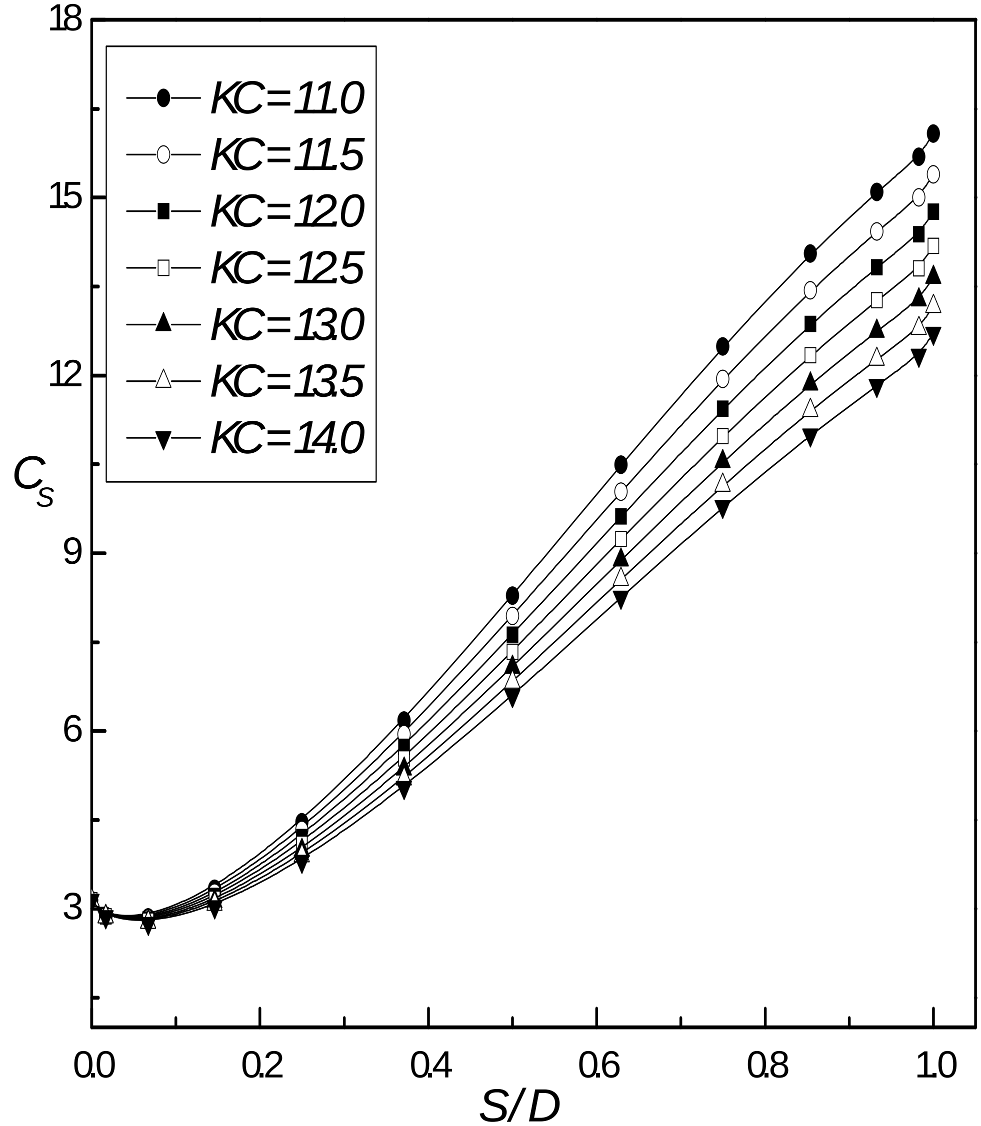

Figure 42. Variation of the slamming coefficient (C_s) with relative submergence (*S/D*) for different Keulegan-Carpenter numbers (*KC*) at wave length-to-amplitude ratio (*L/A*) is110 when diameter-to-wave amplitude ratio (*D/A*) is 0.2 and height-to-wave amplitude ratio (*h/A*) is 0.0.

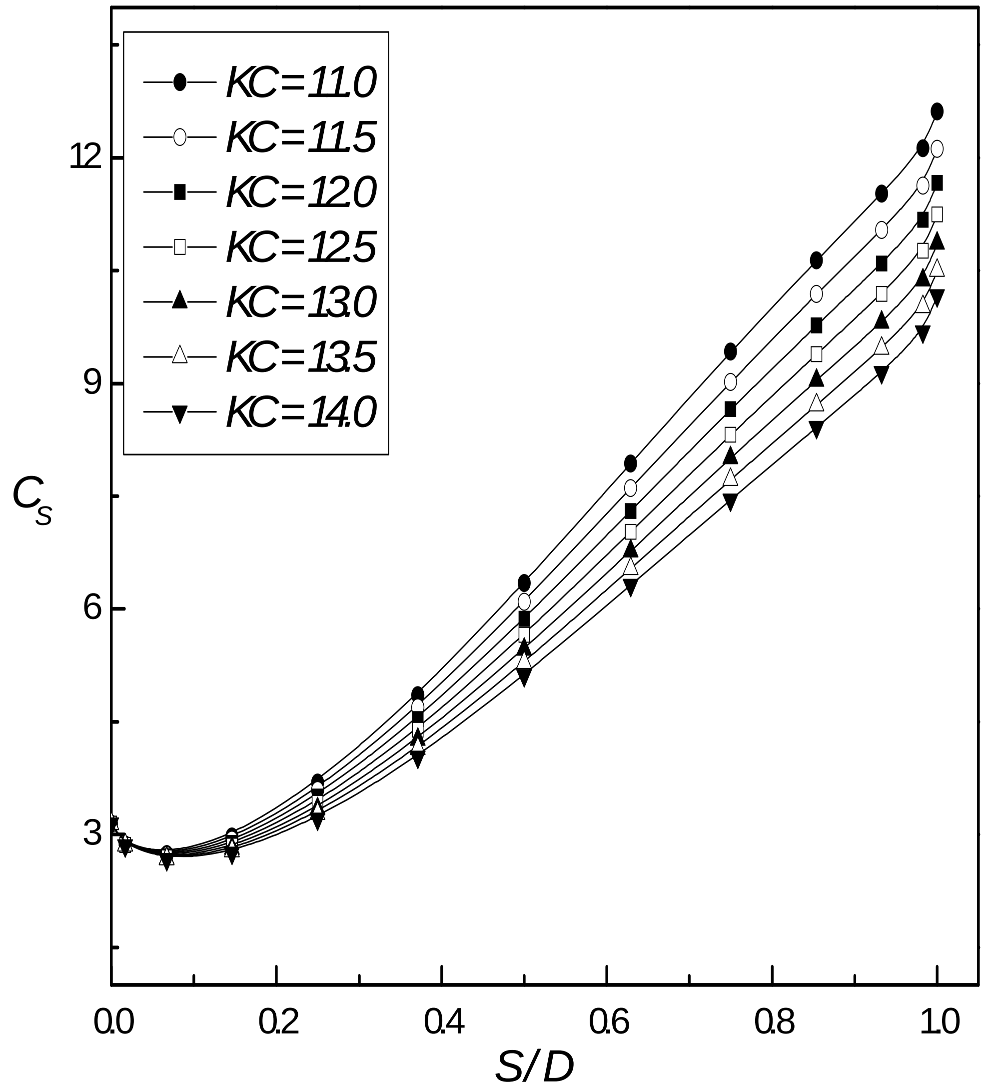

Figure 43. Variation of the slamming coefficient (C_s) with relative submergence (*S/D*) for different Keulegan-Carpenter numbers (*KC*) at wave height-to-amplitude ratio (*h/A*) is equal to 0.0 when *D/A* = 0.2 and *L/A* = 85.

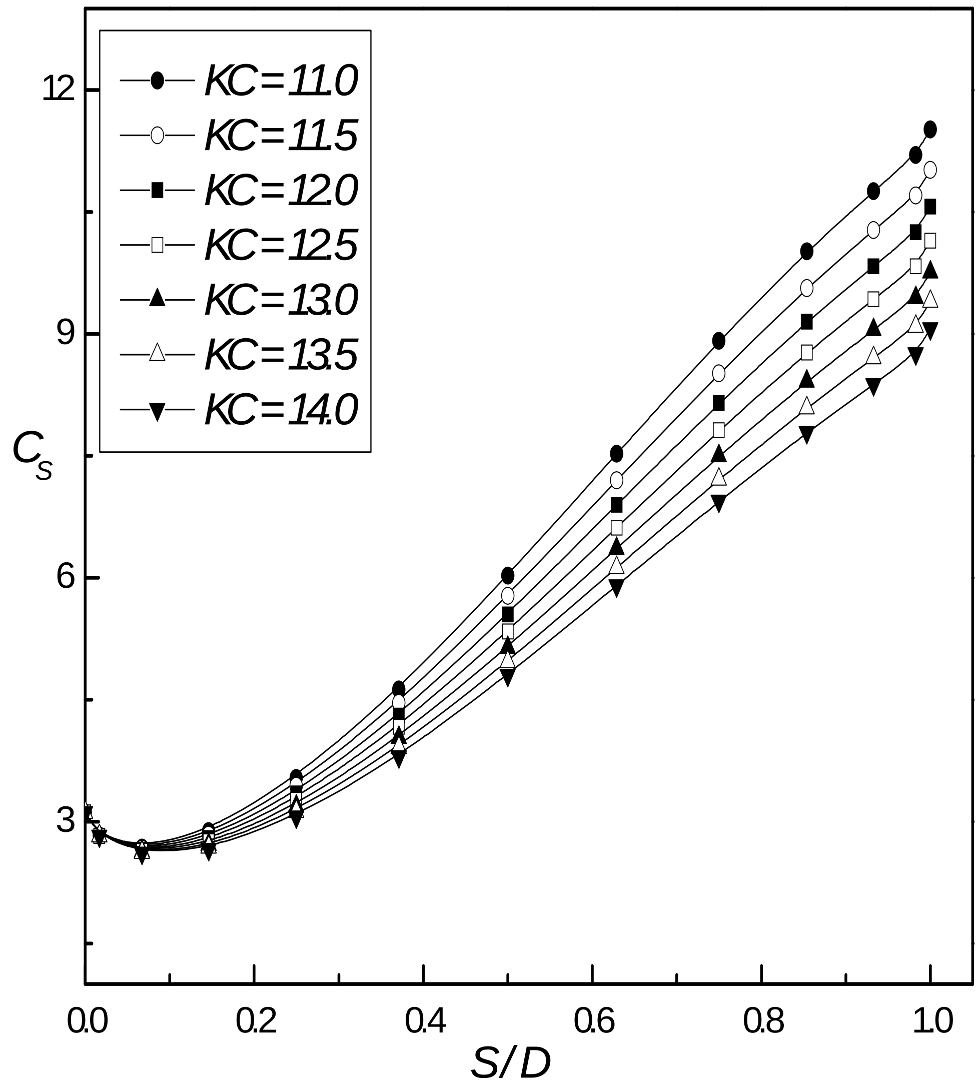

Figure 44. Variation of the slamming coefficient (C_s) with relative submergence (*S/D*) for different Keulegan-Carpenter numbers (*KC*) at wave height-to-amplitude ratio (*h/A*) is equal to 0.1 when *D/A* = 0.2 and *L/A* = 85.

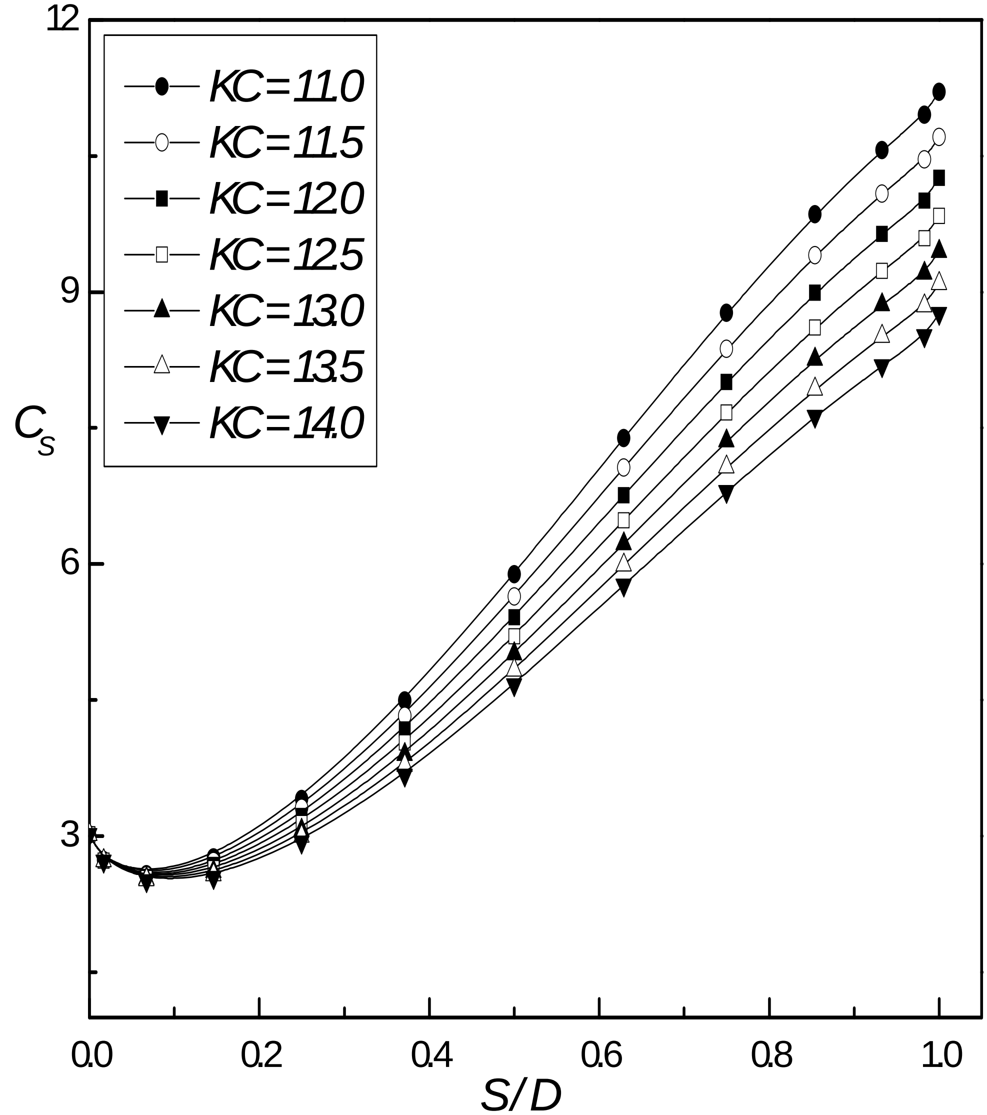

Figure 45. Variation of the slamming coefficient (C_s) with relative submergence (*S/D*) for different Keulegan-Carpenter numbers (*KC*) at wave height-to-amplitude ratio (*h/A*) is equal to 0.2 when *D/A* = 0.2 and *L/A* = 85.

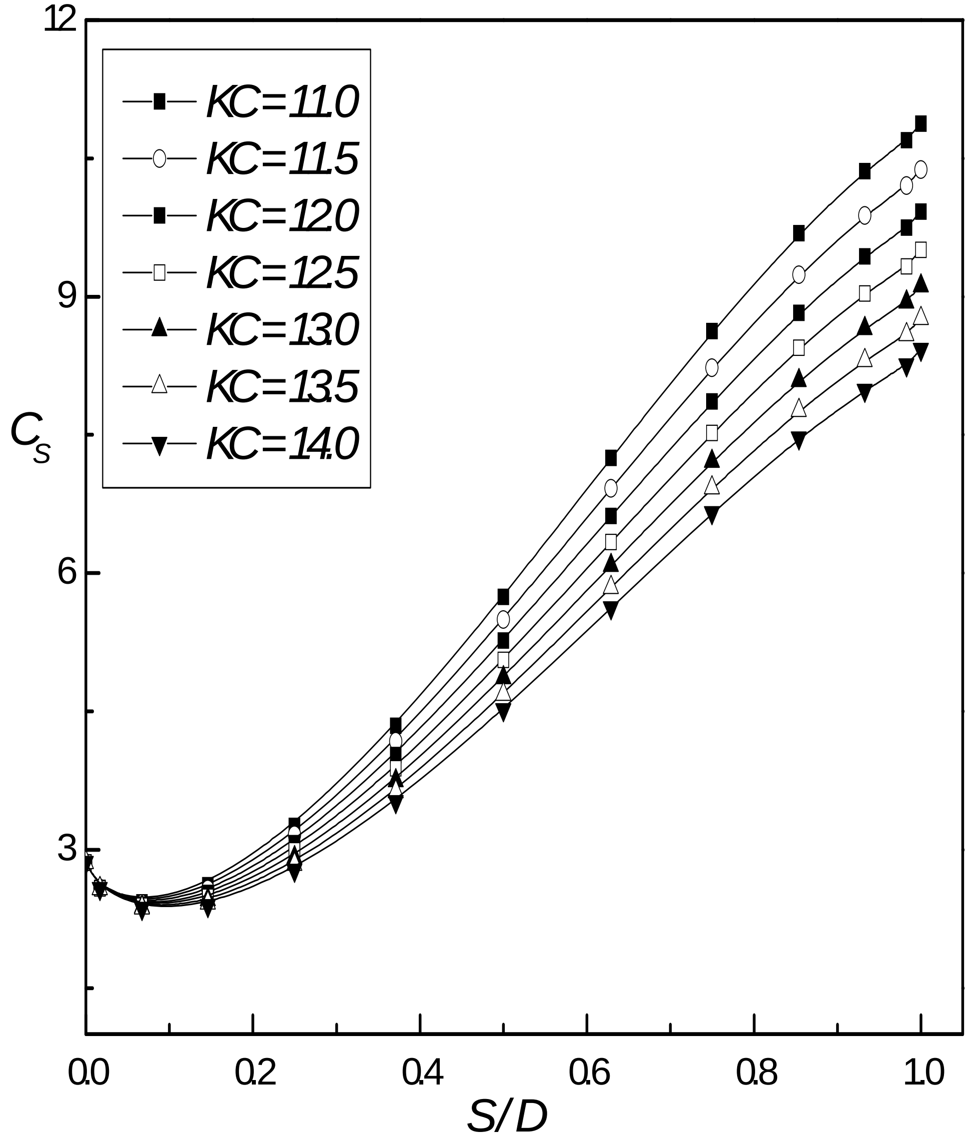

Figure 46. Variation of the slamming coefficient (C_s) with relative submergence (*S/D*) for different Keulegan-Carpenter numbers (*KC*) at wave height-to-amplitude ratio (*h/A*) is equal to 0.3 when *D/A* = 0.2 and *L/A* = 85.

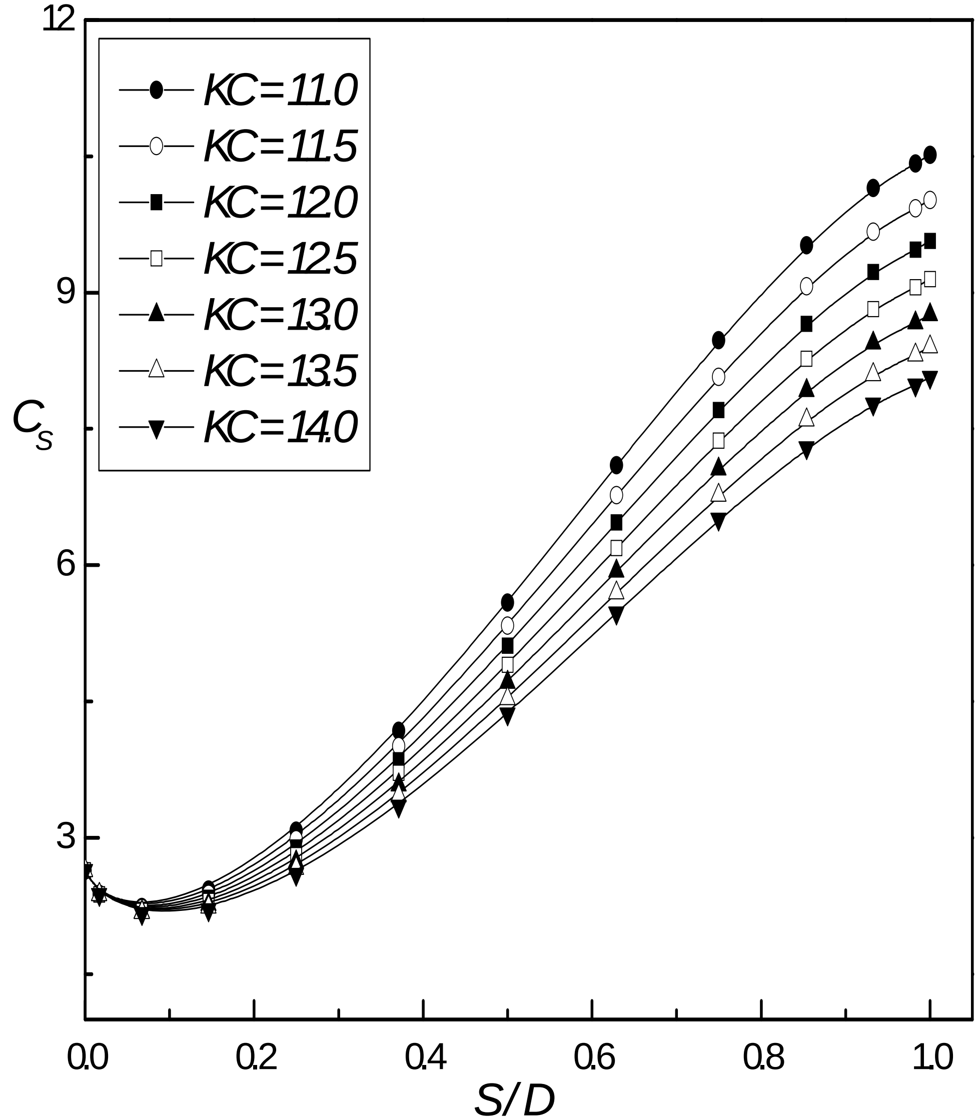

Figure 47. Variation of the slamming coefficient (C_s) with relative submergence (*S/D*) for different Keulegan-Carpenter numbers (*KC*) at wave height-to-amplitude ratio (*h/A*) is equal to 0.4 when *D/A* = 0.2 and *L/A* = 85.

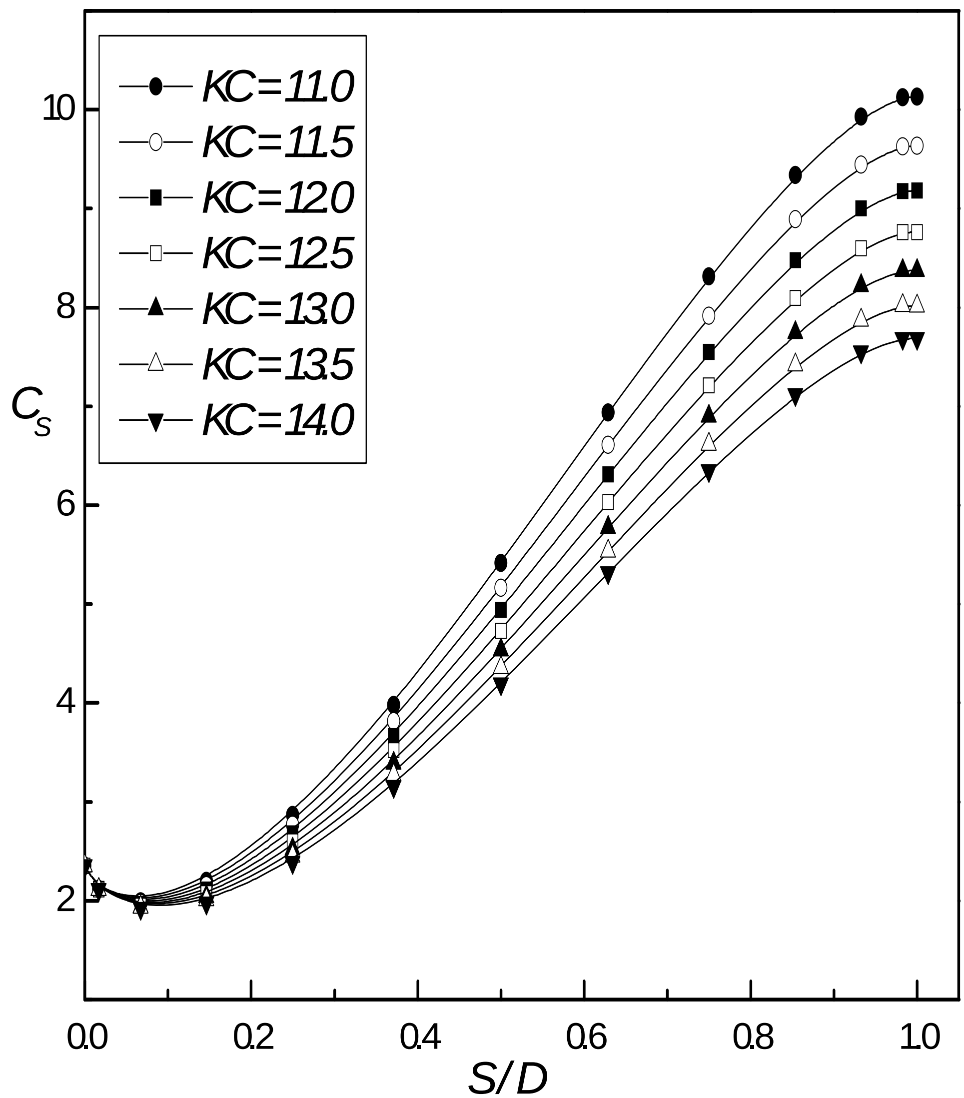

Figure 48. Variation of the slamming coefficient (C_s) with relative submergence (*S/D*) for different Keulegan-Carpenter numbers (*KC*) at wave height-to-amplitude ratio (*h/A*) is equal to 0.5 when *D/A* = 0.2 and *L/A* = 85.

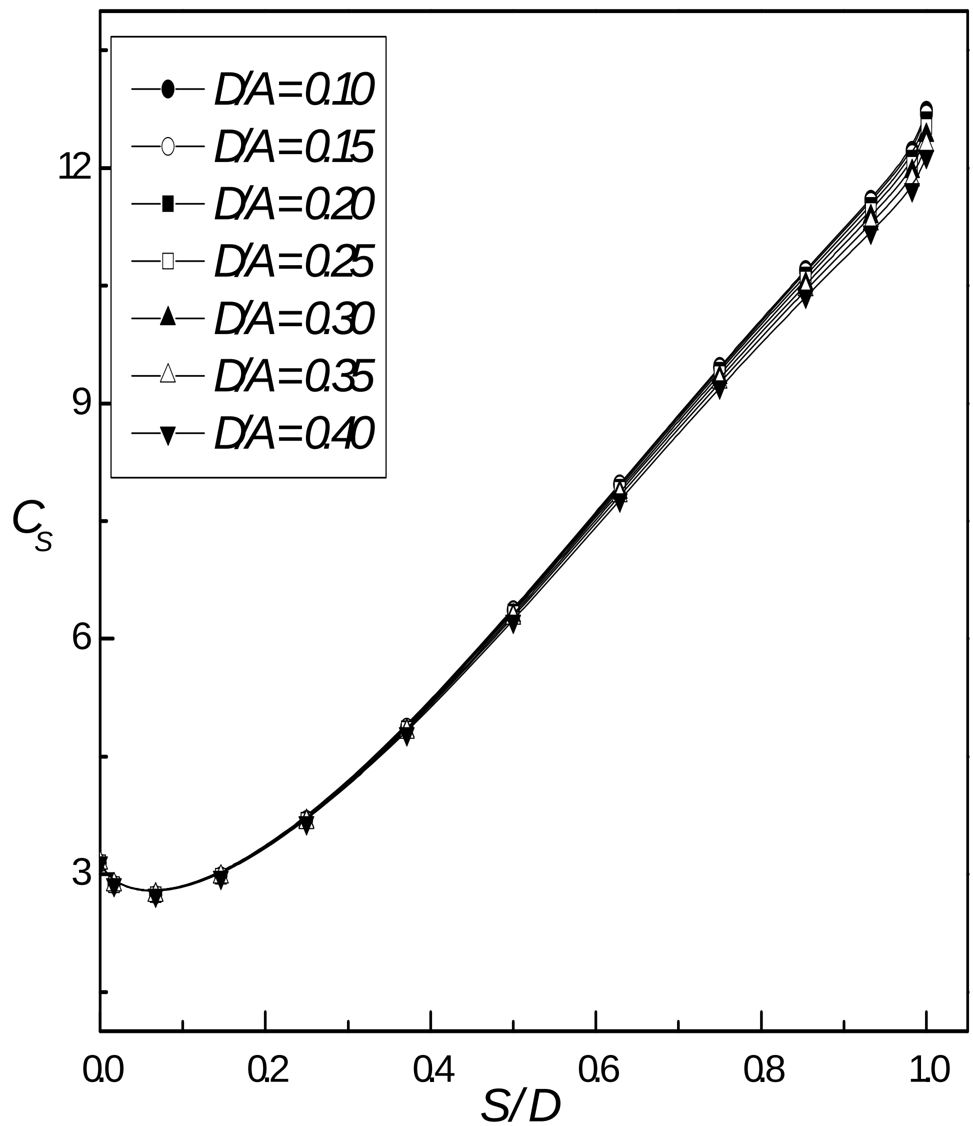

Figure 49. Variation of slamming coefficient (*Cs*) with relative submergence (*S/D*) for different values of cylinder diameter-to-wave amplitude ratio (*D/A*) at height-to-amplitude ratio (*h/A*) is equal to 0.0 when *L/A* = 85 and *KC* = 11

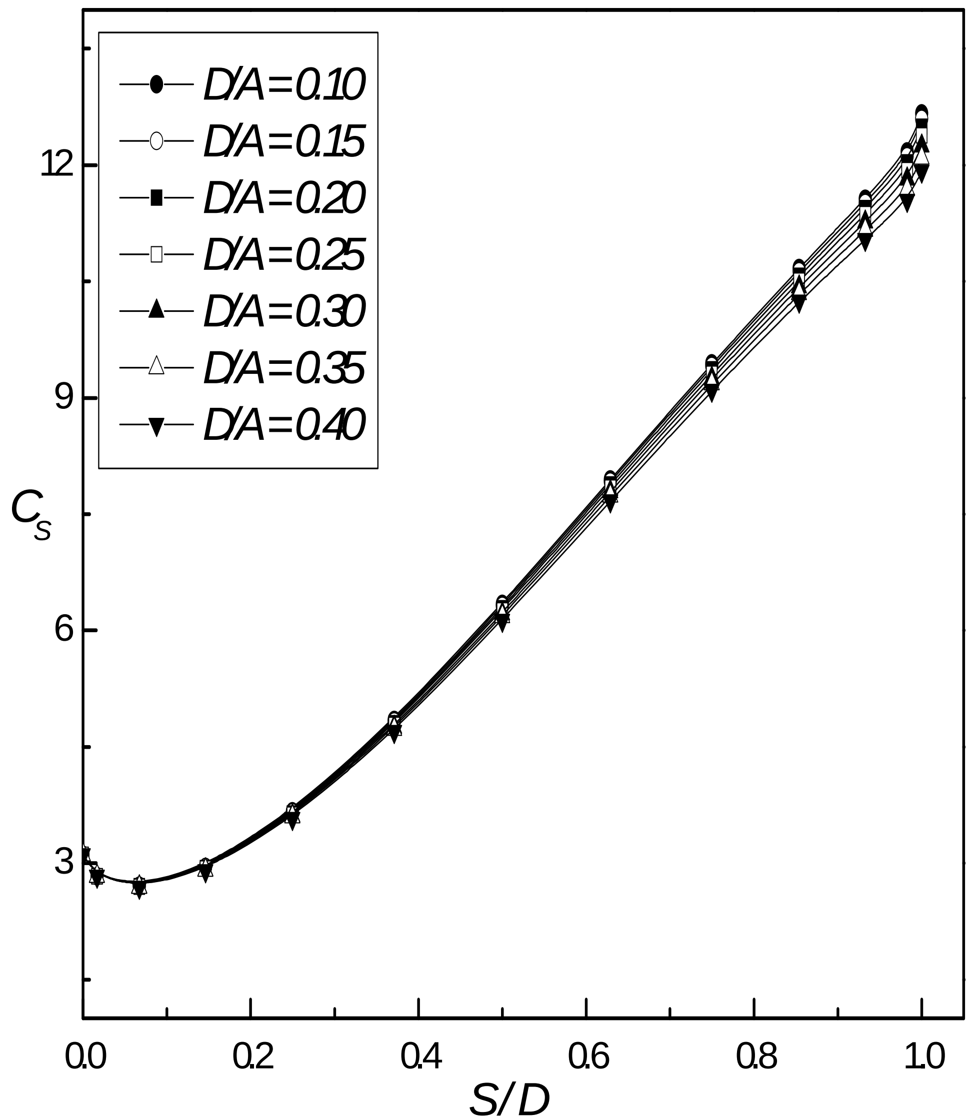

Figure 50. Variation of slamming coefficient (*Cs*) with relative submergence (*S/D*) for different values of cylinder diameter-to-wave amplitude ratio (*D/A*) at height-to-amplitude ratio (*h/A*) is equal to 0.1 when *L/A* = 85 and *KC* = 11

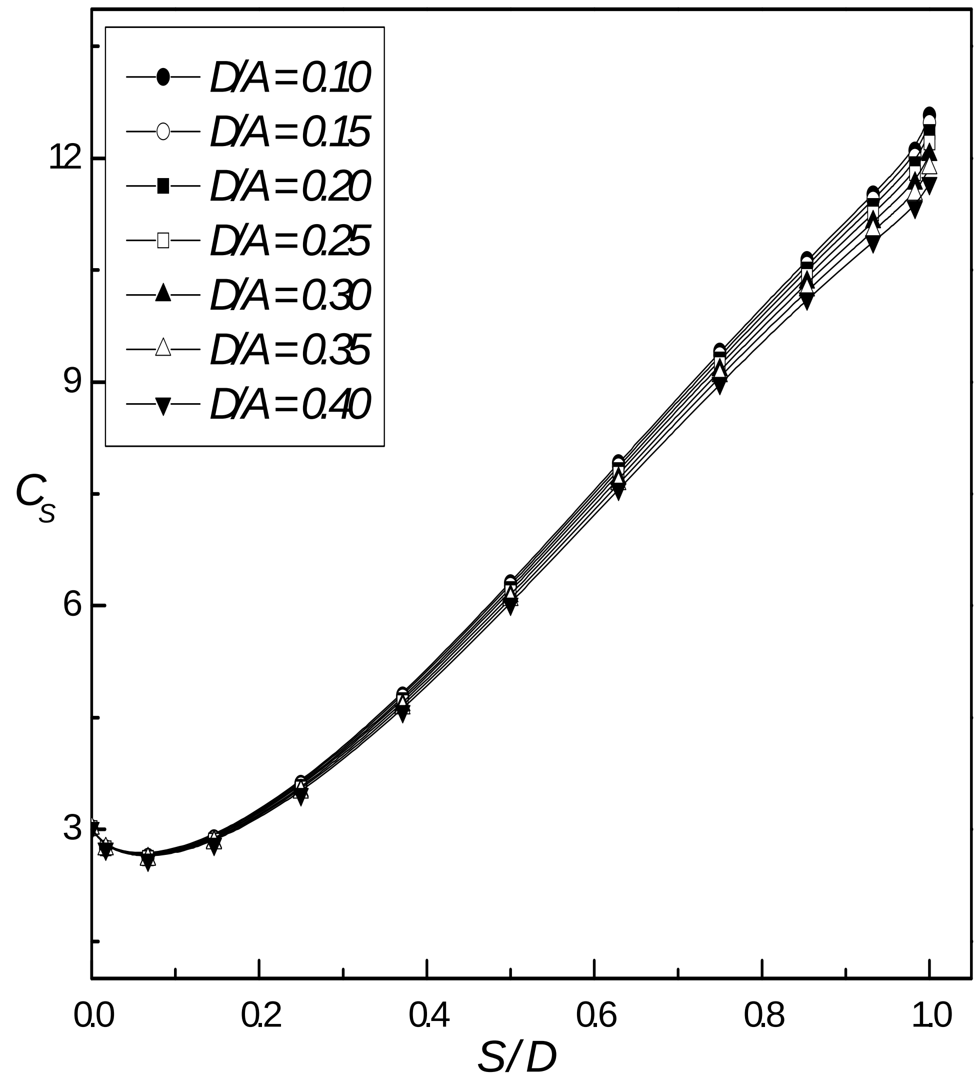

Figure 51. Variation of slamming coefficient (*Cs*) with relative submergence (*S/D*) for different values of cylinder diameter-to-wave amplitude ratio (*D/A*) at height-to-amplitude ratio (*h/A*) is equal to 0.2 when *L/A* = 85 and *KC* = 11

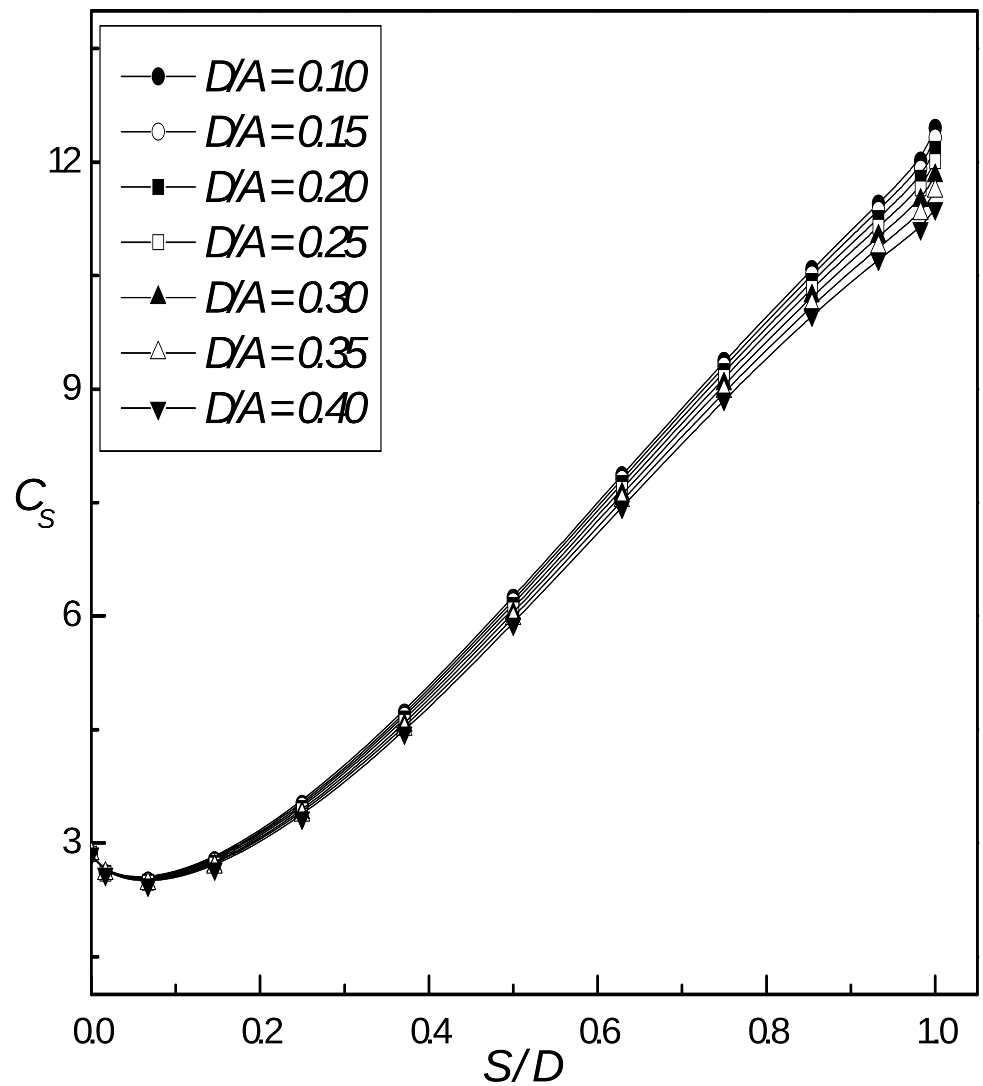

Figure 52. Variation of slamming coefficient (*Cs*) with relative submergence (*S/D*) for different values of cylinder diameter-to-wave amplitude ratio (*D/A*) at height-to-amplitude ratio (*h/A*) is equal to 0.3 when *L/A* = 85 and *KC* = 11

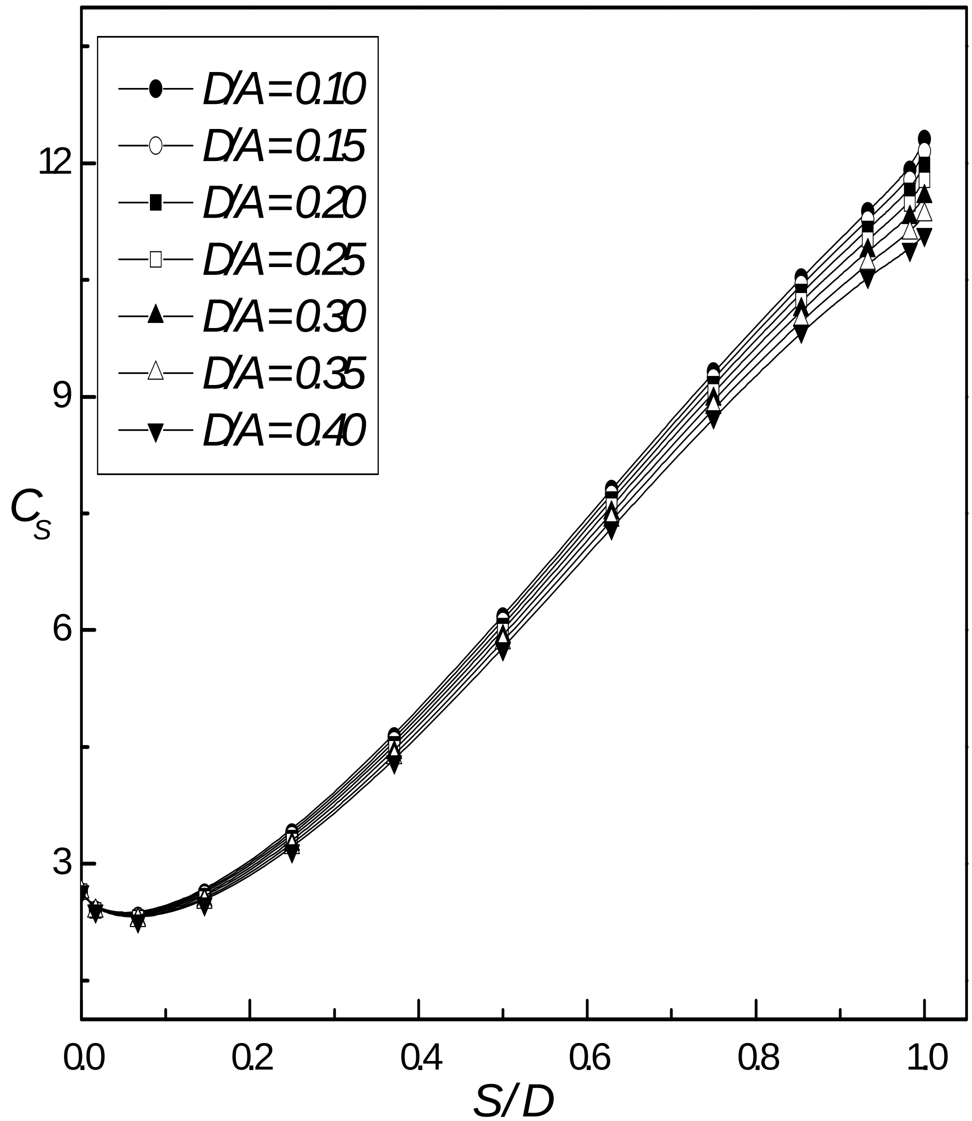

Figure 53. Variation of slamming coefficient (*Cs*) with relative submergence (*S/D*) for different values of cylinder diameter-to-wave amplitude ratio (*D/A*) at height-to-amplitude ratio (*h/A*) is equal to 0.4 when *L/A* = 85 and *KC* = 11

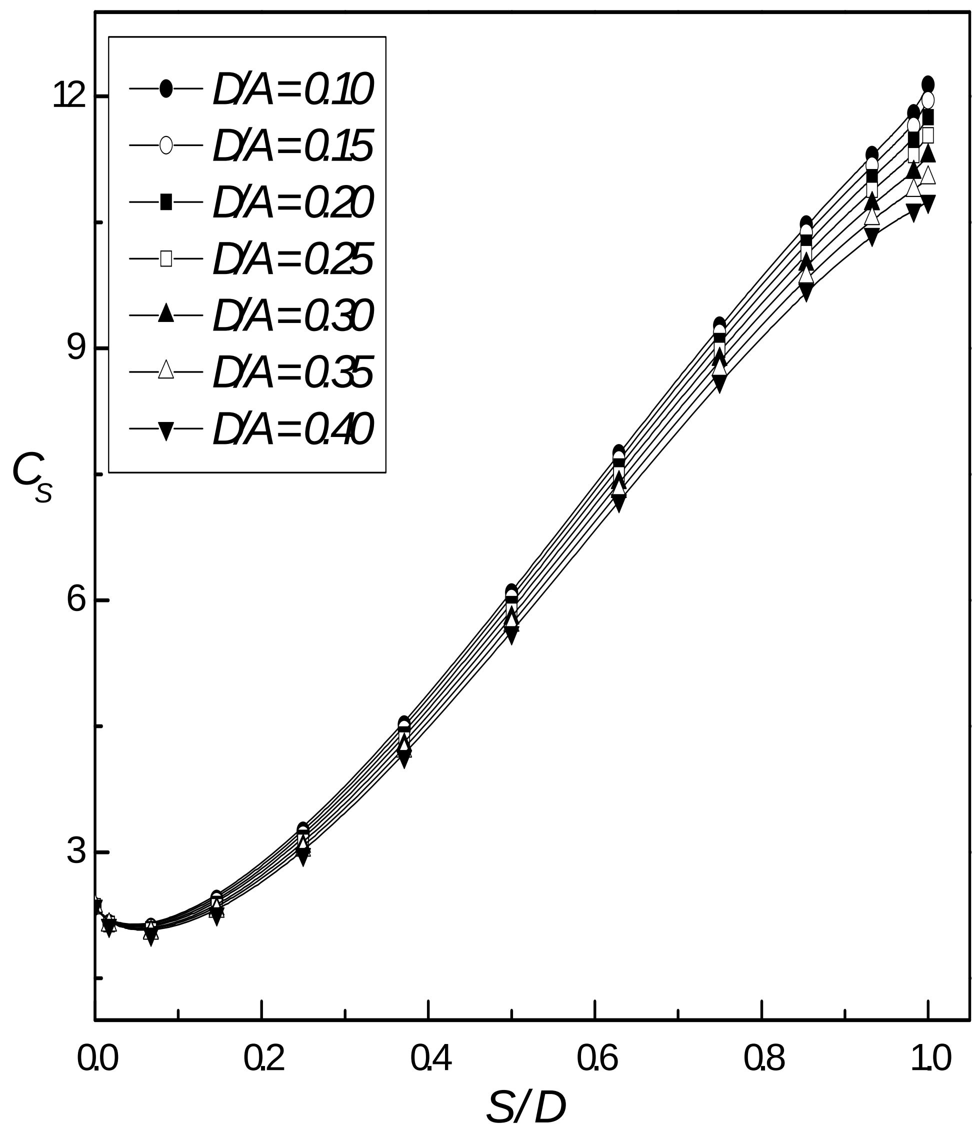

Figure 54. Variation of slamming coefficient (*Cs*) with relative submergence (*S/D*) for different values of cylinder diameter-to-wave amplitude ratio (*D/A*) at height-to-amplitude ratio (*h/A*) is equal to 0.5 when *L/A* = 85 and *KC* = 11

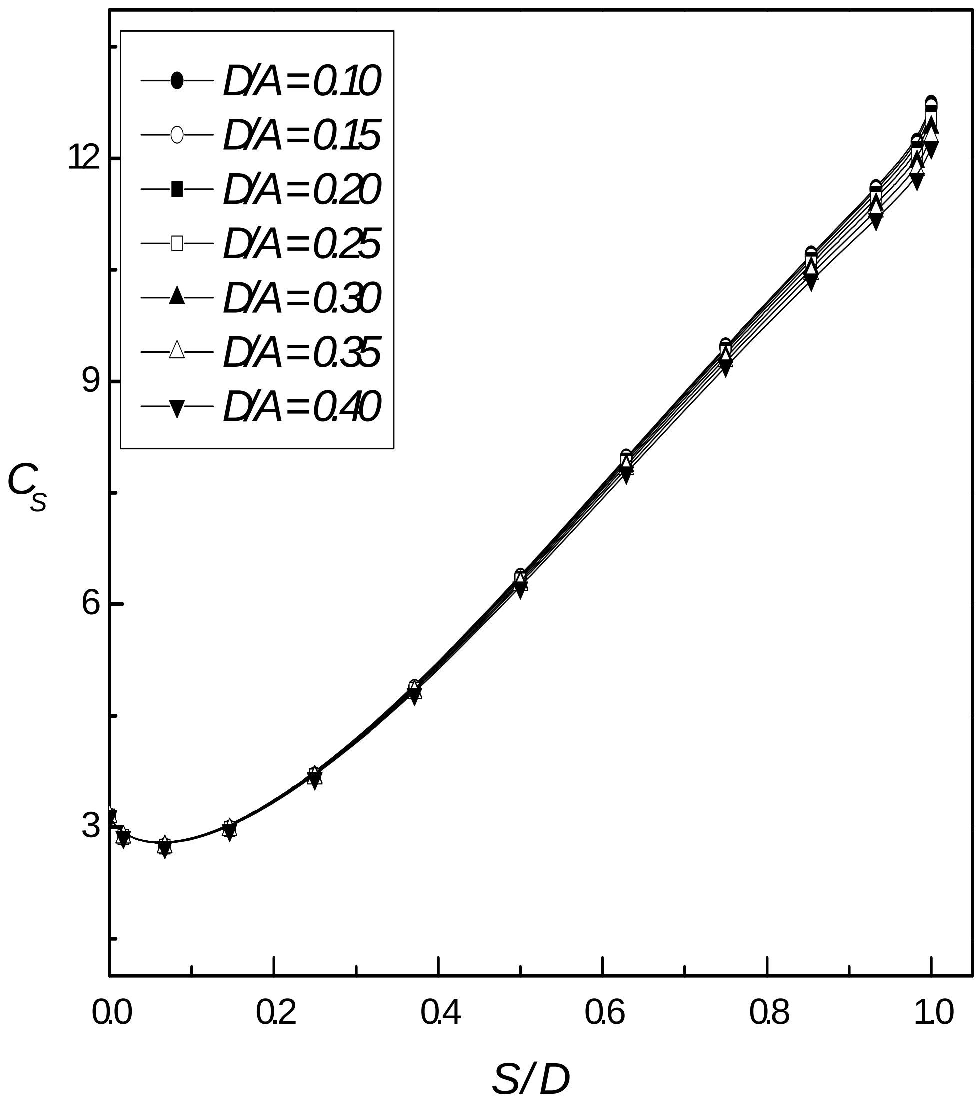

Figure 55. Variation of slamming coefficient (*Cs*) with relative submergence (*S/D*) for different values of cylinder diameter-to-wave amplitude ratio (*D/A*) at wave length-to-amplitude ratio (*L/A*) is equal to 80 when *h/A* = 0.0 and *KC* = 11.

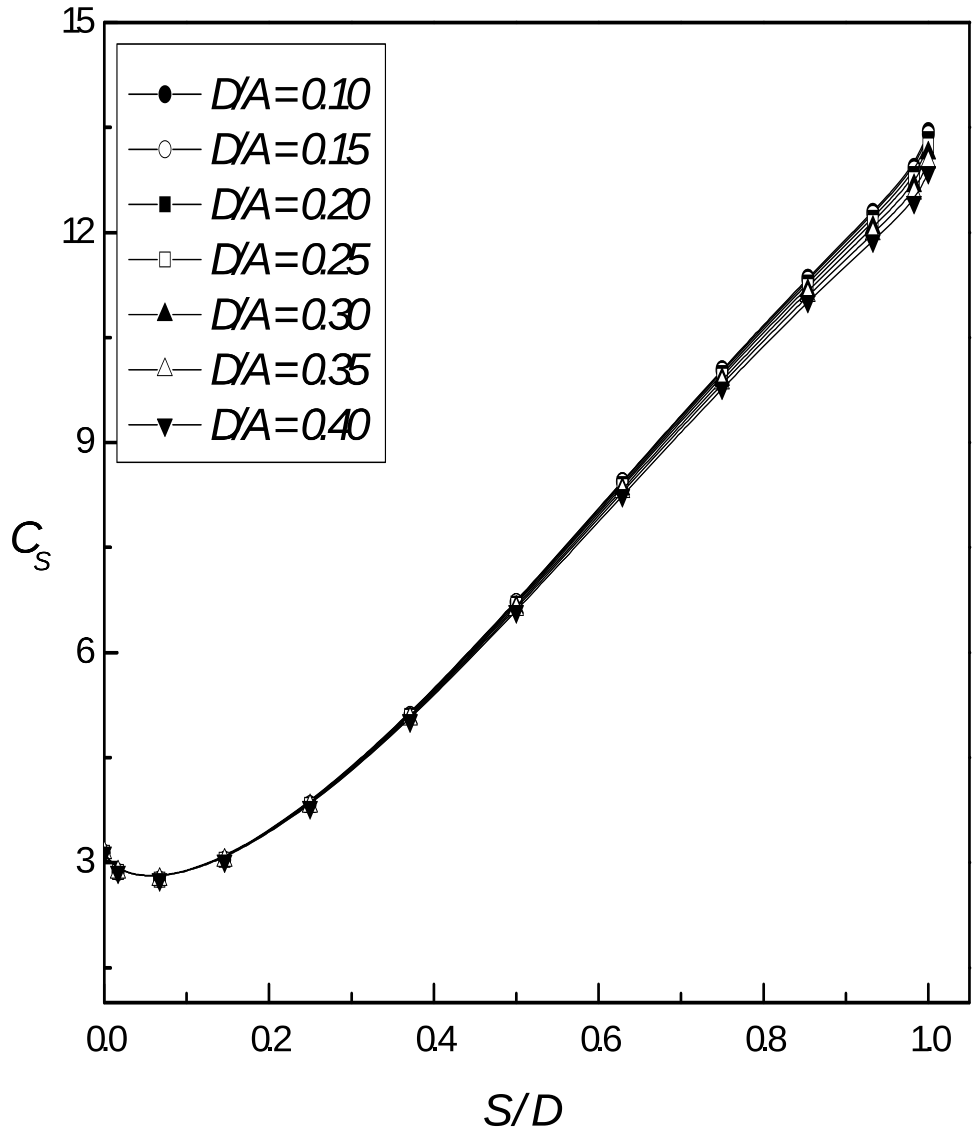

Figure 56. Variation of slamming coefficient (*Cs*) with relative submergence (*S/D*) for different values of cylinder diameter-to-wave amplitude ratio (*D/A*) at wave length-to-amplitude ratio (*L/A*) is equal to 85 when *h/A* = 0.0 and *KC* = 11.

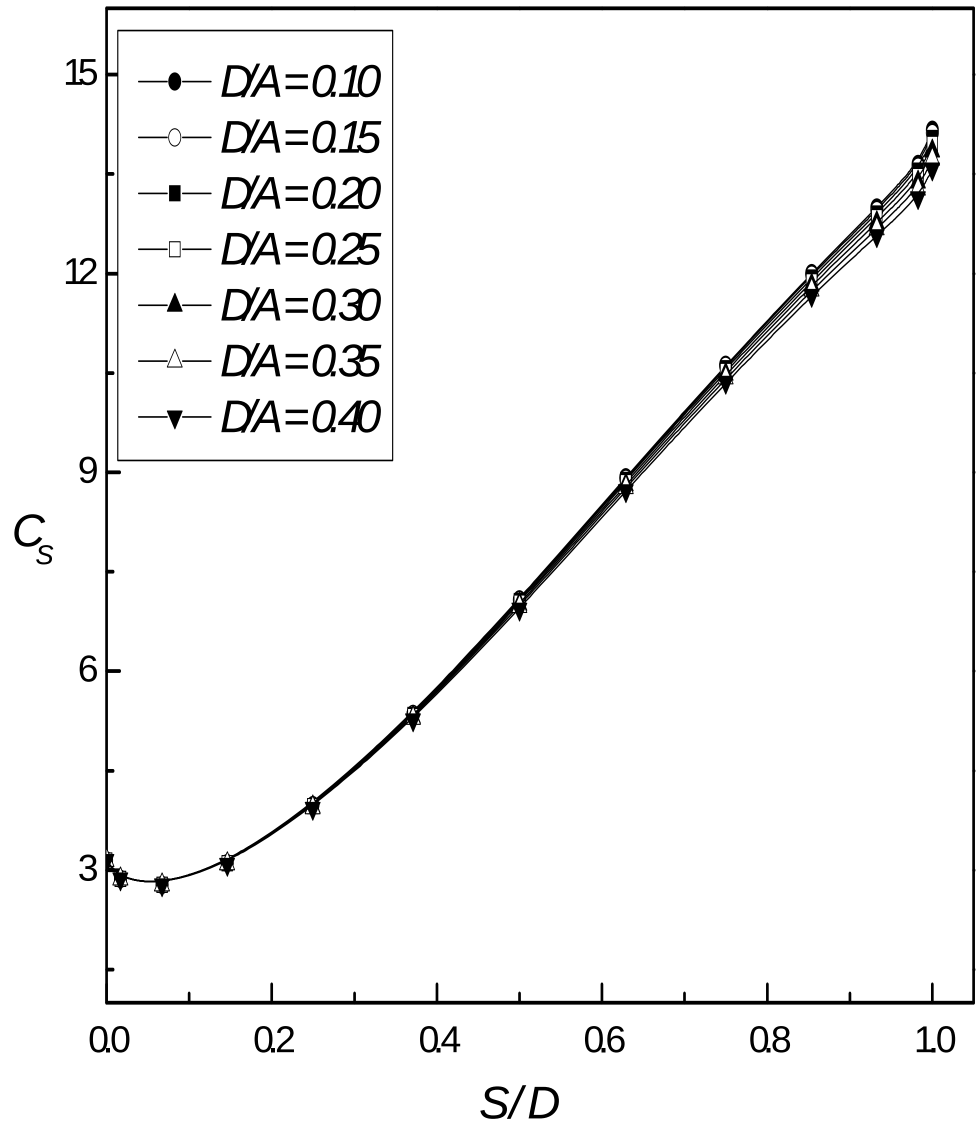

Figure 57. Variation of slamming coefficient (*Cs*) with relative submergence (*S/D*) for different values of cylinder diameter-to-wave amplitude ratio (*D/A*) at wave length-to-amplitude ratio (*L/A*) is equal to 90 when h/A = 0.0 and KC = 11.

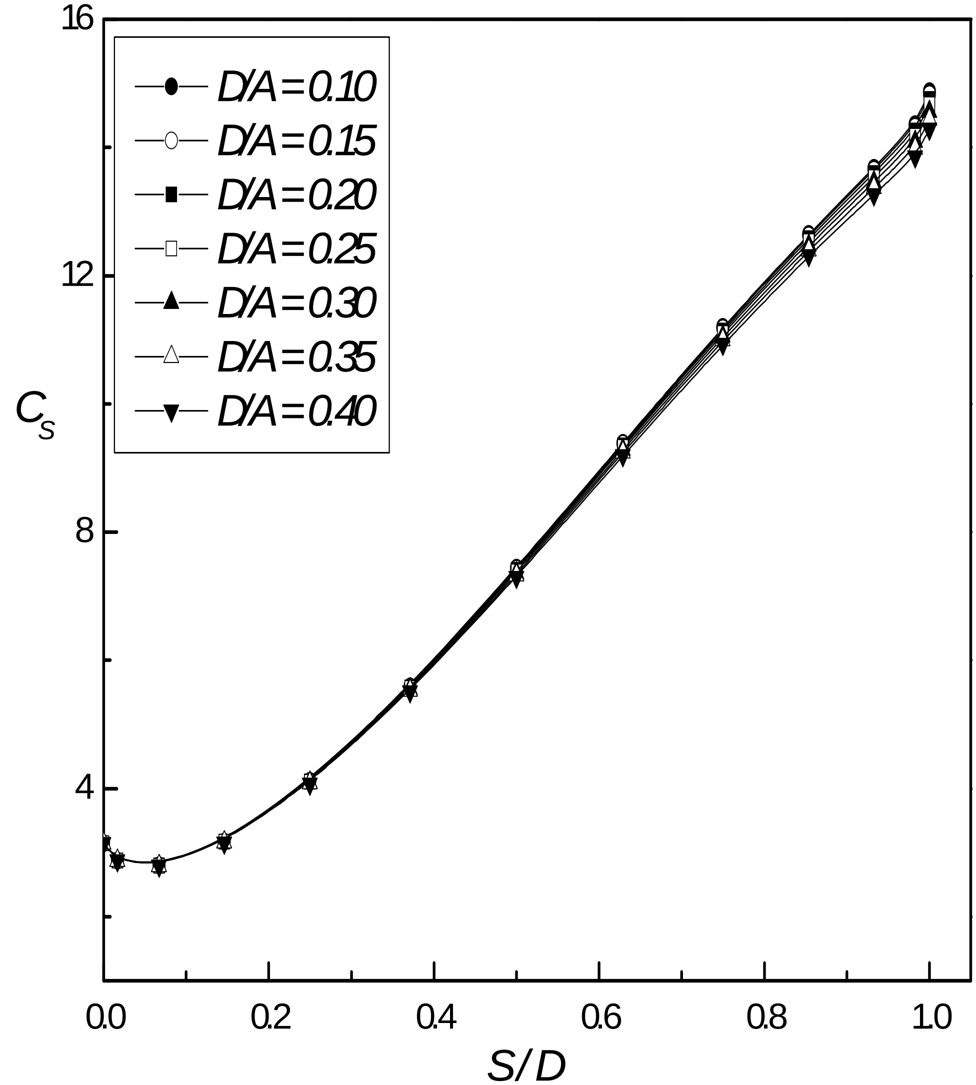

Figure 59. Variation of slamming coefficient (*Cs*) with relative submergence (*S/D*) for different values of cylinder diameter-to-wave amplitude ratio (*D/A*) at wave length-to-amplitude ratio (*L/A*) is equal to 95 when *h/A* = 0.0 and *KC* = 11.

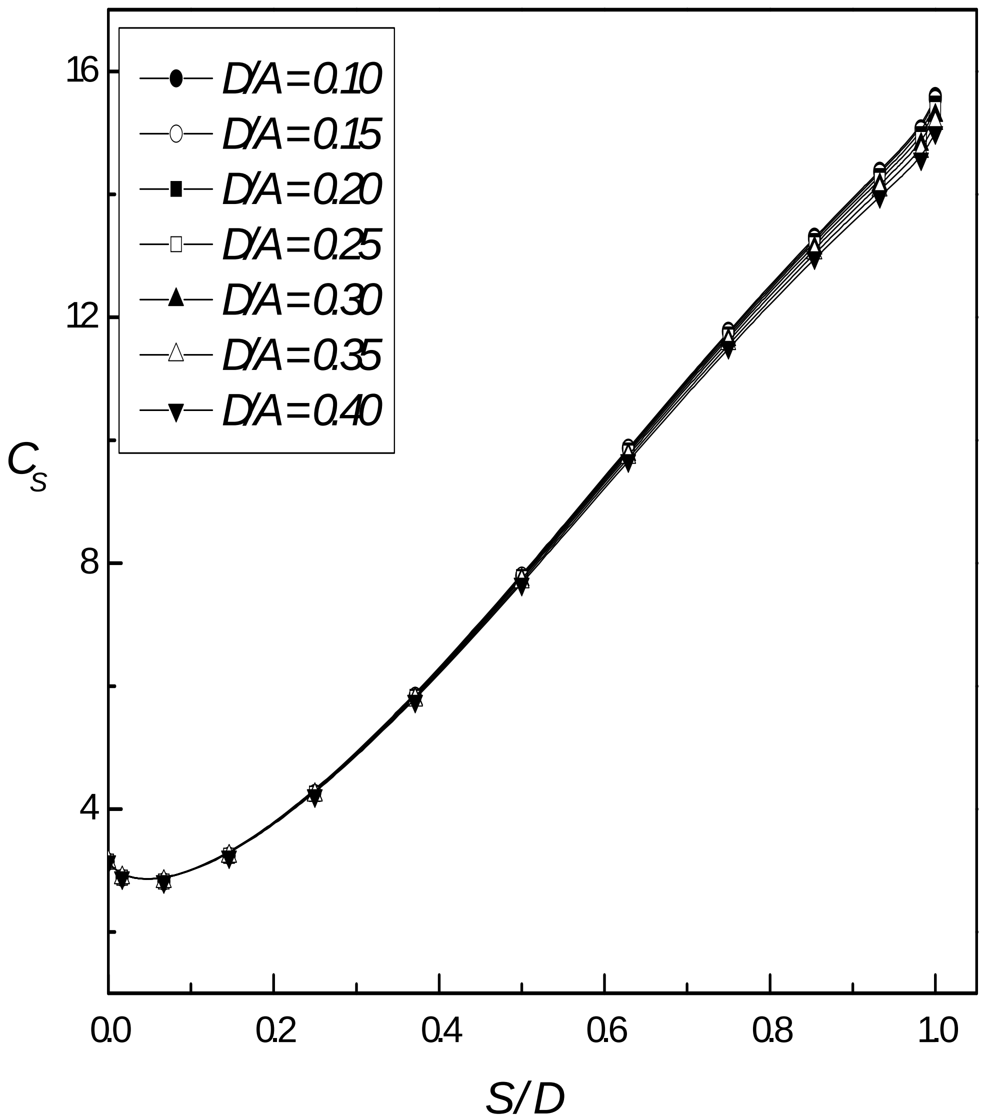

Figure 59. Variation of slamming coefficient (*Cs*) with relative submergence (*S/D*) for different values of cylinder diameter-to-wave amplitude ratio (*D/A*) at wave length-to-amplitude ratio (*L/A*) is equal to 100 when *h/A* = 0.0 and *KC* = 11.

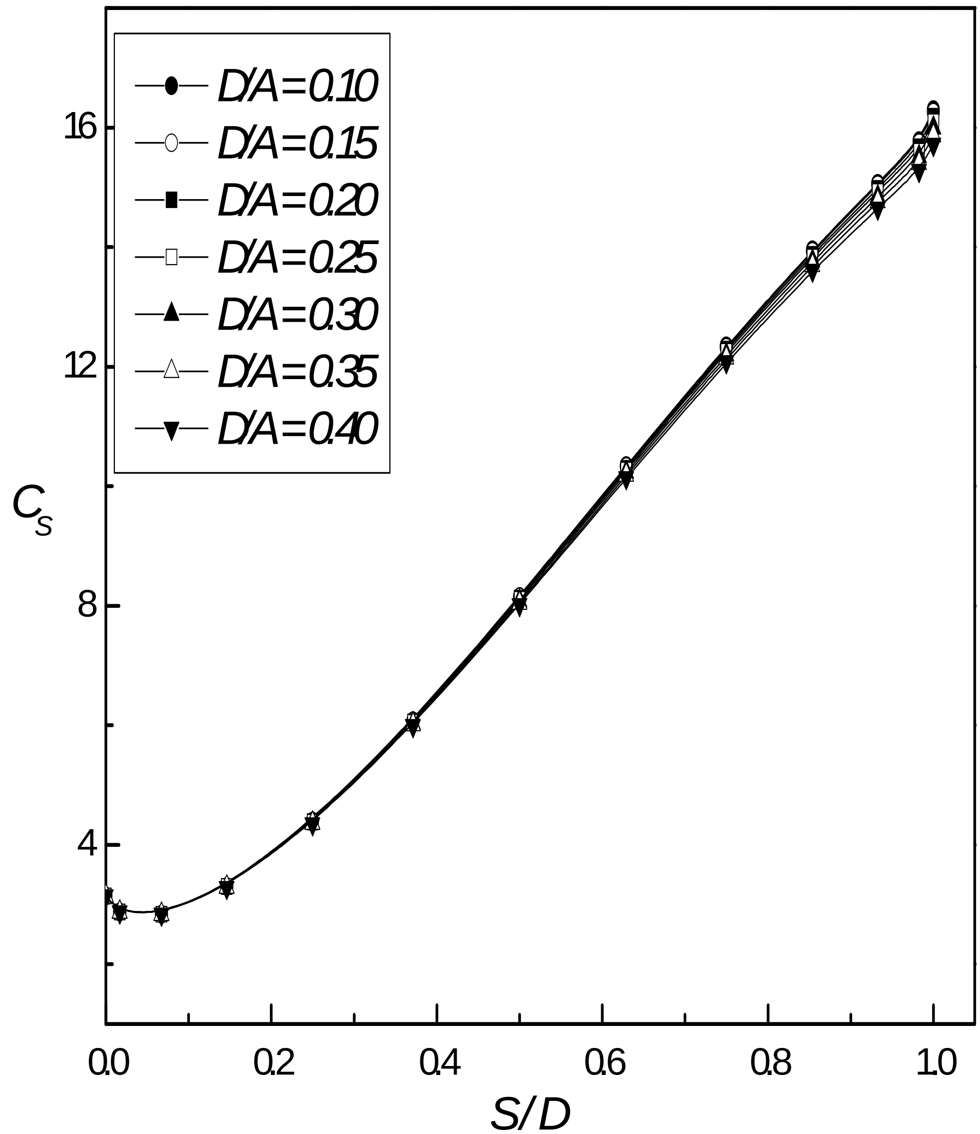

Figure 60. Variation of slamming coefficient (*Cs*) with relative submergence (*S/D*) for different values of cylinder diameter-to-wave amplitude ratio (*D/A*) at wave length-to-amplitude ratio (*L/A*) is equal to 105 when *h/A* = 0.0 and *KC* = 11.

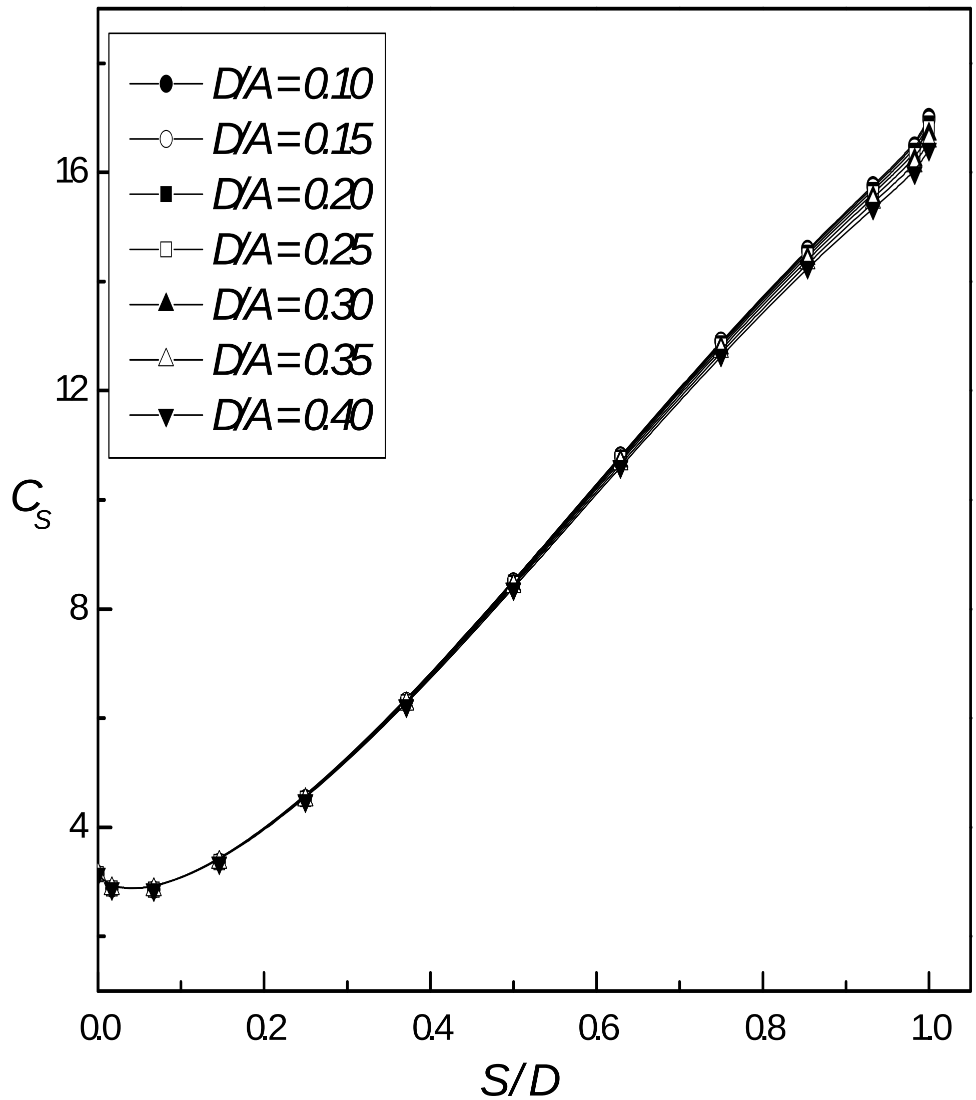

Figure 61. Variation of slamming coefficient (*Cs*) with relative submergence (*S/D*) for different values of cylinder diameter-to-wave amplitude ratio (*D/A*) at wave length-to-amplitude ratio (*L/A*) is equal to 110 when *h/A* = 0.0 and *KC* = 11.

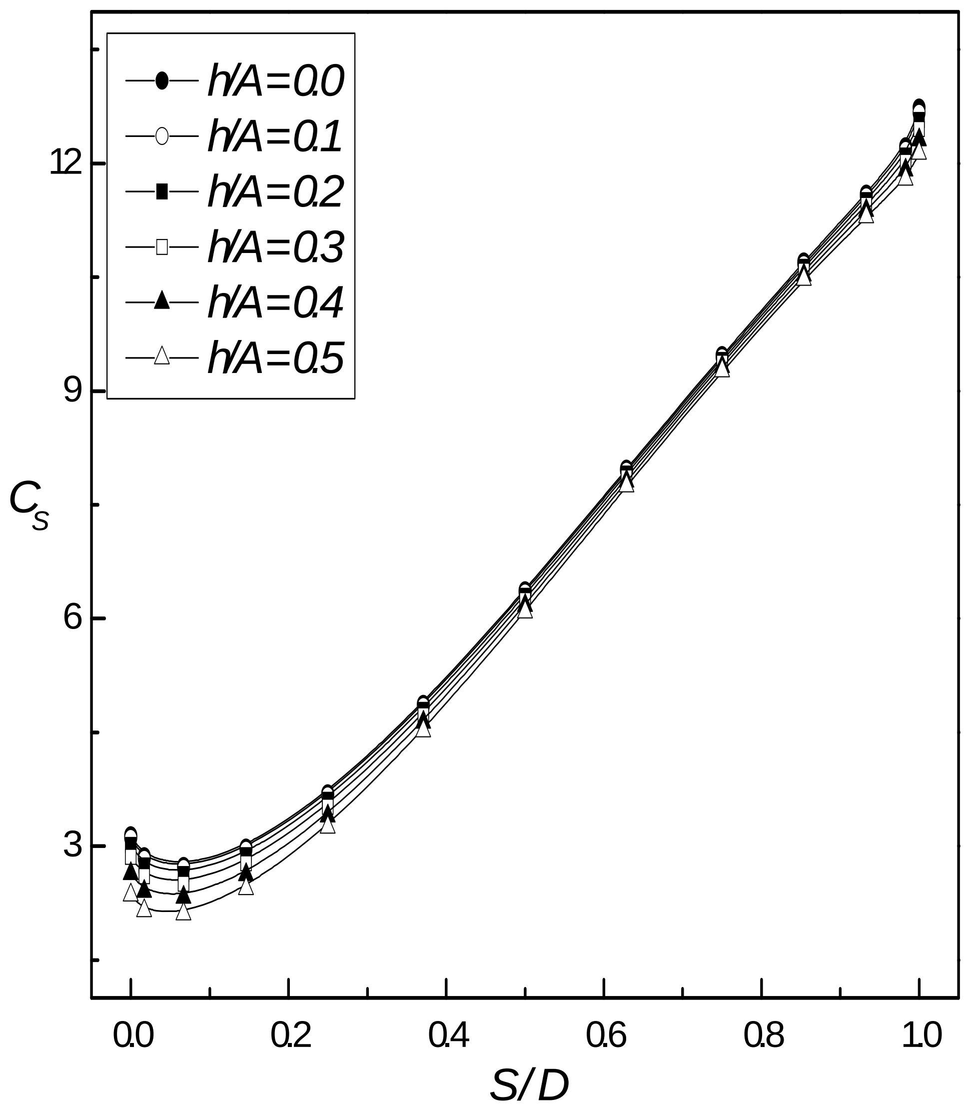

Figure 62. Variation of the slamming coefficient (C_s) with relative submergence (*S/D*) for different values of cylinder height-to-wave amplitude ratio (*h/A*) at diameter-to-wave amplitude ratio (*D/A*) is equal to 0.1 when *L/A* = 85 and *KC* = 11.

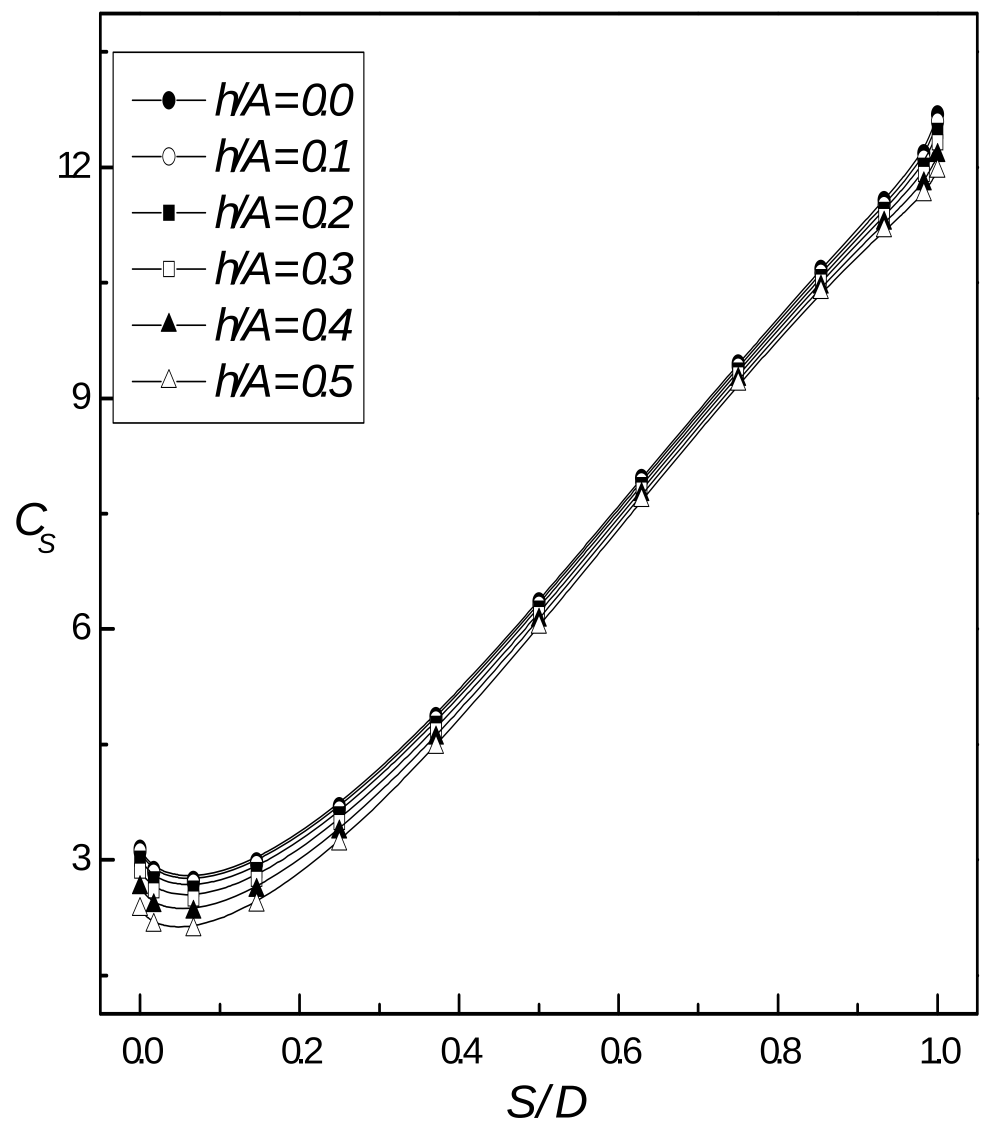

Figure 63. Variation of the slamming coefficient (C_s) with relative submergence (*S/D*) for different values of cylinder height-to-wave amplitude ratio (*h/A*) at diameter-to-wave amplitude ratio (*D/A*) is equal to 0.15 when *L/A* = 85 and *KC* = 11.

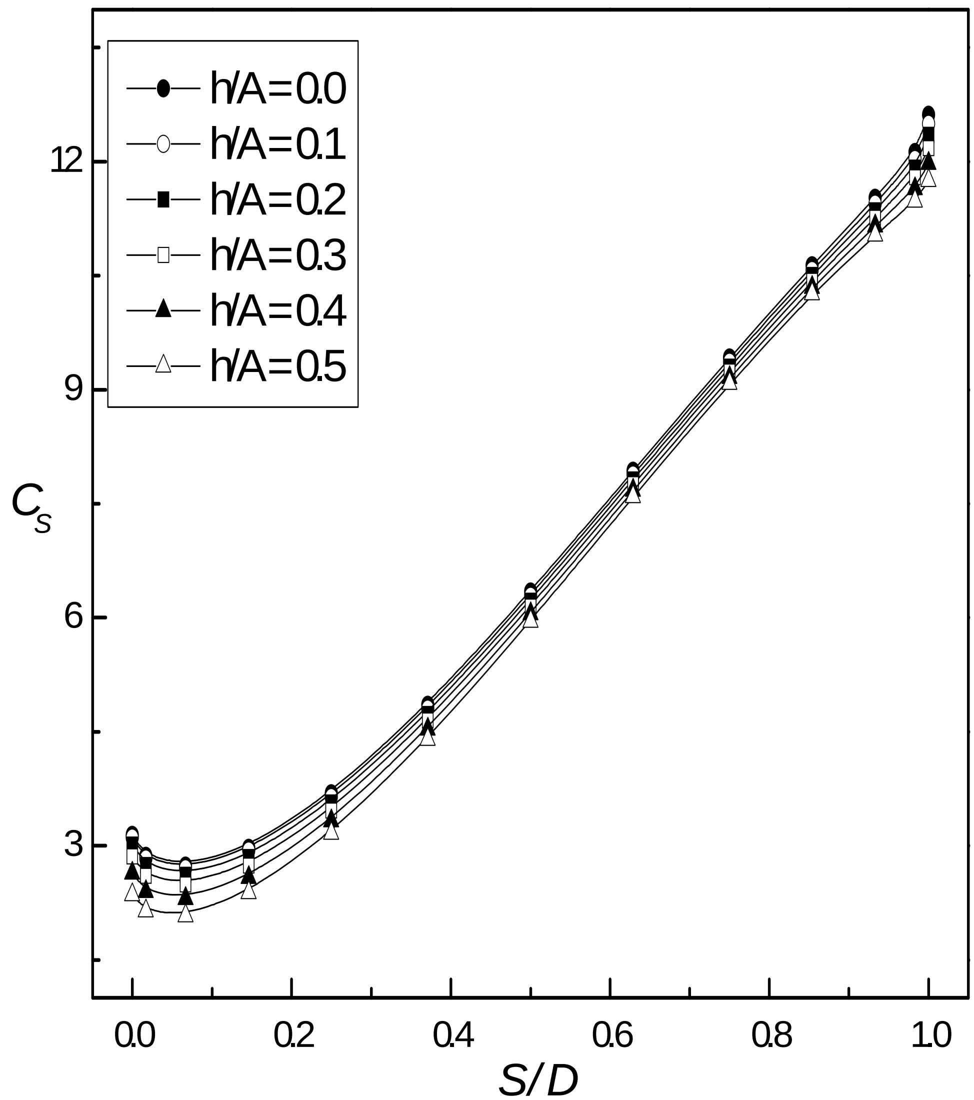

Figure 64. Variation of the slamming coefficient (C_s) with relative submergence (*S/D*) for different values of cylinder height-to-wave amplitude ratio (*h/A*) at diameter-to-wave amplitude ratio (*D/A*) is equal to 0.20 when *L/A* = 85 and *KC* = 11.

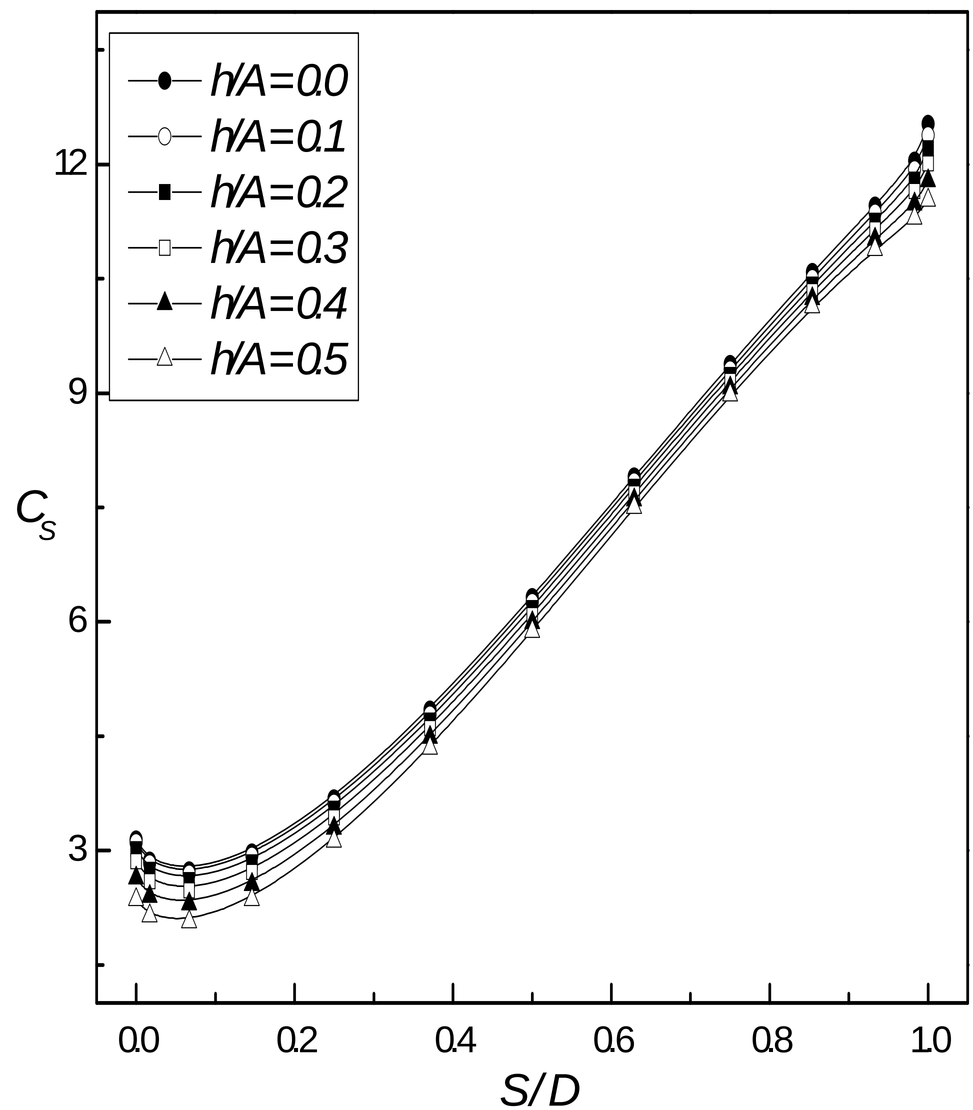

Figure 65. Variation of the slamming coefficient (C_s) with relative submergence (*S/D*) for different values of cylinder height-to-wave amplitude ratio (*h/A*) at diameter-to-wave amplitude ratio (*D/A*) is equal to 0.25 when *L/A* = 85 and *KC* = 11.

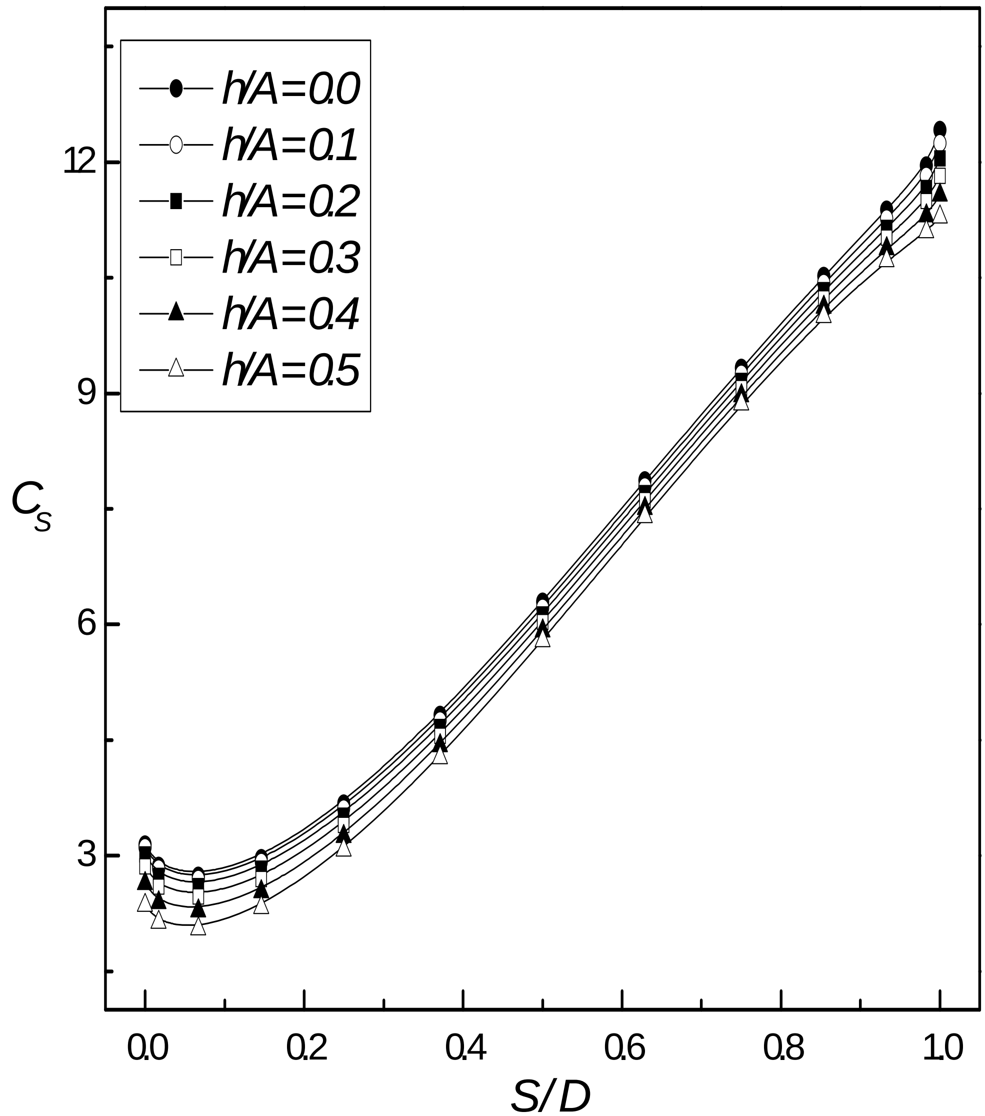

Figure 66. Variation of the slamming coefficient (C_s) with relative submergence (*S/D*) for different values of cylinder height-to-wave amplitude ratio (*h/A*) at diameter-to-wave amplitude ratio (*D/A*) is equal to 0.3 when *L/A* = 85 and *KC* = 11.

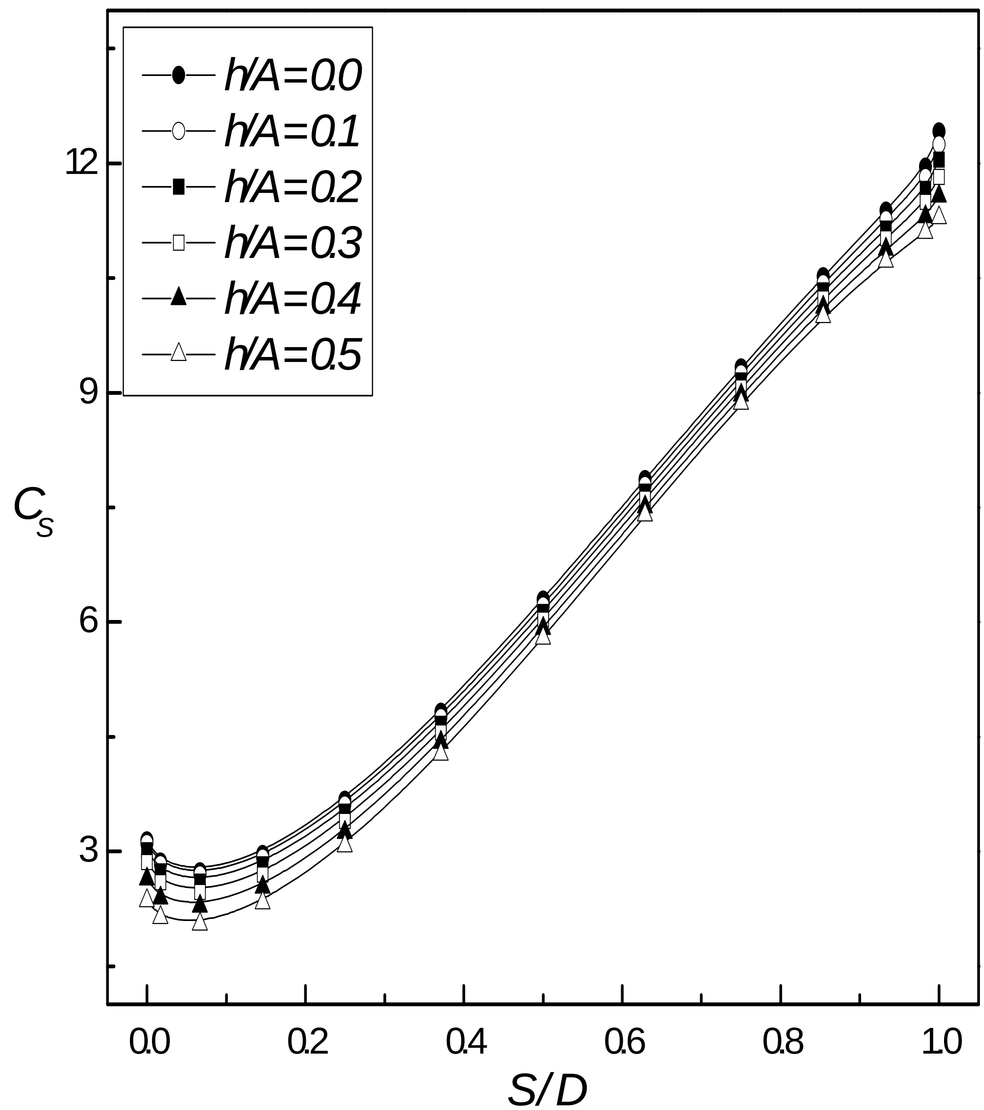

Figure 67. Variation of the slamming coefficient (C_s) with relative submergence (*S/D*) for different values of cylinder height-to-wave amplitude ratio (*h/A*) at diameter-to-wave amplitude ratio (*D/A*) is equal to 0.35 when *L/A* = 85 and *KC* = 11.

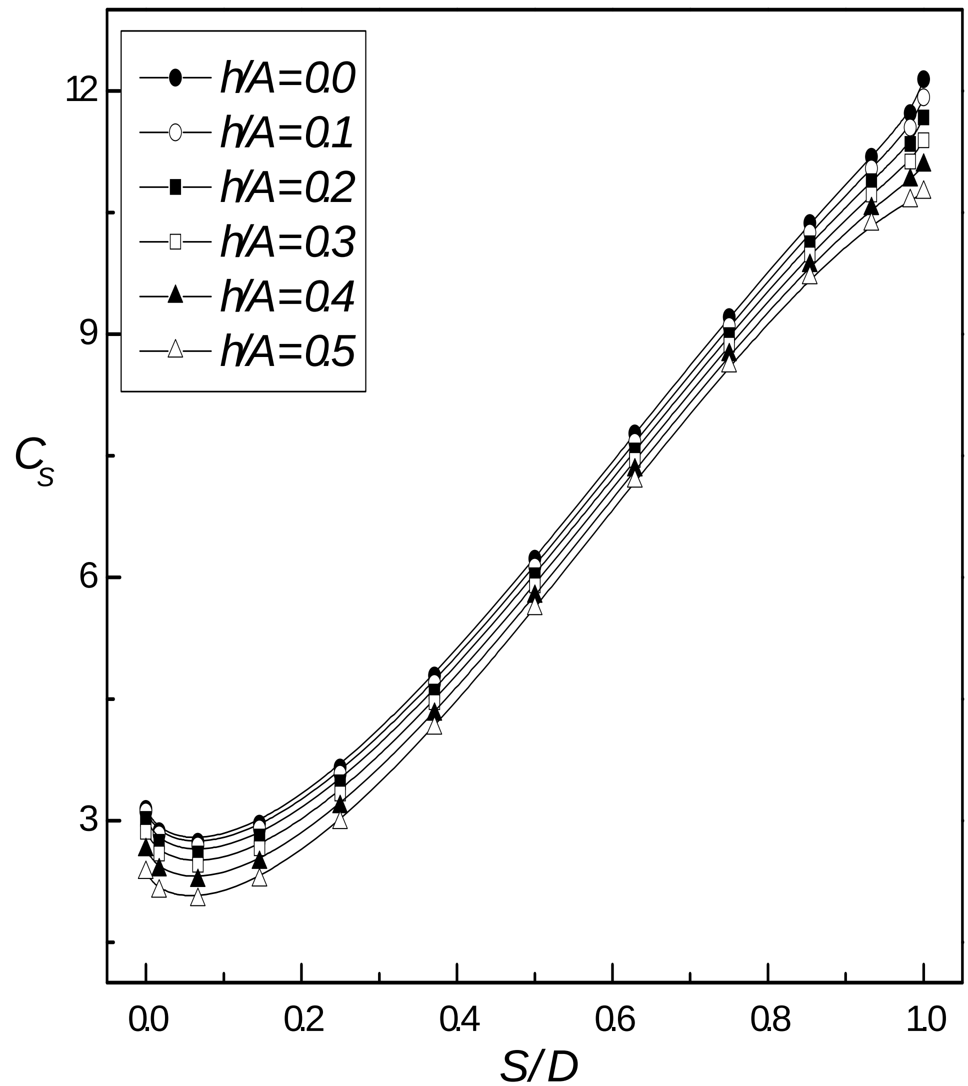

Figure 68. Variation of the slamming coefficient (C_s) with relative submergence (*S/D*) for different values of cylinder height-to-wave amplitude ratio (*h/A*) at diameter-to-wave amplitude ratio (*D/A*) is equal to 0.40 when *L/A* = 85 and *KC* = 11.

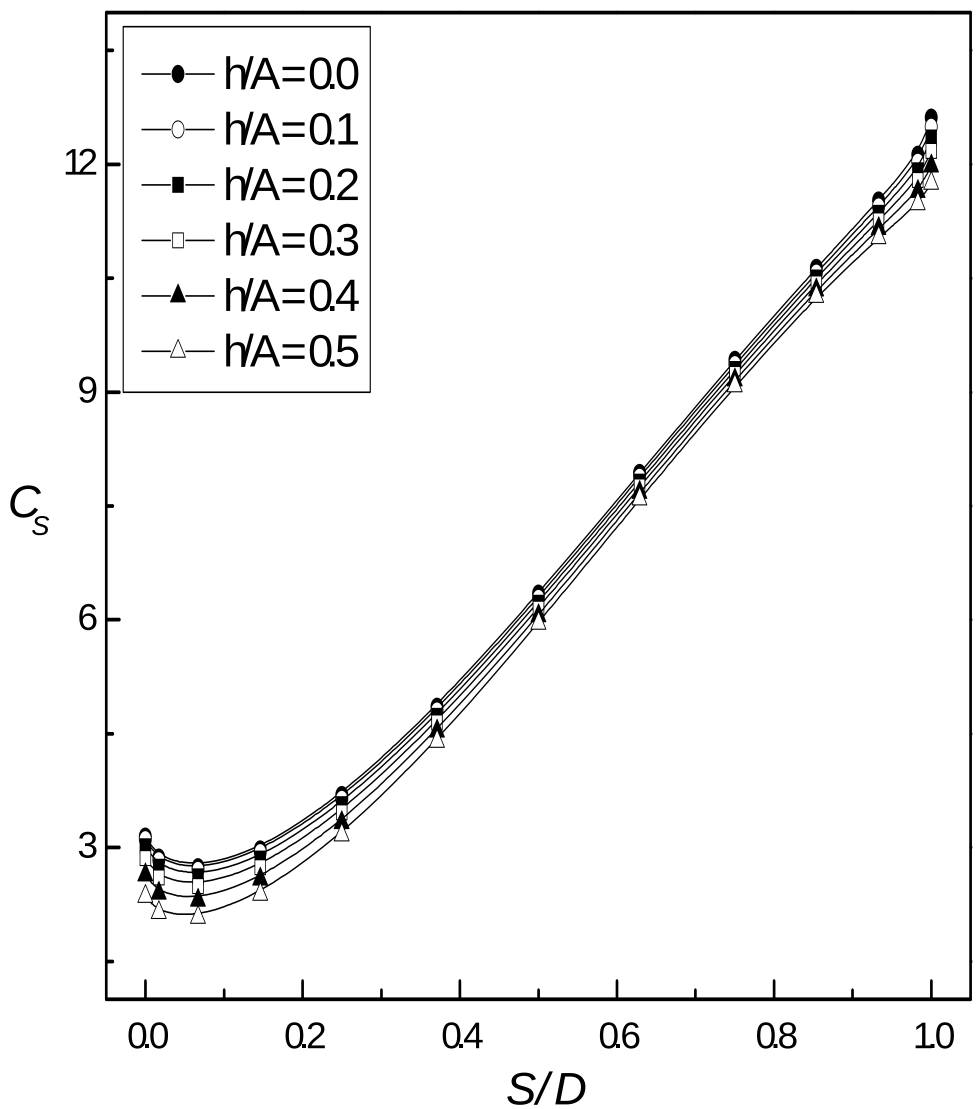

Figure 69. Variation of the slamming coefficient (C_s) with relative submergence (*S/D*) for different values of cylinder height-to-wave amplitude ratio (*h/A*) at length-to-amplitude ratio (*L/A*) is equal to 80 when *D/A* = 0.2 and *KC* = 11.

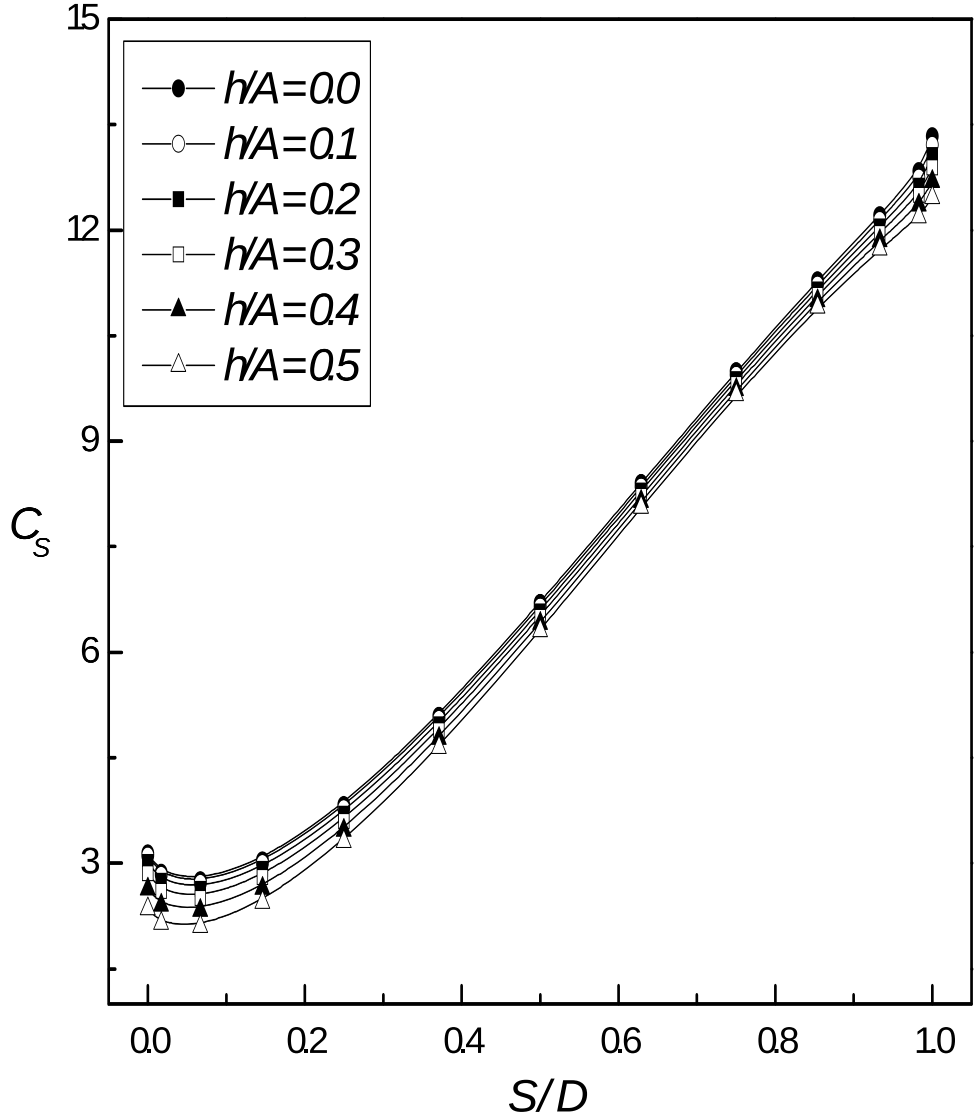

Figure 70. Variation of the slamming coefficient (C_s) with relative submergence (*S/D*) for different values of cylinder height-to-wave amplitude ratio (*h/A*) at length-to-amplitude ratio (*L/A*) is equal to 85 when *D/A* = 0.2 and *KC* = 11.

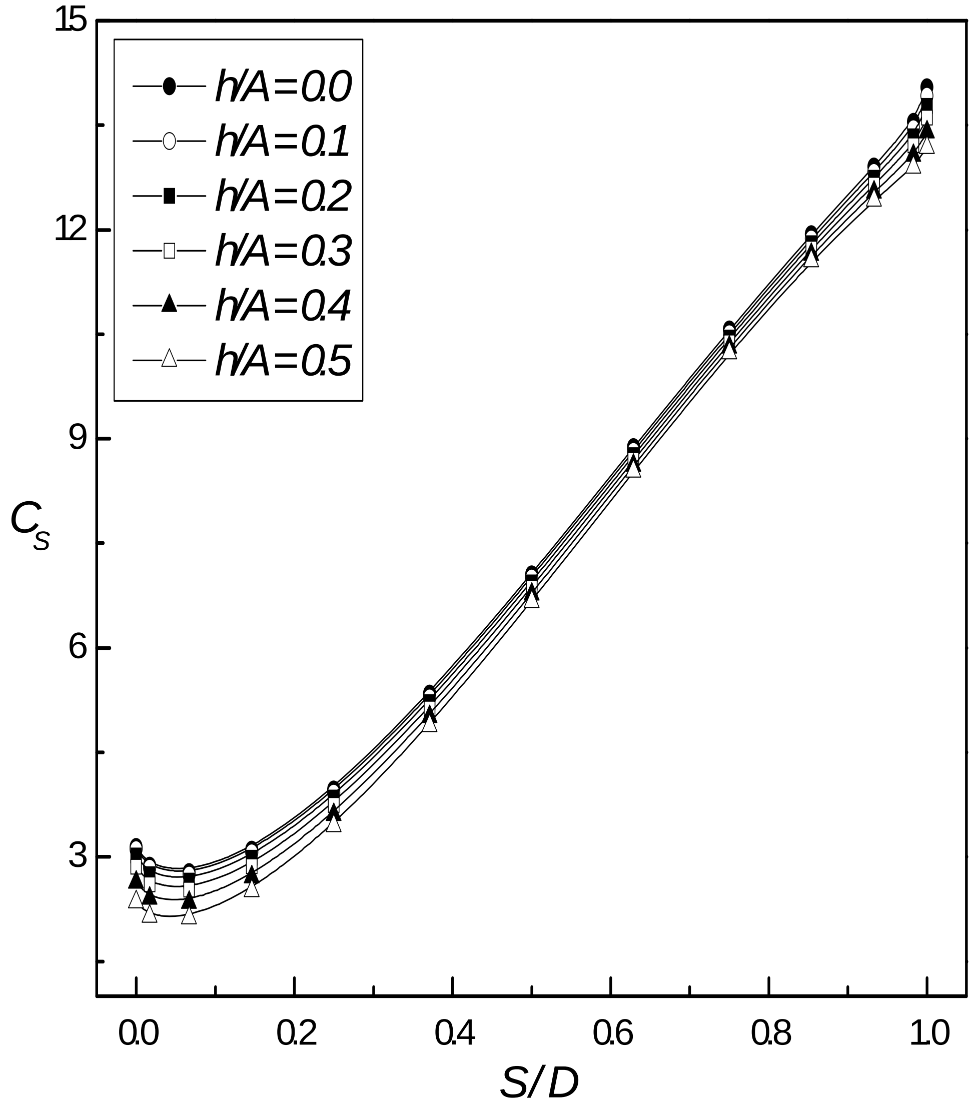

Figure 71. Variation of the slamming coefficient (C_s) with relative submergence (*S/D*) for different values of cylinder height-to-wave amplitude ratio (*h/A*) at wave length-to-amplitude ratio (*L/A*) is equal to 90 when *D/A* = 0.2 and *KC* = 11.

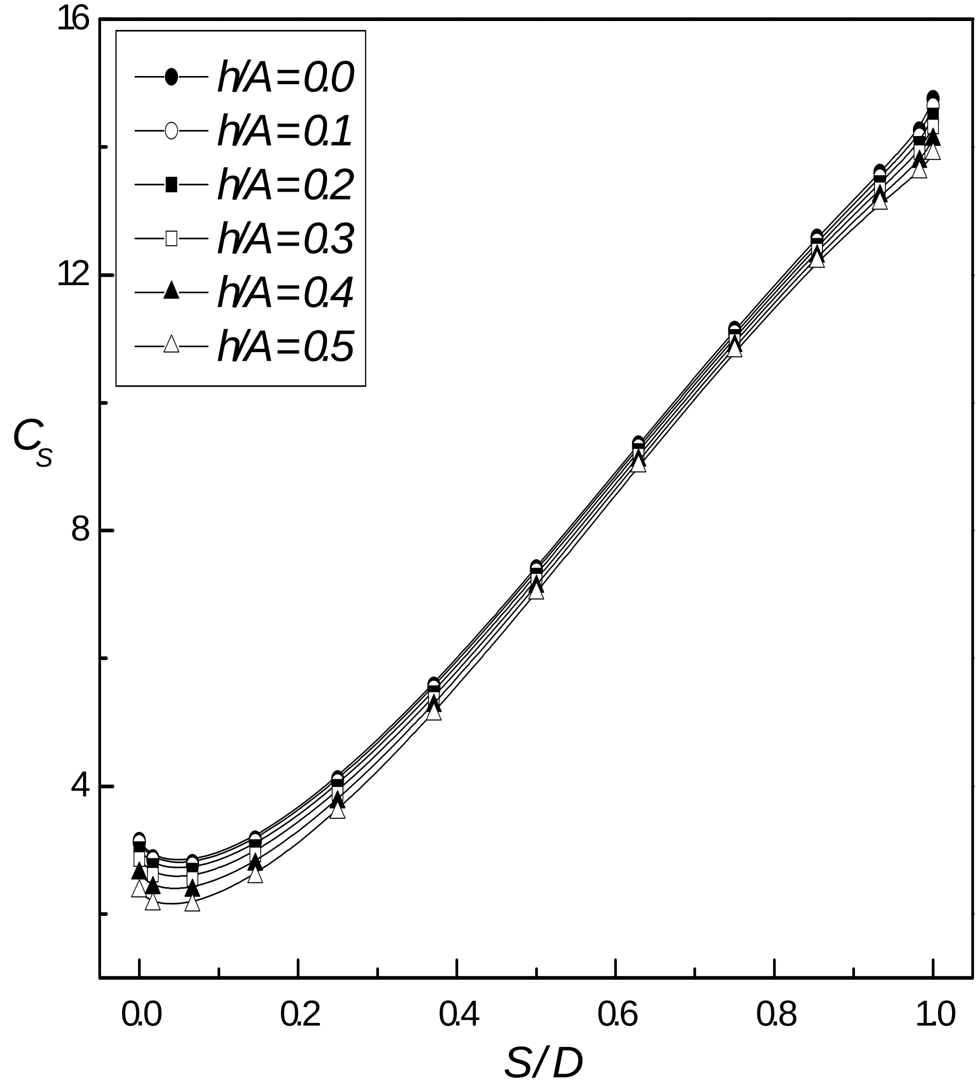

Figure 72. Variation of the slamming coefficient (C_s) with relative submergence (*S/D*) for different values of cylinder height-to-wave amplitude ratio (*h/A*) at wave length-to-amplitude ratio (*L/A*) is equal to 95 when *D/A* = 0.2 and *KC* = 11.

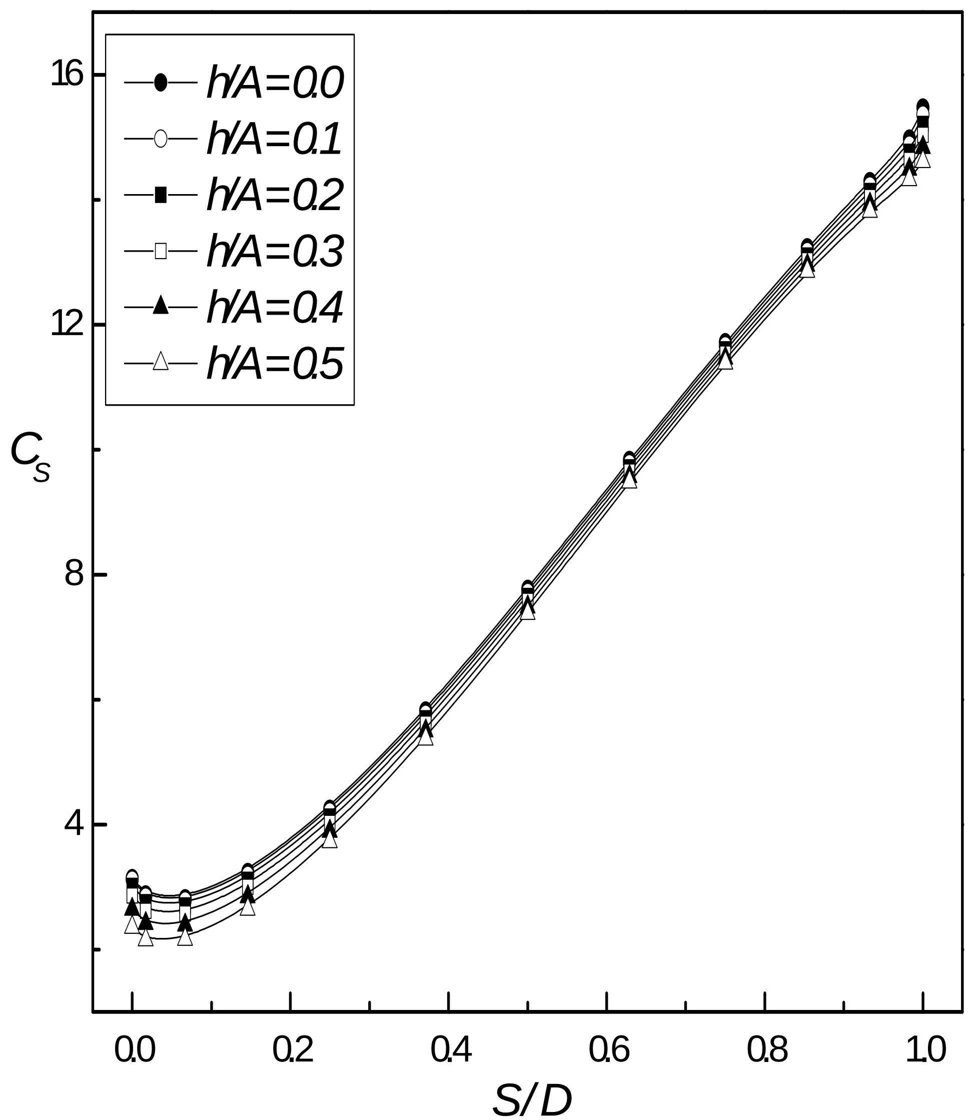

Figure 73. Variation of the slamming coefficient (C_s) with relative submergence (*S/D*) for different values of cylinder height-to-wave amplitude ratio (*h/A*) at wave length-to-amplitude ratio (*L/A*) is equal to 100 when *D/A* = 0.2 and *KC* = 11.

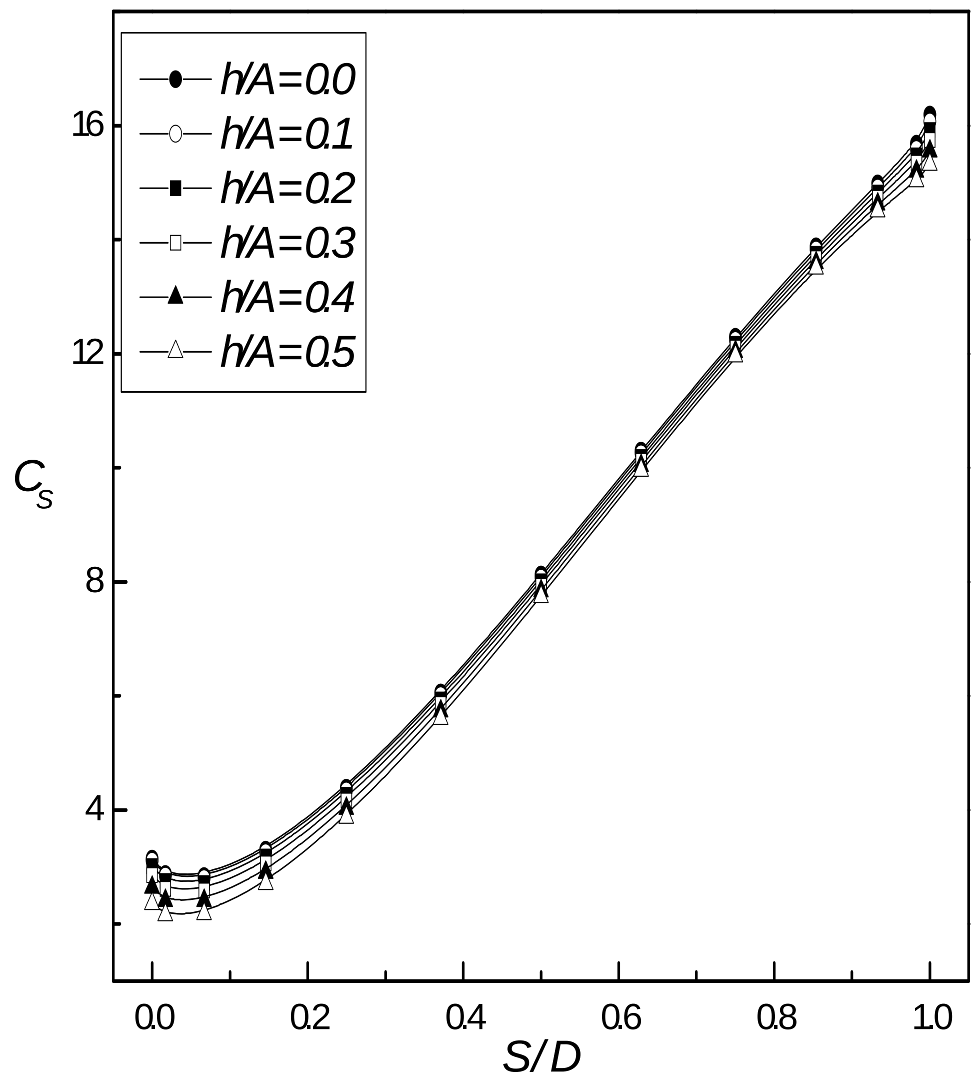

Figure 74. Variation of the slamming coefficient (C_s) with relative submergence (*S/D*) for different values of cylinder height-to-wave amplitude ratio (h/A) at wave length-to-amplitude ratio (*L/A*) is equal to 105 when *D/A* = 0.2 and *KC* = 11.

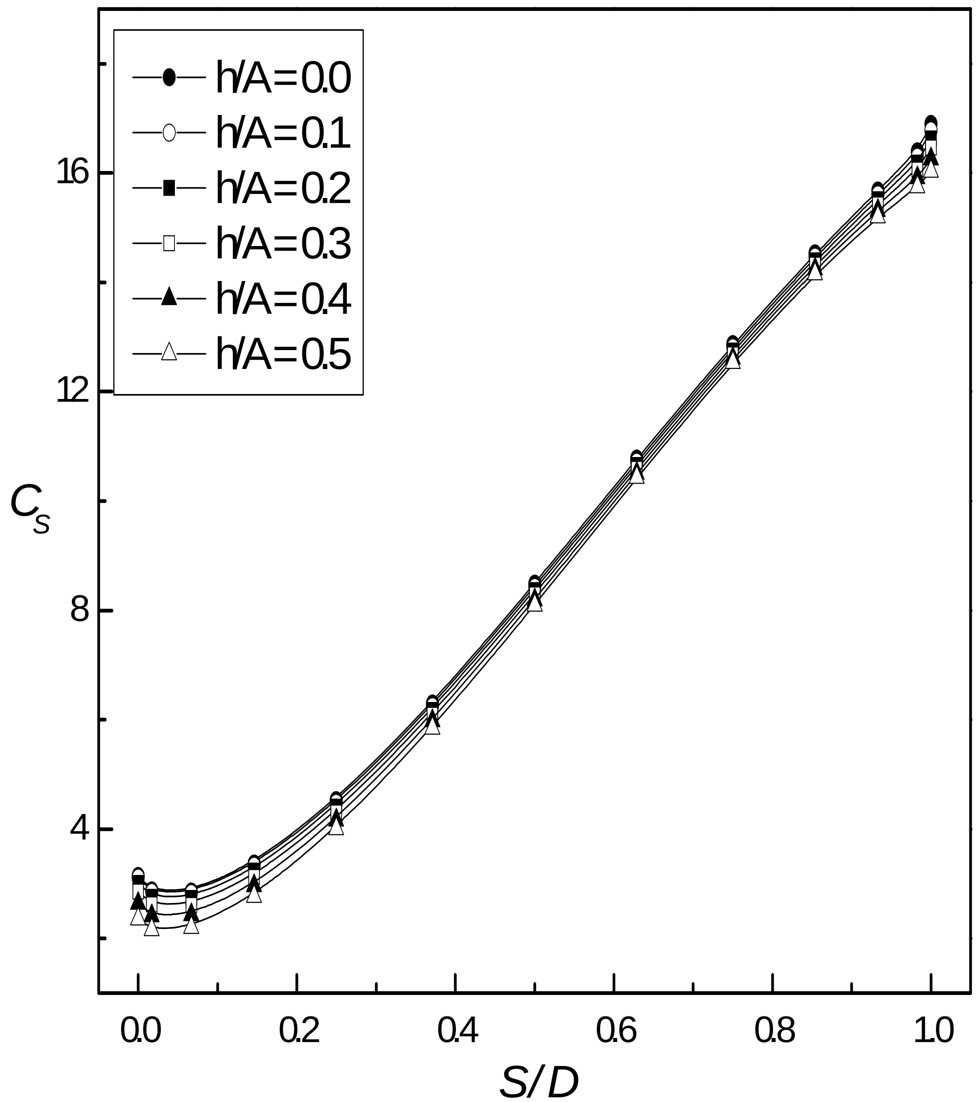

Figure 75. Variation of the slamming coefficient (C_s) with relative submergence (*S/D*) for different values of cylinder height-to-wave amplitude ratio (h/A) at wave length-to-amplitude ratio (*L/A*) is equal to 110 when *D/A* = 0.2 and *KC* = 11.

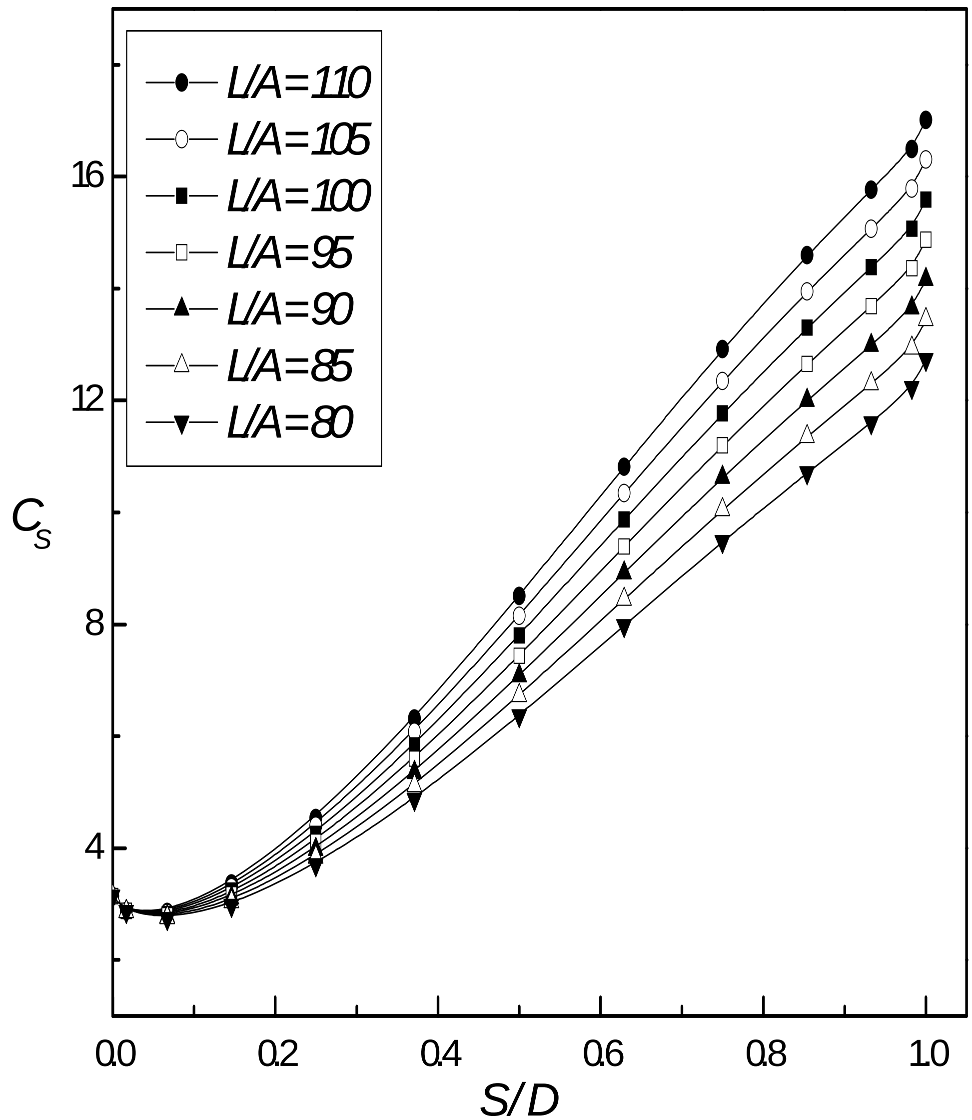

Figure 76. Variation of the slamming coefficient (C_s) with relative submergence (*S/D*) for different values of wave length-to-amplitude ratio (*L/A*) at diameter-to-wave amplitude ratio (*D/A*) is equal to 0.1 when *h/A* = 0.0 and *KC* = 11.

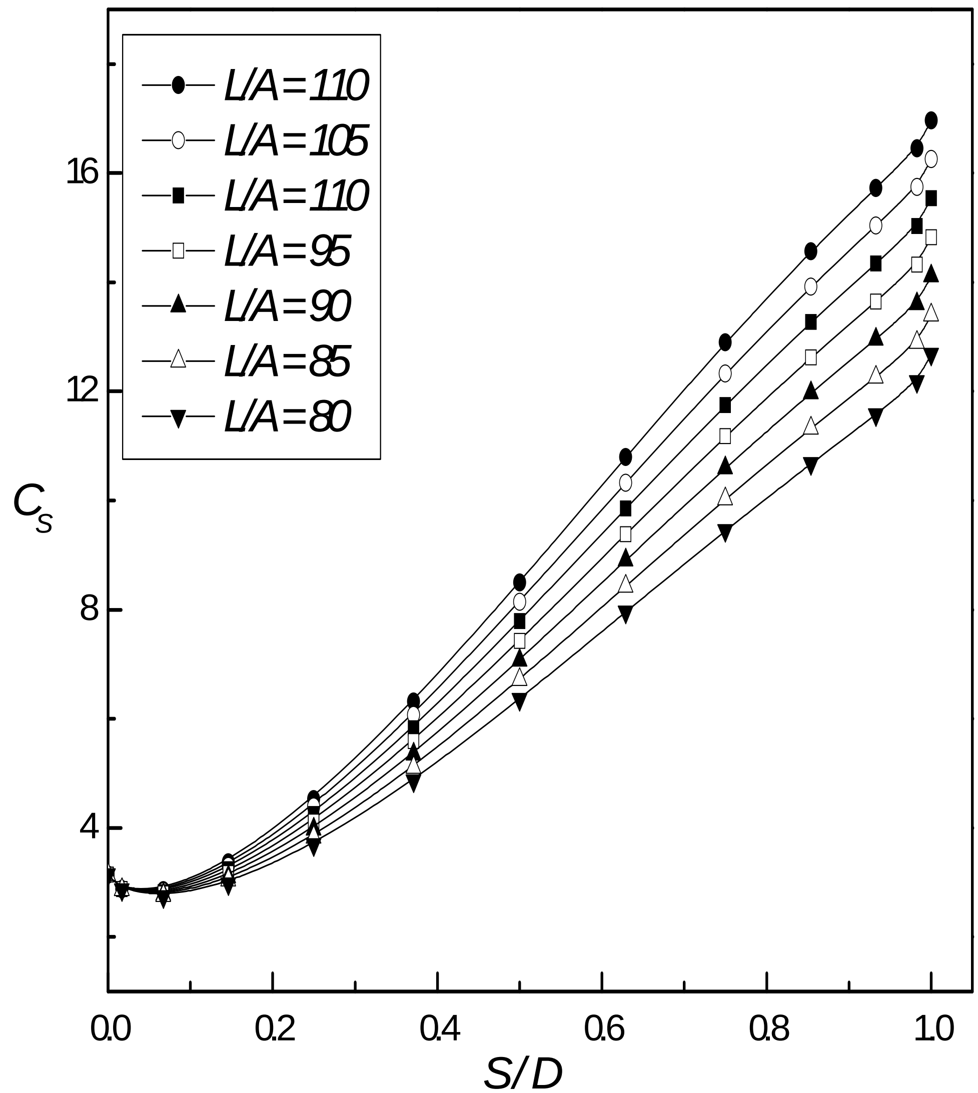

Figure 77. Variation of the slamming coefficient (C_s) with relative submergence (*S/D*) for different values of wave length-to-amplitude ratio (*L/A*) at diameter-to-wave amplitude ratio (*D/A*) is equal to 0.15 when *h/A* = 0.0 and *KC* = 11.

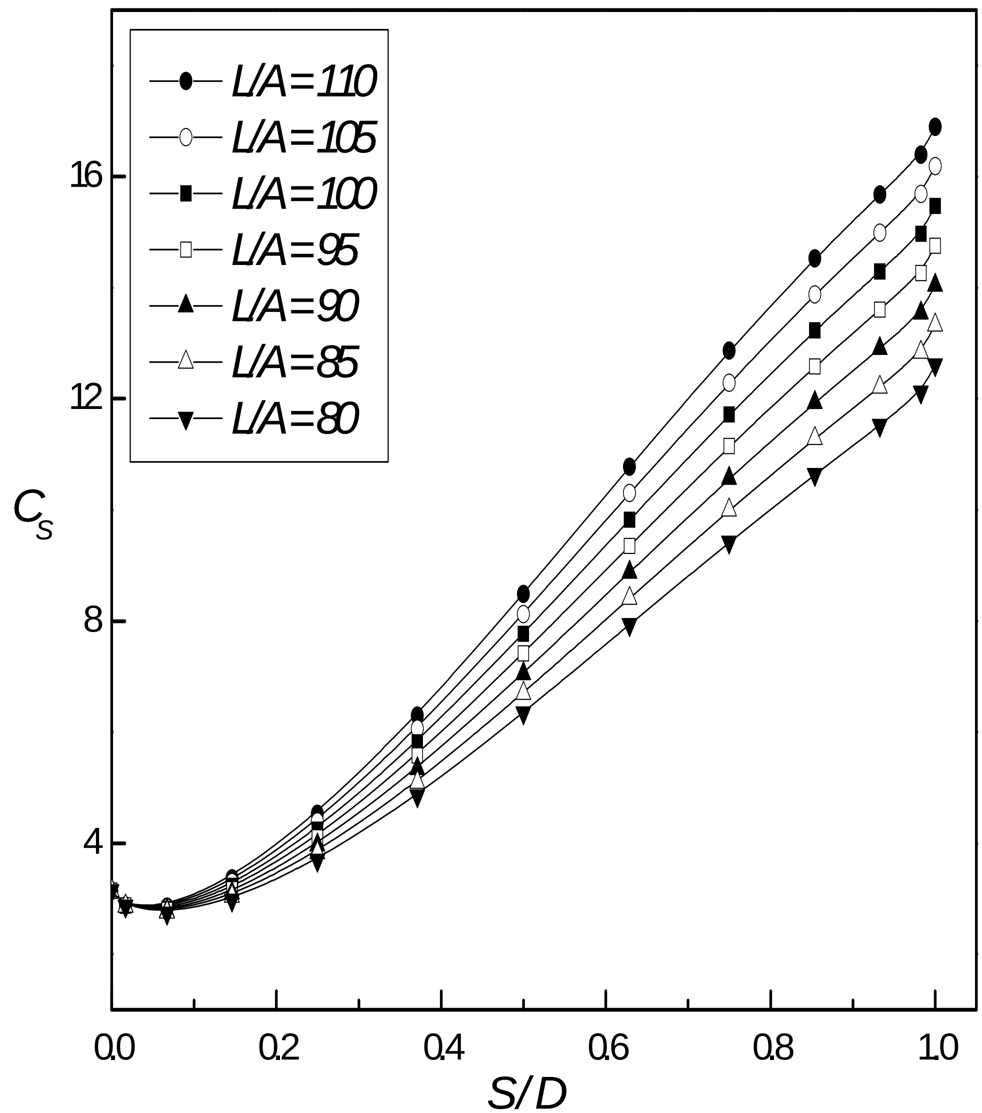

Figure 78. Variation of the slamming coefficient (C_s) with relative submergence (*S/D*) for different values of wave length-to-amplitude ratio (*L/A*) at diameter-to-wave amplitude ratio (*D/A*) is equal to 0.2 when *h/A* = 0.0 and *KC* = 11.

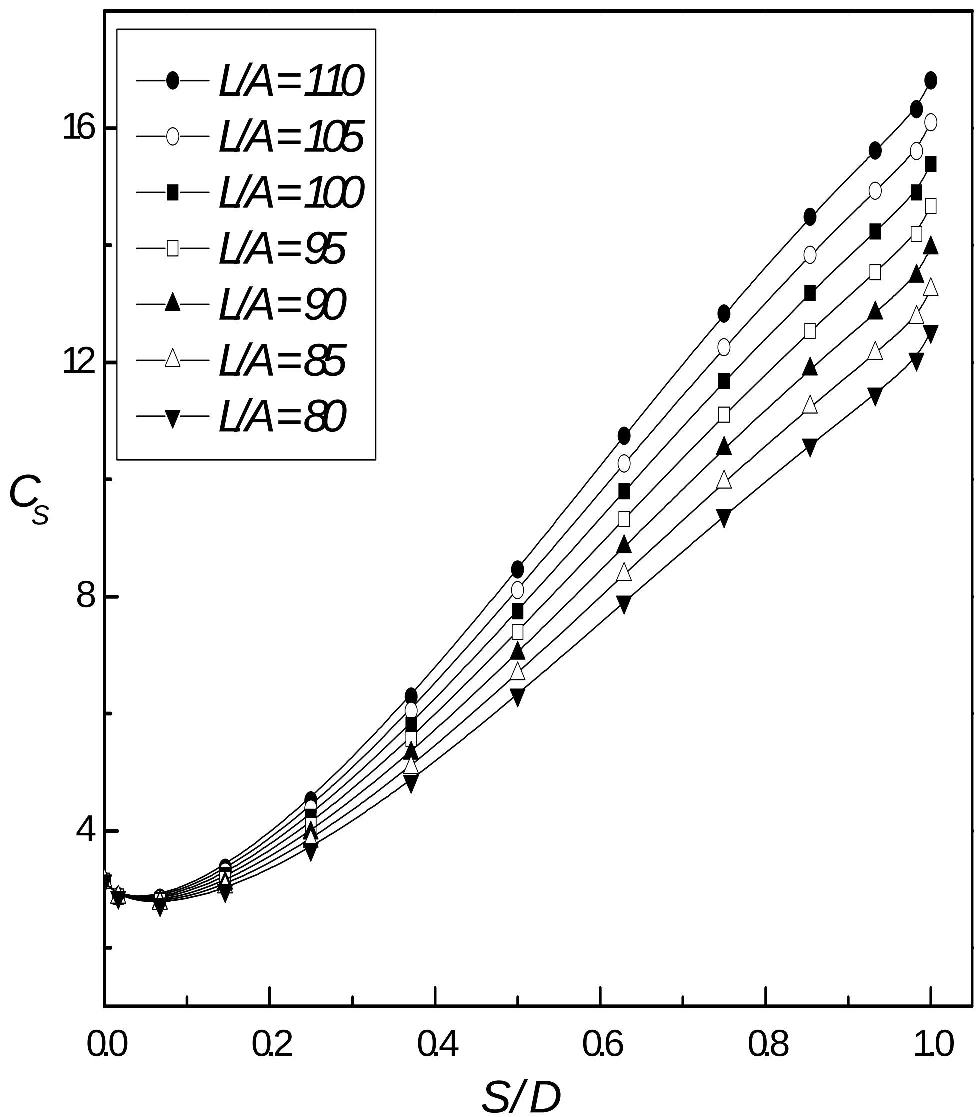

Figure 79. Variation of the slamming coefficient (C_s) with relative submergence (*S/D*) for different values of wave length-to-amplitude ratio (*L/A*) at diameter-to-wave amplitude ratio (*D/A*) is equal to 0.25 when *h/A* = 0.0 and *KC* = 11.

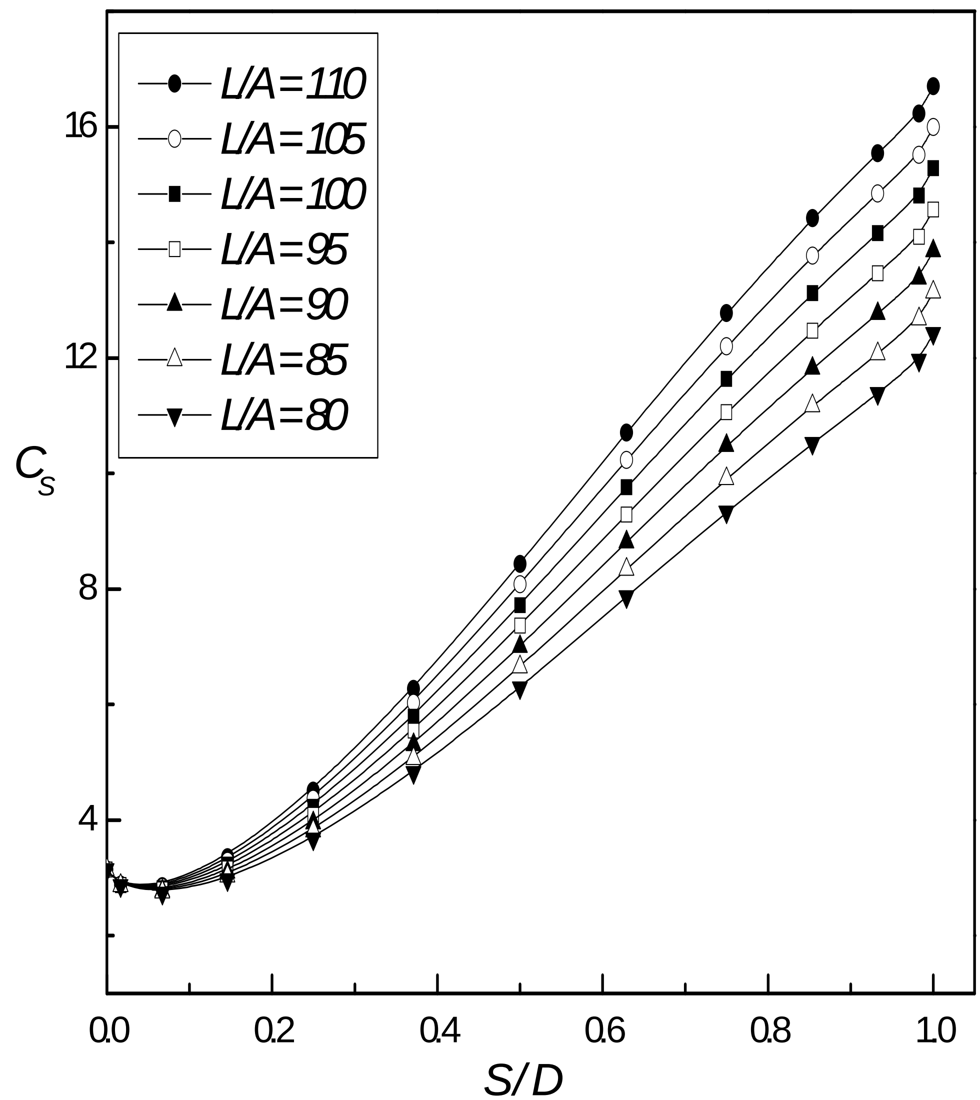

Figure 80. Variation of the slamming coefficient (C_s) with relative submergence (*S/D*) for different values of wave length-to-amplitude ratio (*L/A*) at diameter-to-wave amplitude ratio (*D/A*) is equal to 0.3 when *h/A* = 0.0 and *KC* = 11.

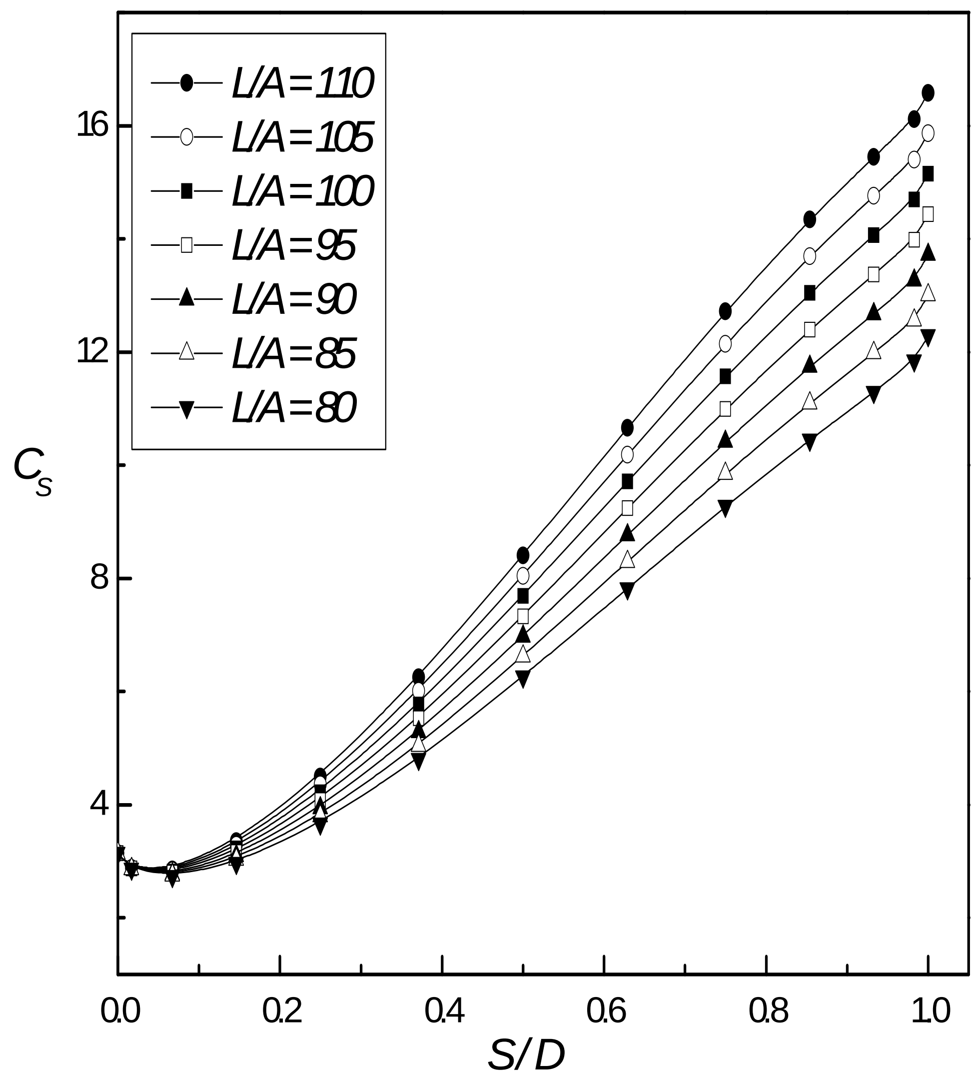

Figure 81. Variation of the slamming coefficient (C_s) with relative submergence (*S/D*) for different values of wave length-to-amplitude ratio (*L/A*) at diameter-to-wave amplitude ratio (*D/A*) is equal to 0.35 when *h/A* = 0.0 and *KC* = 11.

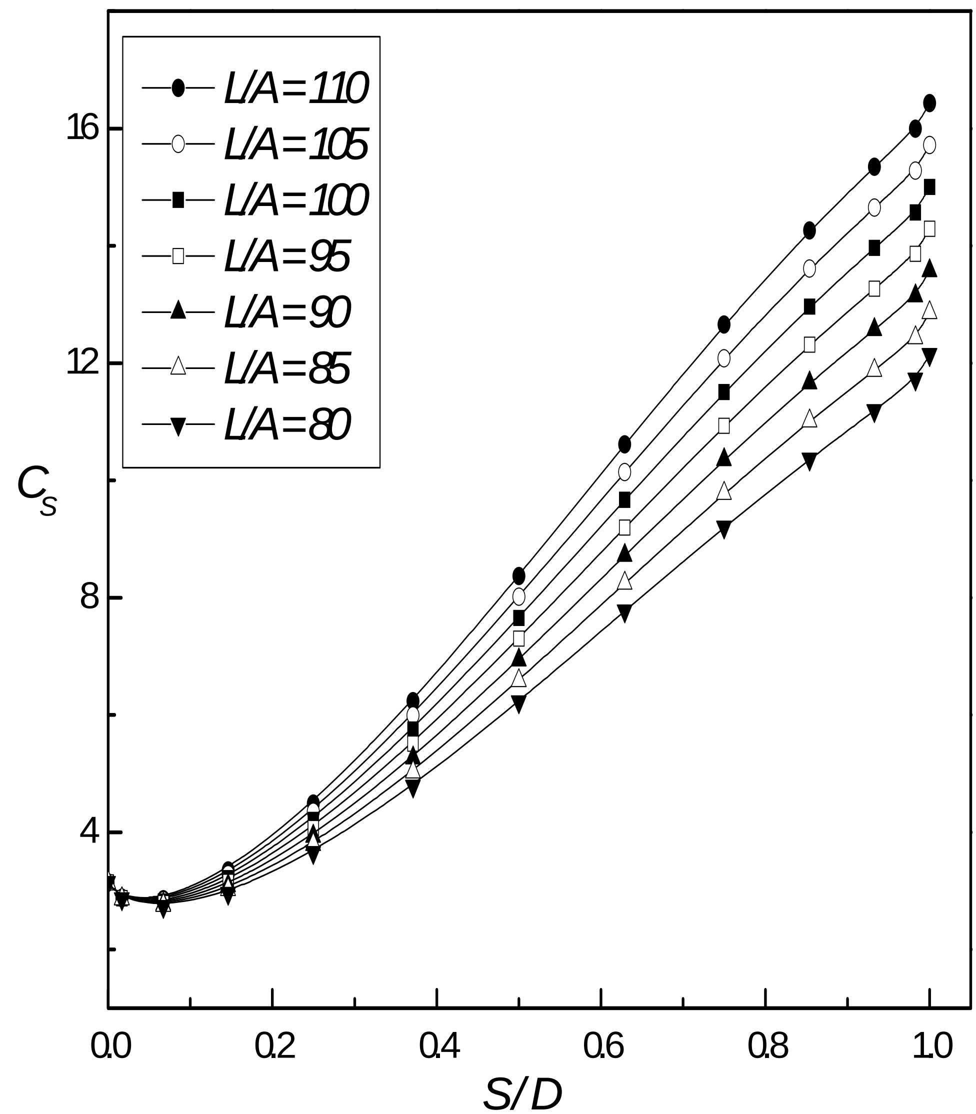

Figure 82. Variation of the slamming coefficient (C_s) with relative submergence (*S/D*) for different values of wave length-to-amplitude ratio (*L/A*) at diameter-to-wave amplitude ratio (*D/A*) is equal to 0.4 when *h/A* = 0.0 and *KC* = 11.

APPENDIX - I

L'Hospital's Rule for Evaluating Functions of Indeterminate Forms

If two functions $\phi(x)$ and $\psi(x)$ vanish at $x = a$, the fraction $\phi(x)/\psi(x)$ is an indeterminate form of the type $0/0$ at $x = a$. To find the limit of $\phi(x)/\psi(x)$, in the case of an indeterminacy of the form $0/0$, the ratio of the functions can be replaced by the ratio of their derivatives, and the limit found of this new ratio. This rule was given by the French mathematician, L' Hospital, and is usually named after him (Smirnov, 1964).

Equation (17) clearly shows that the function $f_2(\theta)$ takes an indeterminate form when θ tends towards 2π. We can apply L'Hospital's rule to evaluate this function as follows:

$$f_2(\theta) = \frac{2\pi^3}{3}\frac{(1-\cos\theta)}{(2\pi-\theta)^2} + \frac{\pi}{3}(1-\cos\theta) + (\sin\theta - \theta) \qquad (17)$$

or,

$$\underset{\theta\to 2\pi}{Lt} f_2(\theta) = \underset{\theta\to 2\pi}{Lt} \frac{2\pi^3(1-Cos\theta)}{3(2\pi-\theta)^2} + 0 + 0 - 2\pi$$

or,

$$\underset{\theta\to 2\pi}{Lt} f_2(\theta) = \underset{\theta\to 2\pi}{Lt} [\frac{2\pi^3 Sin\theta}{-6(2\pi-\theta)}] - 2\pi$$

or,

$$\underset{\theta\to 2\pi}{Lt} f_2(\theta) = \underset{\theta\to 2\pi}{Lt} \frac{2\pi^3 Cos\theta}{6} - 2\pi$$

or,

$$\underset{\theta\to 2\pi}{Lt} f_2(\theta) = \frac{\pi^3}{3} - 2\pi$$

Equation (24) clearly shows that the function $f_3(\theta)$ takes an indeterminate form when θ tends towards zero. We can apply L'Hospital's rule to evaluate this function as follows:

$$f_3(\theta) = \frac{1}{\sin\frac{\theta}{2}}\left[\frac{2\pi^3}{3}\left\{\frac{\sin\theta}{(2\pi-\theta)^2} + \frac{2(1-\cos\theta)}{(2\pi-\theta)^3}\right\} + \frac{\pi}{3}\sin\theta + (\cos\theta - 1)\right] \text{.................}(24)$$

or,

$$\underset{\theta\to 0}{Lt}\, f_3(\theta) = \underset{\theta\to 0}{Lt}\left[\frac{2\pi^3 Sin\theta}{3\sin\frac{\theta}{2}(2\pi-\theta)^2}\right] + \underset{\theta\to 0}{Lt}\left[\frac{4\pi^3(1-Cos\theta)}{3Sin\frac{\theta}{2}(2\pi-\theta)^3}\right] + \underset{\theta\to 0}{Lt}\left[\frac{\pi Sin\theta}{3Sin\frac{\theta}{2}}\right]$$

$$+ \underset{\theta\to 0}{Lt}\left[\frac{Cos\theta - 1}{Sin\frac{\theta}{2}}\right]$$

or,

$$\underset{\theta\to 0}{Lt}\, f_3(\theta) = \underset{\theta\to 0}{Lt}\left[\frac{4\pi^3 Sin\frac{\theta}{2}Cos\frac{\theta}{2}}{3\sin\frac{\theta}{2}(2\pi-\theta)^2}\right] + \underset{\theta\to 0}{Lt}\left[\frac{4\pi^3(1-1+2Sin^2\frac{\theta}{2})}{3Sin\frac{\theta}{2}(2\pi-\theta)^3}\right] + \underset{\theta\to 0}{Lt}\left[\frac{2\pi Sin\frac{\theta}{2}Cos\frac{\theta}{2}}{3Sin\frac{\theta}{2}}\right]$$

$$+ \underset{\theta\to 0}{Lt}\left[\frac{1-2Sin^2\frac{\theta}{2}-1}{Sin\frac{\theta}{2}}\right]$$

or,

$$\underset{\theta\to 0}{Lt}\, f_3(\theta) = \underset{\theta\to 0}{Lt}\left[\frac{4\pi^3 Cos\frac{\theta}{2}}{3(2\pi-\theta)^2}\right] + \underset{\theta\to 0}{Lt}\left[\frac{8\pi^3 Sin\frac{\theta}{2})}{3(2\pi-\theta)^3}\right] + \underset{\theta\to 0}{Lt}\left[\frac{2\pi Cos\frac{\theta}{2}}{3}\right] + \underset{\theta\to 0}{Lt}\left[-2Sin\frac{\theta}{2}\right]$$

or,

$$\underset{\theta\to 0}{Lt}\, f_3(\theta) = \frac{4\pi^3}{12\pi^2} + 0 + \frac{2\pi}{3} + 0$$

or,

$$\underset{\theta\to 0}{Lt}\, f_3(\theta) = \frac{\pi}{3} + 0 + \frac{2\pi}{3} + 0$$

or,

$$\underset{\theta\to 0}{Lt}\, f_3(\theta) = \pi$$

Similarly, equation (24) shows that the function $f_3(\theta)$ takes an indeterminate form when θ tends towards 2π. We can apply L'Hospital's rule to evaluate this function as follows:

$$f_3(\theta) = \frac{1}{\sin\frac{\theta}{2}}\left[\frac{2\pi^3}{3}\left\{\frac{\sin\theta}{(2\pi-\theta)^2} + \frac{2(1-\cos\theta)}{(2\pi-\theta)^3}\right\} + \frac{\pi}{3}\sin\theta + (\cos\theta - 1)\right] \text{..................(24)}$$

or,

$$\underset{\theta\to 2\pi}{Lt}\, f_3(\theta) = \underset{\theta\to 2\pi}{Lt}\left[\frac{2\pi^3 Sin\theta}{3\sin\frac{\theta}{2}(2\pi-\theta)^2}\right] + \underset{\theta\to 2\pi}{Lt}\left[\frac{4\pi^3(1-Cos\theta)}{3Sin\frac{\theta}{2}(2\pi-\theta)^3}\right] + \underset{\theta\to 2\pi}{Lt}\left[\frac{\pi Sin\theta}{3Sin\frac{\theta}{2}}\right]$$
$$+ \underset{\theta\to 2\pi}{Lt}\left[\frac{(Cos\theta-1)}{Sin\frac{\theta}{2}}\right]$$

or,

$$\underset{\theta\to 2\pi}{Lt}\, f_3(\theta) = \underset{\theta\to 2\pi}{Lt}\left[\frac{2\pi^3 .2Sin\frac{\theta}{2}Cos\frac{\theta}{2}}{3\sin\frac{\theta}{2}(2\pi-\theta)^2}\right] + \underset{\theta\to 2\pi}{Lt}\left[\frac{4\pi^3\left(1-1+2Sin^2\frac{\theta}{2}\right)}{3Sin\frac{\theta}{2}(2\pi-\theta)^3}\right]$$
$$+ \underset{\theta\to 2\pi}{Lt}\left[\frac{2\pi Sin\frac{\theta}{2}Cos\frac{\theta}{2}}{3Sin\frac{\theta}{2}}\right] + \underset{\theta\to 2\pi}{Lt}\left[\frac{1-2Sin^2\frac{\theta}{2}-1}{Sin\frac{\theta}{2}}\right]$$

or,

$$\underset{\theta\to 2\pi}{Lt}\, f_3(\theta) = \underset{\theta\to 2\pi}{Lt}\left[\frac{4\pi^3 Cos\frac{\theta}{2}}{3(2\pi-\theta)^2}\right] + \underset{\theta\to 2\pi}{Lt}\left[\frac{8\pi^3 Sin^2\frac{\theta}{2}}{3Sin\frac{\theta}{2}(2\pi-\theta)^3}\right] + \underset{\theta\to 2\pi}{Lt}\left[\frac{2\pi Cos\frac{\theta}{2}}{3}\right]$$
$$+ \underset{\theta\to 2\pi}{Lt}\left[-2Sin\frac{\theta}{2}\right]$$

or,

$$\underset{\theta \to 2\pi}{Lt} f_3(\theta) = \underset{\theta \to 2\pi}{Lt}\left[\frac{4\pi^3(-Sin\frac{\theta}{2}) \times \frac{1}{2}}{-6(2\pi - \theta)}\right] + \underset{\theta \to 2\pi}{Lt}\left[\frac{8\pi^3 Sin\frac{\theta}{2}}{3(2\pi - \theta)^3}\right] + \underset{\theta \to 2\pi}{Lt}\left[\frac{2\pi Cos\frac{\theta}{2}}{3}\right]$$
$$+ \underset{\theta \to 2\pi}{Lt}\left[-2Sin\frac{\theta}{2}\right]$$

or,

$$\underset{\theta \to 2\pi}{Lt} f_3(\theta) = \underset{\theta \to 2\pi}{Lt}\left[\frac{4\pi^3 Sin\frac{\theta}{2}}{12(2\pi - \theta)}\right] + \underset{\theta \to 2\pi}{Lt}\left[\frac{8\pi^3(Cos\frac{\theta}{2}) \times \frac{1}{2}}{-9(2\pi - \theta)^2}\right] + \underset{\theta \to 2\pi}{Lt}\left[\frac{2\pi Cos\frac{\theta}{2}}{3}\right]$$
$$+ \underset{\theta \to 2\pi}{Lt}\left[-2Sin\frac{\theta}{2}\right]$$

or,

$$\underset{\theta \to 2\pi}{Lt} f_3(\theta) = \underset{\theta \to 2\pi}{Lt}\left[\frac{\pi^3(Cos\frac{\theta}{2}) \times \frac{1}{2}}{(-1)}\right] + \underset{\theta \to 2\pi}{Lt}\left[\frac{-2\pi^3 Sin\frac{\theta}{2}}{18(2\pi - \theta)}\right] + \underset{\theta \to 2\pi}{Lt}\left[\frac{2\pi Cos\frac{\theta}{2}}{3}\right]$$
$$+ \underset{\theta \to 2\pi}{Lt}\left[-2Sin\frac{\theta}{2}\right]$$

or,

$$\underset{\theta \to 2\pi}{Lt} f_3(\theta) = \underset{\theta \to 2\pi}{Lt}\left[\frac{\pi^3 Cos\frac{\theta}{2}}{(-6)}\right] + \underset{\theta \to 2\pi}{Lt}\left[\frac{-2\pi^3(Cos\frac{\theta}{2}) \times \frac{1}{2}}{-18}\right] + \underset{\theta \to 2\pi}{Lt}\left[\frac{2\pi Cos\frac{\theta}{2}}{3}\right]$$
$$+ \underset{\theta \to 2\pi}{Lt}\left[-2Sin\frac{\theta}{2}\right]$$

or,

$$\underset{\theta \to 2\pi}{Lt} f_3(\theta) = \underset{\theta \to 2\pi}{Lt}\left[\frac{\pi^3 Cos\frac{\theta}{2}}{(-6)}\right] + \underset{\theta \to 2\pi}{Lt}\left[\frac{-\pi^3 Cos\frac{\theta}{2}}{-18}\right] + \underset{\theta \to 2\pi}{Lt}\left[\frac{2\pi Cos\frac{\theta}{2}}{3}\right] + \underset{\theta \to 2\pi}{Lt}\left[-2Sin\frac{\theta}{2}\right]$$

or,

$$\underset{\theta \to 2\pi}{Lt} f_3(\theta) = \left[\frac{-\pi^3}{6} \times (-1)\right] + \left[\frac{-\pi^3}{18}\right] + \left[\frac{2\pi(-1)}{3}\right] + 0$$

or,

$$\underset{\theta \to 2\pi}{Lt} f_3(\theta) = \frac{\pi^3}{6} - \frac{\pi^3}{18} - \frac{2\pi}{3} + 0$$

or,

$$\underset{\theta \to 2\pi}{Lt} f_3(\theta) = \frac{3\pi^3 - \pi^3}{18} - \frac{2\pi}{3}$$

or,

$$\underset{\theta \to 2\pi}{Lt} f_3(\theta) = \frac{\pi^3}{9} - \frac{2\pi}{3}$$